

**UNIVERSIDADE FEDERAL DE MINAS GERAIS**  
**PROGRAMA DE PÓS-GRADUAÇÃO EM ENGENHARIA MECÂNICA**

CLEISON HENRIQUE DE PAULA

**THERMO-ECONOMIC AND ENVIRONMENTAL ANALYSIS OF A  
REFRIGERATION SYSTEM OPERATING WITH ECOLOGICAL REFRIGERANTS**

Belo Horizonte

2021

Cleison Henrique de Paula

**THERMO-ECONOMIC AND ENVIRONMENTAL ANALYSIS OF A  
REFRIGERATION SYSTEM OPERATING WITH ECOLOGICAL REFRIGERANTS**

Thesis submitted to the Graduate Program in Mechanical Engineering of the Federal University of Minas Gerais, as a partial requirement to obtain the title of Doctor in Mechanical Engineering.

Concentration area: Energy and Sustainability

Advisor: Prof. Dr. Antônio Augusto Torres  
Maia

Belo Horizonte

2021

P324t Paula, Cleison Henrique de.  
Thermo-economic and environmental analysis of a refrigeration system operating with ecological refrigerants [recurso eletrônico] / Cleison Henrique de Paula. - 2021.  
1 recurso online (113 f. : il., color.) : pdf.

Orientador: Antônio Augusto Torres Maia.

Tese (doutorado) - Universidade Federal de Minas Gerais, Escola de Engenharia.

Apêndices: f. 89-113.

Bibliografia: f. 83-88.  
Exigências do sistema: Adobe Acrobat Reader.

1. Engenharia mecânica - Teses. 2. Análise ambiental - Teses.  
3. Modelos matemáticos - Teses. 4. Refrigeração - Teses. I. Maia, Antônio Augusto Torres. II. Universidade Federal de Minas Gerais. Escola de Engenharia. III. Título.

CDU: 621(043)



UNIVERSIDADE FEDERAL DE MINAS GERAIS  
ESCOLA DE ENGENHARIA  
PROGRAMA DE PÓS-GRADUAÇÃO EM ENGENHARIA MECÂNICA

FOLHA DE APROVAÇÃO

**THERMO-ECONOMIC AND ENVIRONMENTAL ANALYSIS OF A REFRIGERATION SYSTEM OPERATING WITH ECOLOGICAL REFRIGERANTS**

**CLEISON HENRIQUE DE PAULA**

Tese submetida à Banca Examinadora designada pelo Colegiado do Programa de Pós-Graduação em Engenharia Mecânica da Universidade Federal de Minas Gerais, constituída pelos Professores: Dr. Antônio Augusto Torres Maia (Orientador-Departamento de Engenharia Mecânica/UFMG), Dr. Juan José Garcia Pabón (Instituto de Engenharia Mecânica/UNIFEI), Dr. Willian Moreira Duarte (Centro Universitário de Belo Horizonte/UniBH), Dr. Luben Cabezas Gómez (Departamento de Engenharia Mecânica/USP), Dr. Raphael Nunes de Oliveira (Departamento de Engenharia Mecânica/UFMG), como parte dos requisitos necessários à obtenção do título de "**Doutor em Engenharia Mecânica**", na área de concentração de "Engenharia e Sustentabilidade".

Tese aprovada no dia 28 de maio de 2021.

Por:



Documento assinado eletronicamente por **Antonio Augusto Torres Maia, Professor do Magistério Superior**, em 24/06/2021, às 20:41, conforme horário oficial de Brasília, com fundamento no art. 5º do [Decreto nº 10.543, de 13 de novembro de 2020](#).



Documento assinado eletronicamente por **Juan Jose Garcia Pabon, Usuário Externo**, em 28/06/2021, às 10:46, conforme horário oficial de Brasília, com fundamento no art. 5º do [Decreto nº 10.543, de 13 de novembro de 2020](#).



Documento assinado eletronicamente por **Willian Moreira Duarte, Usuário Externo**, em 28/06/2021, às 15:49, conforme horário oficial de Brasília, com fundamento no art. 5º do [Decreto nº 10.543, de 13 de novembro de 2020](#).



Documento assinado eletronicamente por **Raphael Nunes de Oliveira, Servidor(a)**, em 02/07/2021, às 09:48, conforme horário oficial de Brasília, com fundamento no art. 5º do [Decreto nº 10.543, de 13 de novembro de 2020](#).



Documento assinado eletronicamente por **Luben Cabezas Gómez, Usuário Externo**, em 09/07/2021, às 11:56, conforme horário oficial de Brasília, com fundamento no art. 5º do [Decreto nº 10.543, de 13 de novembro de 2020](#).



A autenticidade deste documento pode ser conferida no site [https://sei.ufmg.br/sei/controlador\\_externo.php?acao=documento\\_conferir&id\\_orgao\\_acesso\\_externo=0](https://sei.ufmg.br/sei/controlador_externo.php?acao=documento_conferir&id_orgao_acesso_externo=0), informando o código verificador **0798971** e o código CRC **A5CADEC0**.

## PREFACE

This thesis is the result of research conducted in the last three years at the group of refrigeration and heating (GREA) at Federal University of Minas Gerais (UFMG) under the supervision of Prof. Dr. Antônio Augusto Torres Maia and Prof. Dr. Willian Moreira Duarte. During this time, **four** journal papers and **two** congress paper related to this research were produced and they are listed below:

1. **de Paula, C.H.**, Duarte, W. M., Rocha, T. T. M., de Oliveira, R. N., Maia, A. A. T. Optimal design and environmental, energy and exergy analysis of a vapor compression refrigeration system using R290, R1234yf, and R744 as alternatives to replace R134a. **International Journal of Refrigeration** 113 (2020) 10-20. **Number of citations until 06/17/2021: 22.**
2. **de Paula, C.H.**, Duarte, W. M., Rocha, T. T. M., de Oliveira, R. N., de Paoli Mendes, R., Maia, A. A. T. Thermo-economic and environmental analysis of a small capacity vapor compression refrigeration system using R290, R1234yf, and R600a. **International Journal of Refrigeration** 118 (2020) 250-260. **Number of citations until 06/17/2021: 5.**
3. **de Paula, C.H.**, Duarte, W. M., Rocha, T. T. M., de Oliveira, R. N., Maia, A. A. T. Energetic, exergetic, environmental and economic assessment of a cascade refrigeration system operating with five different ecological refrigerant pairs. **International Journal of Air-Conditioning and Refrigeration**. **Status: this paper went through the first revision.**
4. Rocha, T. T. M., **de Paula, C.H.**, Cangussu, V. M., Maia, A. A. T., de Oliveira, R. N. Effect of surface roughness on the mass flow rate predictions for adiabatic capillary tubes. **International Journal of Refrigeration** 118 (2020) 269-278. **Number of citations until 06/17/2021: 3.**
5. **De Paula, Cleison**; Moreira Duarte, Willian; Torres Martins Rocha, Thiago; Nunes, Raphael; Maia, Antônio. Environmental and energy performance evaluation of the R1234yf as an environmentally friendly alternative to R134a. In: 25<sup>th</sup> ABCM International Congress of Mechanical Engineering (2019).
6. **De Paula, Cleison**; Moreira Duarte, Willian; Maia, Antônio. Thermo-economic and environmental analysis of a small capacity vapor compression refrigeration system using R744 as a replacement for R134a. In: 18th ABCM Brazilian Congress of Thermal Sciences and Engineering (2020).

This document was written considering the guidelines of Brazilian Association of Technical Standards, however, for the decimal separator it was used point (.) instead of comma (,).

## ACKNOWLEDGEMENT

I would like to thank my LORD and Savior JESUS CHRIST, for salvation, for life, for health, for patience, provision and completion of this doctorate. Lord JESUS must increase, but I must decrease!

I would like to thank all my family, especially my parents, José Maria and Ângela Cleide, my beloved siblings, Poliana, Júlio César, Alesi, and Alessandra, for their affection, love, patience and support.

In addition, I would like to thank Prof. Ricardo Koury for the guidance and help that were essential for me to get an opportunity to study in the Graduate Program in Mechanical Engineering, as a doctorate candidate. I have faith in JESUS that one day we will meet again in the arms of the heavenly Father in a place of peace, joy, and rest for our souls.

I would like to thank my advisor, Prof. Antônio Maia, and Prof. Willian Duarte, for patience and attention. Furthermore, I would like to thank professors Luiz Machado and Raphael Nunes for all their help.

I would like to thank GREA (Cooling and Heating Group of the Graduate Program in Mechanical Engineering/UFMG) for all their help and learning over these years.

I would like to thank Tiago Paulino, Thiago Torres, Leonardo Victor, Ramon, Cássio Cançado, Sabrina Rabelo, Túlio da Mota, Ivana Macedo, Henrique Neiva, Valdson, Leandro Cristino and Marina Cândida for all help during the PhD course.

This work was supported by the Fundação de Amparo à Pesquisa do Estado de Minas Gerais (FAPEMIG) and the Conselho Nacional de Desenvolvimento Científico e Tecnológico (CNPq). This study was financed in part by the Coordenação de Aperfeiçoamento de Pessoal de Nível Superior - Brasil (CAPES) - Finance Code 001.

Finally, I would like to thank the LORD JESUS CHRIST for the lives of my beloved brothers of the Assembly of God and Betel Baptist Churches for the prayers and beautiful words given in various services.

## ABSTRACT

This thesis presents a mathematical model of a vapor compression refrigeration system operating under steady-state conditions. This model was used to design an energy-efficient system, with low cost, that operates with the most appropriate ecological refrigerant in terms of overall environmental impact, focusing the refrigerants R290, R600a, R744, and R1234yf. The environmental analysis was performed based on Total Equivalent Warming Impact, while the thermo-economic analysis was performed based on Coefficient of Performance, Exergy Efficiency, and Total Plant Cost Rate. For the reference cooling capacities evaluated, the thermo-economic and environmental analysis indicated that the system with R290 has higher energy, exergy, environmental, and economic performance among the evaluated systems for the studied thermodynamic conditions. Therefore, the system operating with R290 is the most suitable to replace systems with R134a. Finally, analyzing the three cost rates related to Total Plant Cost Rate in each system for both reference cooling capacities analyzed, it was noted that the operational cost rate was the most relevant cost, while the penalty cost rate due to carbon dioxide emission was the least relevant cost.

**Keywords:** Thermo-economic and environmental analysis. Ecological refrigerants. Steady-state model. Vapor compression refrigeration system.

## RESUMO

Esta tese apresenta um modelo matemático de um sistema de refrigeração por compressão de vapor operando em regime permanente. Este modelo foi usado para projetar um sistema eficiente do ponto de vista energético, com baixo custo, que opera com o refrigerante ecológico mais adequado em termos de impacto ambiental global, concentrando-se nos refrigerantes R290, R600a, R744 e R1234yf. A análise ambiental foi realizada com base no Impacto Total de Aquecimento Equivalente, enquanto a análise termo-econômica foi realizada com base no Coeficiente de Performance, Eficiência Exergética e Taxa de Custo Total da Planta. Para as capacidades de refrigeração nominais avaliadas, a análise termo-econômica e ambiental indicou que o sistema com R290 apresenta maior desempenho energético, exergético, ambiental e econômico entre os sistemas avaliados para as condições termodinâmicas estudadas. Portanto, o sistema operando com R290 é o mais adequado para substituir sistemas com R134a. Por fim, analisando as três taxas de custo relacionadas à Taxa de Custo Total da Planta em cada sistema para as capacidades de refrigeração nominais analisadas, observou-se que a taxa de custo operacional foi o custo mais relevante, enquanto a taxa de custo de penalidade devido à emissão de dióxido de carbono foi o custo menos relevante.

**Palavras-chave:** Análise termo-econômica e ambiental. Refrigerantes ecológicos. Modelo estático. Sistema de refrigeração por compressão de vapor.



## LIST OF FIGURES

FIGURE 2.1 – The context historical of refrigeration from 1834 to the current scenario .. .....	25
FIGURE 2.2 – Published papers focusing the refrigerants R744, R290, R600a, R1270, R1234yf in Gustav Lorentzen Conference . .....	25
FIGURE 2.3 – Published papers focusing the refrigerants R744, R290, R600a, R1270, R1234yf in International Journal of Refrigeration. ....	26
FIGURE 2.4 – Schematic view of refrigeration system.....	27
FIGURE 2.5 – Schematic plant diagram. ....	28
FIGURE 2.6 – Refrigeration facility diagram. ....	29
FIGURE 2.7 – Schematic diagram of the experimental facility.....	30
FIGURE 3.1 – Scheme of the input and output variables of the model. ....	41
FIGURE 3.2 – Refrigerant plant layout under study.....	41
FIGURE 3.3 – Geometric characteristic of evaporator and condenser/gas cooler.....	42
FIGURE 3.4 – Subcritical refrigeration cycle: R290, R600a, R134a, R1234yf. ....	56
FIGURE 3.5 – Transcritical refrigeration cycle: R744 . ....	56
FIGURE 3.6 – Steps performed by the program to calculate the output variables. ....	58
FIGURE 4.1 – COP behavior for the VCRS as a function of $T_{\text{evap}}$ and $T_{\text{cond}}$ for $\dot{Q}_{\text{evap.ref}} =$ 0.5 kW .....	60
FIGURE 4.2 – COP behavior for the VCRS as a function of $T_{\text{evap}}$ and $T_{\text{cond/gc}}$ for $\dot{Q}_{\text{evap.ref}} =$ 1.2 kW. ....	61
FIGURE 4.3 - COP behavior for three different compression procedures as a function of $T_{\text{evap}}$ .....	62
FIGURE 4.4 - $\eta_{\text{exergy}}$ behavior for the VCRS as a function of $T_{\text{evap}}$ and $T_{\text{cond}}$ for $\dot{Q}_{\text{evap.ref}} =$ 0.5 kW. ....	64
FIGURE 4.5 – Exergy destruction (W) in each component of the VCRS and $\dot{E}_{\text{dest,total}}$ (W) for $\dot{Q}_{\text{evap.ref}} = 0.5\text{kW}$ , $T_{\text{evap}} = -3^{\circ}\text{C}$ and $T_{\text{cond}} = 45^{\circ}\text{C}$ .....	65
FIGURE 4.6 – Exergy destruction (W) in each component of the VCRS and $\dot{E}_{\text{dest,total}}$ (W) for $\dot{Q}_{\text{evap.ref}} = 0.5\text{kW}$ , $T_{\text{evap}} = -5^{\circ}\text{C}$ and $T_{\text{cond}} = 50^{\circ}\text{C}$ .....	65
FIGURE 4.7 - $\eta_{\text{exergy}}$ behavior for the VCRS as a function of $T_{\text{evap}}$ and $T_{\text{cond/gc}}$ for $\dot{Q}_{\text{evap.ref}} =$ 1.2kW .....	66

FIGURE 4.8 – Exergy destruction (W) in each component of the VCRS and $\dot{E}_{dest,total}$ (W) for $\dot{Q}_{evap.ref} = 1.2kW$ , $T_{evap} = -5^{\circ}C$ and $T_{cond/gc} = 45^{\circ}C$ .....	.67
FIGURE 4.9 – Exergy destruction (W) in each component of the VCRS and $\dot{E}_{dest,total}$ (W) for $\dot{Q}_{evap.ref} = 1.2kW$ , $T_{evap} = -3^{\circ}C$ and $T_{cond/gc} = 50^{\circ}C$ .....	.68
FIGURE 4.10 - $\eta_{exergy}$ behavior for two different compression procedures as a function of $T_{evap}$ .....	69
FIGURE 4.11 - TEWI behavior for the VCRS as a function of $T_{evap}$ and $T_{cond}$ for $\dot{Q}_{evap.ref} = 0.5 kW$ .....	70
FIGURE 4.12 - TEWI behavior for the VCRS as a function of $T_{evap}$ and $T_{cond/gc}$ for $\dot{Q}_{evap.ref} = 1.2 kW$ .....	71
FIGURE 4.13 - $\dot{C}_{total}$ behavior for the VCRS as a function of $T_{evap}$ and $T_{cond}$ for $\dot{Q}_{evap.ref} = 0.5 kW$ .....	73
FIGURE 4.14 - $\dot{C}_{total}$ behavior for the VCRS as a function of $T_{evap}$ and $T_{cond/gc}$ for $\dot{Q}_{evap.ref} = 1.2 kW$ .....	74
FIGURE 4.15 – $\dot{C}_{total}$ , $\dot{C}_{cm}$ , $\dot{C}_{op}$ , $\dot{C}_{env}$ ( <b>R\$/year</b> ) related to each system for $\dot{Q}_{evap.ref} = 0.5 kW$ , $T_{evap} = -3^{\circ}C$ and $T_{cond} = 45^{\circ}C$ .....	75
FIGURE 4.16 – $\dot{C}_{total}$ , $\dot{C}_{cm}$ , $\dot{C}_{op}$ , $\dot{C}_{env}$ ( <b>R\$/year</b> ) related to each system for $\dot{Q}_{evap.ref} = 1.2 kW$ , $T_{evap} = -3^{\circ}C$ and $T_{cond/gc} = 45^{\circ}C$ .....	76

## LIST OF TABLES

TABLE 1.1 – Papers on VCRS (vapor compression refrigeration system) operating with ecological refrigerants. ....	21
TABLE 1.2 – Papers on the economic viability of the VCRS with ecological refrigerants. ....	22
TABLE 2.1 – Relevant papers on VCRS operating with ecological refrigerants. ....	31
TABLE 2.2 – Correlations as a function of Nusselt number for internal and single-phase flow. ....	33
TABLE 2.3 – Main information about Shah’s (2017) correlation. ....	34
TABLE 2.4 – Flow regimes of the correlation proposed by Shah (2016).....	36
TABLE 2.5 – Hughmark correlation parameters. ....	37
TABLE 3.1 – Main properties of the selected refrigerants. ....	40
TABLE 3.2 – Compressors selected for reference cooling capacity of 0.5 kW.....	47
TABLE 3.3 – Compressors selected for reference cooling capacity of 1.2 kW.....	47
TABLE 3.4 – Global and volumetric efficiency curves for reference cooling capacity of 0.5kW. ....	47
TABLE 3.5 – Global and volumetric efficiency curves for reference cooling capacity of 1.2 kW. ....	48
TABLE 3.6 – Capital cost function of the main components. ....	53
TABLE 3.7 – Thermodynamic considerations adopted to perform the simulation. ....	55
TABLE 3.8 – Considerations for calculating of the TEWI parameter.....	57
TABLE 3.9 – Input parameters to calculate the Total plant cost rate. ....	57
TABLE 4.1 – TEWI values related to direct and indirect emissions. ....	72
TABLE 4.2 – Geometric, energy, exergy, economic and environmental characteristics of each evaluated system for $\dot{Q}_{\text{evap.ref}} = 0.5 \text{ kW}$ , $T_{\text{evap}} = -3^{\circ}\text{C}$ and $T_{\text{cond}} = 45^{\circ}\text{C}$ .....	77
TABLE 4.3 – Geometric, energy, exergy, economic and environmental characteristics of VCRS for $\dot{Q}_{\text{evap.ref}} = 1.2 \text{ kW}$ , $T_{\text{evap}} = -3^{\circ}\text{C}$ and $T_{\text{cond/gc}} = 45^{\circ}\text{C}$ .....	77
TABLE 4.4 – Values obtained for other variables for each evaluated system.....	78
TABLE 4.5 – Summary of the parameters compared in each refrigeration system analyzed ....	80

## ABBREVIATIONS

ASHRAE	American Society of Heating, Refrigerating and Air-Conditioning Engineers
COP	coefficient of performance [dimensionless]
ED	expansion device
EES	engineering equation solver
EEV	electronic expansion valve
GWP	global warming potential [dimensionless]
IEACS	indirect expansion air-conditioning system
LCCP	life cycle climate performance
ODP	ozone depletion potential [dimensionless]
TEV	thermostatic expansion valve
TEWI	total equivalent warming impact [kgco <sub>2</sub> ]
R134a	refrigerant also known as HFC-134a
R1234yf	refrigerant 2,3,3,3-Tetrafluoropropene
R1234ze	refrigerant 1,3,3,3-Tetrafluoropropene
R1270	code used to identify Propylene
R290	code used to identify Propane when used as refrigerant
R744	code used to identify carbon dioxide or CO <sub>2</sub> when used as refrigerant
R600a	code used to identify isobutane when used as refrigerant
VCRS	vapor compression refrigeration system
IHX	internal heat exchanger

## NOMENCLATURE

### Exceptions

$A_0, A_1, \dots, A_N$	generics constants, units vary throughout the text
$B_n$	generics constants (n= 1, 2, 3...)
$D_h$	hydraulic diameter [m]
$i_{lv}$	specific enthalpy of vaporization [kJ/kg]
$K_H$	Hughmark correlation parameter [dimensionless]
$R^2$	adjustment coefficient [dimensionless]
$Z_H$	Hughmark correlation parameter [dimensionless]

### Greek symbols

$A$	void fraction
$\alpha_{\text{recup}}$	refrigerant life recovery rate [%]
$\beta$	CO <sub>2</sub> emission factor [kgCO <sub>2</sub> /kWh]
$\Phi$	maintenance factor [dimensionless]
$k$	thermal conductivity [W/mK]
$\eta_{\text{exergy}}$	exergy efficiency [dimensionless]
$\eta_{\text{global}}$	compressor global efficiency [dimensionless]
$\eta_v$	compressor volumetric efficiency [dimensionless]
$\eta_{\text{pump}}$	pump overall efficiency [dimensionless]
$\mu$	dynamic viscosity [Pa · s]
$\rho$	density [kg/m <sup>3</sup> ]
$\sigma'$	surface tension [N/m]

$\gamma$	slip [dimensionless]
$\chi$	Martinelli parameter [dimensionless]
$\Delta P_{\text{cond/gc}}$	pressure drop on the waterside in the condenser/gas cooler [kPa]
$\Delta P_{\text{evap}}$	pressure drop on the waterside in the evaporator [kPa]
$\Delta T_{\text{ml}}$	logarithmic mean temperature difference [°C]
$\Delta T_{\text{sup}}$	superheating degree [°C]
$\Delta T_{\text{sub}}$	subcooling degree [°C]
$\dot{V}$	volumetric flow [m <sup>3</sup> /s]
$V_{\text{cil}}$	compressor displacement volume [m <sup>3</sup> ]
$\theta$	inclination [°]

### Latin symbols

A	area [m <sup>2</sup> ]
$C_{p_w}$	specific heat of water at constant pressure [kJ/kgK]
$C_{\text{CO}_2}$	unit damage cost of carbon dioxide emission [USD/kgCO <sub>2</sub> ]
$C_{\text{ele}}$	electricity unit cost
$\dot{C}_{\text{CM}}$	capital and maintenance cost rate [R\$/year]
$\dot{C}_{\text{env}}$	penalty cost rate due to CO <sub>2</sub> emission [R\$/year]
$\dot{C}_{\text{op}}$	operational cost rate [R\$/year]
$\dot{C}_{\text{total}}$	total plant cost rate [R\$/year]
CRF	capital recovery factor [dimensionless]
$C_{\text{comp}}$	capital cost function of the compressor
$C_{\text{cond/gc}}$	capital cost function of the condenser/gas cooler
$C_{\text{evap}}$	capital cost function of the evaporator

$C_{p;cond/gc}$	capital cost function of the pump related to the condenser/gas cooler circuit
$C_{p;evap}$	capital cost function of the pump related to the evaporator circuit
$C_{TEV}$	capital cost function of the thermostatic expansion valve
$D$	diameter [m]
$D_{oi}$	outer diameter of the inner tube [m]
$D_{REF}$	refrigerant diameter or inner diameter of the inner tube [m]
$D_W$	water diameter or inner diameter of the outer tube [m]
$E_{annual}$	annual electricity consumption of the equipment [kWh/year]
$\dot{E}_{dest,total}$	total exergy destruction [kW]
$\dot{E}_{dest}$	exergy destruction [kW]
$\dot{E}_X$	exergy of the flow [kW]
$F$	friction factor
$g$	gravitational acceleration [ $m/s^2$ ]
$G$	mass velocity [ $kg/m^2s$ ]
$H$	convective coefficient [ $W/m^2K$ ]
$\bar{h}_{ref}$	average convective coefficient of the refrigerant [ $W/m^2K$ ]
$\bar{h}_{w;cond/gc}$	average convective heat transfer coefficient of the water flowing through the condenser/gas cooler [ $W/m^2K$ ]
$\bar{h}_{w;evap}$	average convective heat transfer coefficient of the water flowing through the evaporator [ $W/m^2K$ ]
$I$	specific enthalpy [kJ/kg]
$iR$	interest rate [%]
$L_{HE}$	heat exchanger length [m]
$L_{pipe}$	pipe length [m]
$L_{total}$	total length of the pipe [m]

$L_{\text{rate}}$	annual rate of refrigerant emitted [%]
$L_{\text{time}}$	life of the refrigeration system [years]
$\dot{m}$	mass flow rate [kg/s]
$\dot{m}_{\text{ref}}$	refrigerant mass flow rate [kg/s]
$\dot{m}_{\text{w;cond/gc}}$	water mass flow rate at the condenser/gas cooler [kg/s]
$\dot{m}_{\text{w;evap}}$	water mass flow rate at the evaporator [kg/s]
$m_{\text{ref;HE}}$	refrigerant charge inside the heat exchanger [kg]
$m_{\text{ref;pipe}}$	refrigerant charge inside the pipe between components [kg]
$m_{\text{ref;total}}$	refrigerant charge of the system [kg]
$N$	rotation speed of the compressor [rpm]
$N$	refrigeration plant lifetime [years]
$P$	pressure [kPa]
$p_{\text{red}}$	reduced pressure [dimensionless]
$q$	heat flux [ $\text{W}/\text{m}^2$ ]
$\dot{Q}_{\text{evap}}$	cooling capacity [kW]
$\dot{Q}_{\text{evap.ref}}$	reference cooling capacity [kW]
$\dot{Q}_{\text{cond/gc}}$	heat transfer rate at the condenser/gas cooler [kW]
$R$	rugosity [m]
$r_p$	compressor pressure ratio [dimensionless]
$S$	entropy [kJ/kg K]
$T$	temperature [ $^{\circ}\text{C}$ ]
$\text{TEWI}$	total equivalent warming impact [ $\text{kgCO}_2$ ]
$\text{TEWI}_{\text{Direct}}$	TEWI due to direct emissions [ $\text{kgCO}_2$ ]
$\text{TEWI}_{\text{INDirect}}$	TEWI due to indirect emissions [ $\text{kgCO}_2$ ]



$T_{oper}$	refrigeration system daily operation time [h/day]
$T_{wci}$	water temperature at the condenser/gas cooler inlet [°C]
$T_{wco}$	water temperature at the condenser/gas cooler outlet [°C]
$T_{wi}$	water temperature at the evaporator inlet [°C]
$T_{wo}$	water temperature at the evaporator outlet [°C]
$U$	overall heat transfer coefficient [ $W/m^2K$ ]
$v$	vapor velocity [dimensionless]
$V$	velocity [m/s]
$V_{CW}$	chilled water volume [liters]
$V_{HW}$	hot water volume [liters]
$x$	vapor quality [dimensionless]
$Z$	position [m]
$\dot{W}_{pump,cond/gc}$	electrical power consumption by the pump in the condenser/gas cooler [kW]
$\dot{W}_{pump,evap}$	electrical power consumption by the pump in the evaporator [kW]
$\dot{W}_{comp}$	electrical power consumption in the compressor [kW]
$\dot{W}_{total}$	total electrical power consumption by the system [kW]

### **Dimensionless numbers**

$Bo$	Boiling number
$Co$	convection number
$Fr$	Froude number
$Nu$	Nusselt number
$Pr$	Prandtl number
$Re$	Reynolds number

$W_e$  Weber number

### Common subscripts

0 dead state

1 evaporator outlet

2 condenser/gas cooler inlet

3 condenser/gas cooler outlet

4 evaporator inlet

Cond/gc condenser or gas cooler/condensation or gas cooling

eq Equivalent

evap evaporator/evaporation

exp expansion device

hom Homogeneous

i Inner

L liquid phase

local Local

ref or REF Refrigerant

V vapor phase

# SUMMARY

<b>1. INTRODUCTION .....</b>	<b>21</b>
1.1. General objective .....	23
1.2. Specific objectives .....	23
<b>2. LITERATURE REVIEW .....</b>	<b>24</b>
2.1. Ecological refrigerants.....	24
2.2. Works in the literature on VCRS operating with ecological refrigerants.....	26
2.3. Convective heat transfer coefficients.....	32
2.3.1. Internal single-phase flow in circular section ducts .....	32
2.3.2. Internal two-phase flow in circular section ducts.....	33
2.3.2.1. Boiling heat transfer coefficient .....	34
2.3.2.2. Condensation heat transfer coefficient .....	35
2.3.2.3. Determination of void fraction .....	36
2.4. Environmental metrics for vapor compression refrigeration systems .....	37
2.5. Concluding remarks .....	38
<b>3. METHODOLOGY .....</b>	<b>40</b>
3.1. Ecological refrigerants selected for analysis .....	40
3.2. Mathematical modeling .....	40
3.3. Evaporator model.....	42
3.4. Condenser/gas cooler model.....	44
3.5. Compressor model .....	45
3.5.1 Commercial compressor selection for each refrigerant .....	46
3.6. Energy performance.....	49
3.7. Environmental performance .....	49
3.8. Exergy performance.....	52

3.9	Economic performance .....	53
3.10	Selection process of the commercial diameters .....	54
3.11	Simulation parameters .....	55
3.12	Model solution path .....	57
<b>4</b>	<b>RESULTS AND DISCUSSION.....</b>	<b>60</b>
4.1	Energy analysis .....	60
4.2	Exergy analysis .....	63
4.3	Environmental analysis.....	70
4.4	Economic analysis .....	73
<b>5</b>	<b>CONCLUSIONS.....</b>	<b>81</b>
	<b>REFERENCES .....</b>	<b>83</b>
	<b>APPENDIX A – R290 COMPRESSOR EFFICIENCY MAP DATA .....</b>	<b>89</b>
	<b>APPENDIX B – R134a COMPRESSOR EFFICIENCY MAP DATA .....</b>	<b>92</b>
	<b>APPENDIX C – R600a COMPRESSOR EFFICIENCY MAP DATA .....</b>	<b>94</b>
	<b>APPENDIX D – R1234yf COMPRESSOR EFFICIENCY MAP DATA.....</b>	<b>96</b>
	<b>APPENDIX E – R744 COMPRESSOR EFFICIENCY MAP DATA .....</b>	<b>98</b>
	<b>APPENDIX F – CATALOG CONCERNING THE GEOMETRIC ASPECTS OF COPPER TUBES USED IN THE SIMULATION.....</b>	<b>100</b>
	<b>APPENDIX G – METHOD USED TO SELECT OF COMMERCIAL DIAMETERS FOR EACH REFRIGERANT.....</b>	<b>101</b>

# 1. INTRODUCTION

Since the 1990s, vapor compression refrigeration systems operating with R134a have been widely used for heating (heat pump) and cooling (refrigerator) applications. According to Gill et al. (2019), these systems with R134a have high energy consumption and produce significant environmental impact due to high GWP. According to de Paula et al. (2020a), refrigerants with high GWP are classified as greenhouse gases. The control and elimination of these gases were proposed in the Kyoto protocol, and restrictions were reaffirmed in the Kigali amendment in 2016. Motivated by this imminent need to reformulate the old vapor compression refrigeration systems, several researches have carried out works oriented to develop energy-efficient vapor compression refrigeration systems that operate with ecological refrigerants (low GWP). Among these works, can be highlighted the following papers presented in Tab.1.1.

Table 1.1: Papers on VCRS (vapor compression refrigeration system) operating with ecological refrigerants.

Paper	Contribution of paper
de Paula et al. (2020a)	The authors developed a steady-state model of a VCRS that produces 1200 liters of chilled water (5°C) for an indirect expansion air-conditioning system and 600 liters of hot water (40°C) for bath. This model was used to compare the environmental, energy, and exergy performance of R290, R1234yf, R744 with R134a.
Faria et al. (2016)	The authors developed a dynamic model to investigate the behavior of the solar evaporator and expansion valve assembly of a heat pump operating with R744 under transient and steady operational conditions. The conditions analyzed were solar radiation, ambient temperature, wind speed, and atmosphere conditions.
Nunes et al. (2015)	The authors developed a steady-state model for a capillary tube of a heat pump operating with R744. Besides, the model was also used to determine the minimum diameter of the capillary tube for different conditions.
Duarte et al. (2019a)	The authors developed a steady-state model to select the most suitable refrigerant for direct expansion solar assisted heat pump. The parameters analyzed were COP, TEWI, environmental temperature, solar radiation and wind speed.
Rabelo et al. (2019a)	The authors developed a steady-state model and performed an experimental analysis to evaluate the influence of the expansion valve opening on the pressure, the power consumption of the compressor, COP, mass flow rate and difference of enthalpy of a small size solar assisted heat pump.
Sun et al. (2020)	The authors developed a steady-state model to investigate the energy and exergy performance of R513a as drop-in replacement for R134a. This paper examines the entire system operating zone to identify the performance differences in cooling capacity, COP, exergy destruction rate, and exergy efficiency between R513a and R134a systems.
Paulino et al. (2019)	The authors developed a dynamic model to analyze the evaporator response of a direct expansion solar assisted heat pump operating with R744 to sudden variations in the solar radiation through two strategies. The effects of solar radiation on evaporation temperature and superheating degree were analyzed.
de Paula et al. (2019)	The authors developed a steady-state model of a VCRS to compare the environmental and energy performance of the R1234yf with R134a.
Garcia et al. (2018)	The authors developed a dynamic model to evaluate the possibility of the R1234yf to be a drop-in replacement for a pre-designed VCRS with R134a. This paper includes the characterization of the control system.
Jarall S. (2012)	The author developed a steady-state model and performed an experimental analysis to investigate the energy performance of R1234yf as drop-in replacement for R134a. The analyzed parameters were COP, compressor efficiency, and evaporator cooling effect.
Sánchez et al. (2017)	The authors developed a steady-state model and performed an experimental analysis to evaluate the energy performance of R1234yf, R1234ze(E), R600a, R290, R152a as drop-in replacement for R134a. The evaluated parameters were COP, mass flow rate, power consumption, and discharge temperature.

As noted in Tab. 1.1, the strategy adopted by the authors to develop energy-efficient VCRS was to build mathematical models. In general terms, most of these papers developed steady-state models to compare the energy and/or exergy performance. In contrast, the minority of these papers developed dynamic models to determine the operational condition in which the proposed system operates with the highest efficiency.

Another essential factor in this process is economic viability. A system operating with ecological refrigerant should also have a competitive cost to become a good candidate to replace the old refrigeration systems with non-ecological refrigerants (high GWP). In recent years, some papers have been published in the literature focusing on the economic viability of these new systems. In this context, can be highlighted the following papers presented in Tab. 1.2.

Table 1.2: Papers on the economic viability of the VCRS with ecological refrigerants.

Paper	Parameters studies
Roy and Mandal (2019)	The authors developed a steady-state model to assess the energy, exergy, and economic performance of a VCRS operating with R152a, R600a, and R1234ze. This model used a multi-objective function to determine the optimum performance of the system for each refrigerant.
Fazelpour and Morosuk (2014)	The authors developed a theoretical model to assess the energy, exergy, and economic performance of a transcritical VCRS operating with R744.
Aminyavari et al. (2014)	The authors developed a model of a R744/R717 cascade VCRS to analyze energy, exergy, and economic performance. This model used a genetic algorithm technique to optimize the design parameters of the system.
Baakeem et al. (2018)	The authors developed a theoretical model to investigate the energy, exergy, and economic performance of a multistage VCRS operating with eight different fluids. This model used an optimization technique to maximize the COP of the system by varying four optimization variables.
Rabelo et al. (2019b)	The authors performed an economic analysis comparing the payback period of a heat pump operating with R290 and R134a on an electrical heater.
Karakurt et al. (2016)	The authors evaluated the effects of superheating and subcooling on the exergy and economic performance of a VCRS operating with different refrigerants (R152a, R134a, R290), operational conditions, heat exchangers effectiveness and isentropic efficiency.
Keshtkar and Talebizadeh (2019)	The authors developed a model to optimize a cascade VCRS operating with R744/R134a based on a thermo-economic analysis. The model used a genetic algorithm and a TOPSIS decision-making procedure with Pareto boundary to perform the optimization task.

In most of these studies, economic performance was calculated based on the total plant cost rate, and only some studies were based on other parameters, such as the payback time, as noted in Tab. 1.2. On the other hand, the authors did not evaluate the individual contribution of each cost rate linked to the total plant cost rate. This information is extremely relevant because it indicates the points that make the system more expensive. Also, these works did not quantify the overall environmental impact produced by their systems. This information is crucial to develop a system that operates with ecological

refrigerant because it clearly shows whether this system is adapted to replace an old system with non-ecological refrigerant.

Given this scenario, many studies still need to be carried out to develop designs energy-efficient refrigeration systems, economically viable, and that operate with ecological refrigerants. Therefore, to contribute to this current development, this doctoral thesis has the following objectives described below:

### **1.1. General objective**

The main goal of this thesis is to perform an energy, exergy, environmental and economic analysis of a vapor compression refrigeration system operating with different ecological refrigerants and a non-ecological refrigerant to determine the most suitable ecological refrigerant for the proposed system.

### **1.2. Specific objectives**

- To develop a mathematical model of a vapor compression refrigeration system operating under steady-state conditions.
- To check the following information regarding the VCRS in the literature: most studied ecological refrigerants in recent years, evaporation and condensation/gas cooling temperatures commonly adopted, and configurations used.
- To use commercial diameters to model the heat exchangers (evaporator and condenser/gas cooler) and volumetric and global efficiency curve obtained from commercial compressors available in the market.
- To quantify the overall environmental impact produced by the VCRS through Total Equivalent Warming Impact (TEWI).
- To perform a thermo-economic analysis of the VCRS using the Coefficient of performance (COP), Exergy Efficiency ( $\eta_{\text{exergy}}$ ) and total plant cost rate ( $\dot{C}_{\text{total}}$ ).
- To compare the TEWI, COP,  $\eta_{\text{exergy}}$  and  $\dot{C}_{\text{total}}$  of the VCRS operating with different ecological refrigerants and a non-ecological refrigerant.

## 2. LITERATURE REVIEW

In this chapter, the following information necessary for the development of the proposed steady-state model is presented: ecological refrigerants most studied in vapor compression refrigeration systems in recent years, thermodynamic condition used in these systems, correlations used to calculate the heat transfer coefficient by convection for single-phase and two-phase flow and the main topics analyzed in the steady-state models present in the literature.

### 2.1. Ecological refrigerants

In 1834, the Englishman Jacob Perkins developed and patented a vapor compression refrigeration system operating with ethyl ether to produce ice. However, this prototype began to be commercially designed only from the 1850s (Çengel and Boles, 2007). From the 1850s to the 1920s, natural refrigerants (R744, R717 and hydrocarbons) were predominantly used in vapor compression refrigeration systems, but the use of these refrigerants was drastically reduced from the 1930s due to the advent of synthetic refrigerants (CFCs and HCFCs).

From the 1930s to the mid-1980s, CFCs and HCFCs were used extensively in refrigeration and air conditioning systems. In the late 1980s, the international community established the Montreal protocol to eliminate these synthetic refrigerants due to their high ozone depletion potential (ODP). This high ODP index is related to the presence of the chlorine molecule in the structure of both CFCs and HCFCs. Thus, HFCs refrigerants were developed in the early 1990s, with HFC-134a being widely used in domestic refrigeration systems. These refrigerants have a null ODP and do not contain the chlorine molecule in their structure. However, in the late 1990s, the international community established the Kyoto protocol to control and phase out HFCs over the years due to their high global warming potential (GWP).

From the mid-2010s, the 21<sup>st</sup> United Nations Climate Change Conference and Kigali amendment proposed regulations to accelerate the elimination process of these refrigerants with high GWP, termed as non-ecological refrigerants. Therefore, the current scenario is marked by the search for ecological refrigerants (low GWP) to replace non-ecological refrigerants. This historical context of refrigeration described above is presented in the timeline shown in FIG. 2.1.



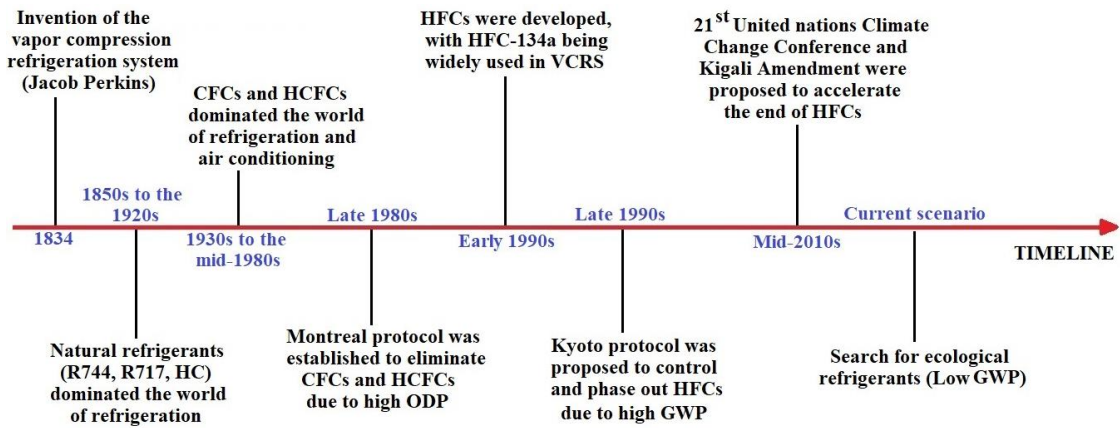


FIGURE 2.1: Historical context of refrigeration from 1834 to the current scenario.

To identify the ecological refrigerants (low GWP and null ODP) most used in VCRS in recent years, some works presented in the Gustav Lorentzen Conference on natural refrigerants and the International Journal of Refrigeration were evaluated. FIG. 2.2 shows the published papers in the Gustav Lorentzen Conference from 2000 to 2018. The published articles in the International Journal of Refrigeration in the period from 2009 to 2018 are presented in FIG. 2.3.

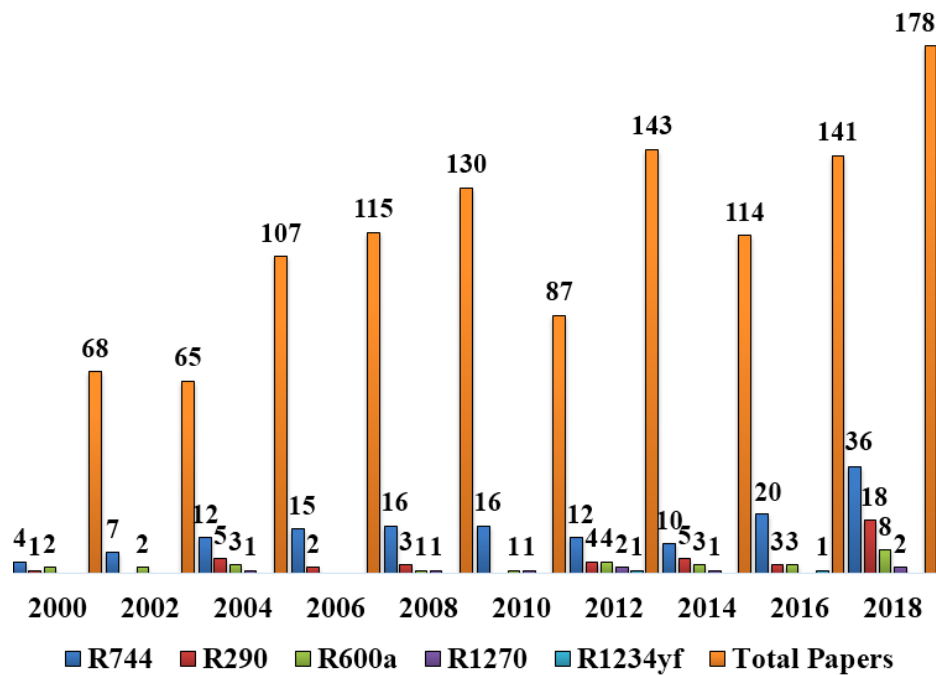


FIGURE 2.2: Published papers focusing the refrigerants R744, R290, R600a, R1270, R1234yf in Gustav Lorentzen Conference.

SOURCE: de Paula et. al (2020a, p.12).

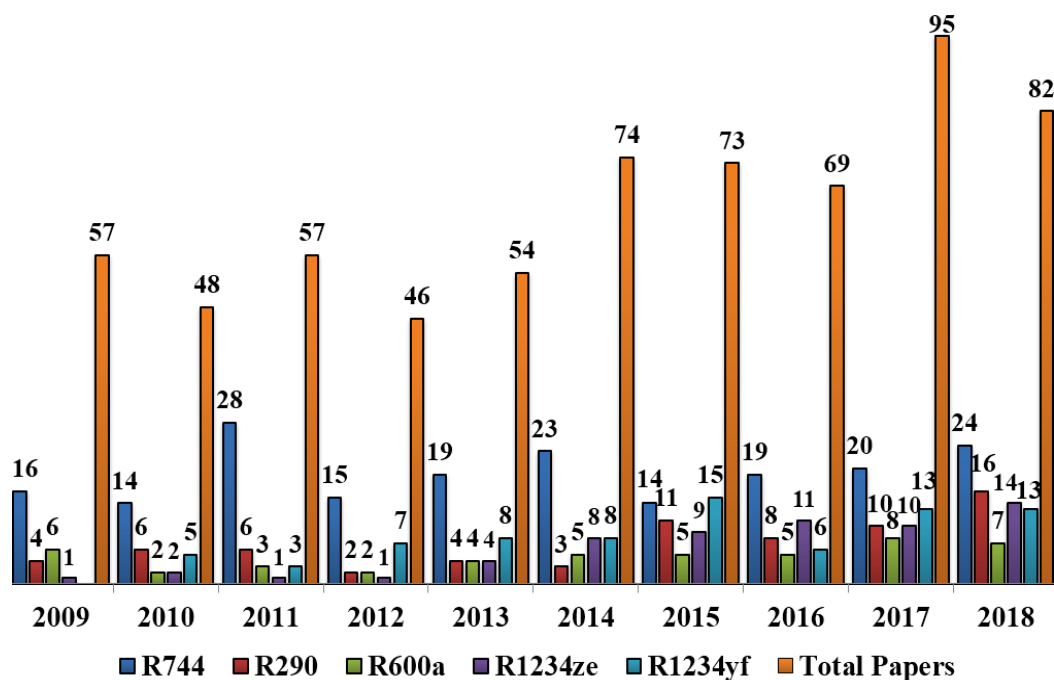


FIGURE 2.3: Published papers focusing the refrigerants R744, R290, R600a, R1234ze, R1234yf in International Journal of Refrigeration.

SOURCE: de Paula et. al (2020a, p.12).

By analyzing the data presented in FIG. 2.2 and FIG. 2.3, it is noted that the ecological refrigerants commonly evaluated in both situations are carbon dioxide (R744), propane (R290), isobutane (R600a) and hydrofluorolefins (R1234yf). It is observed that the interest in these ecological refrigerants has been gradually increasing in recent years. Among the mentioned refrigerants, R744 is the most studied while the others are less especially R600a. However, it is also noted that the number of papers focusing on these refrigerants is still a topic little examined in the literature in relation to the total number of papers.

## 2.2. Works in the literature on VCRS operating with ecological refrigerants

For VCRS operating with R290, R600a, R744, and R1234yf, an extensive research was performed. Information regarding configuration type, ranges considered for volumetric and global efficiency, COP, evaporation and condensation/gas cooling temperatures, cooling capacity, and the expansion device type used, were extracted from the most relevant papers found.

Jarall S. (2012) carried out a theoretical and experimental study of a VCRS with R1234yf. A schematic view of this system can be seen in FIG 2.4. In this system, the

evaporator and the condenser are plate-type heat exchangers, the compressor is hermetic and rotary, and its expansion device is a thermostatic expansion valve (TEV).

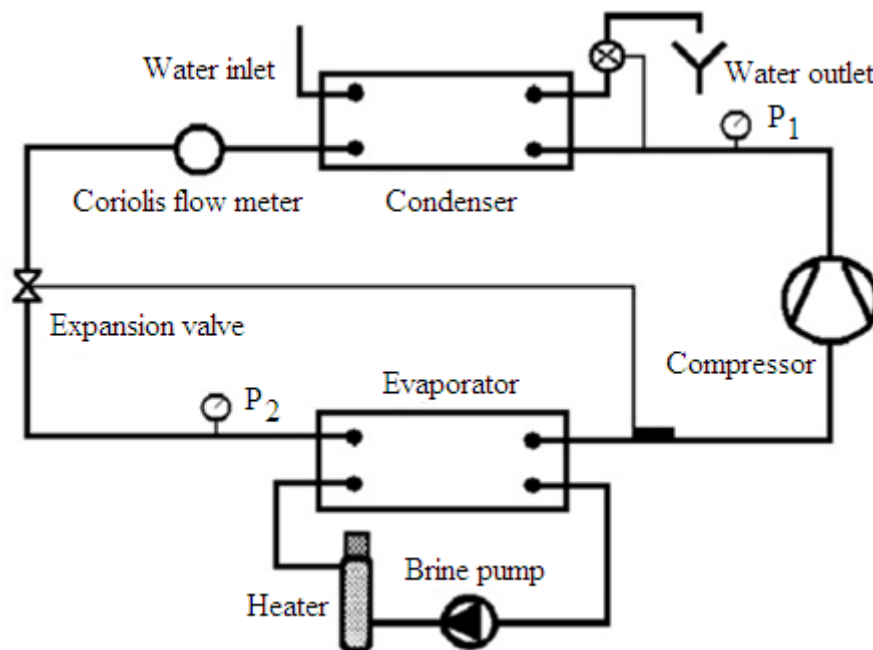


FIGURE 2.4 – Schematic view of refrigeration system.  
SOURCE – Jarall S. (2012, p. 1672).

First, the global efficiency of the compressor was evaluated for two different condensation temperatures ( $40^{\circ}\text{C}$  and  $45^{\circ}\text{C}$ ) with the evaporation temperature ranging from  $-8^{\circ}\text{C}$  to  $15.5^{\circ}\text{C}$ . The results show that the global efficiency varies from 44.53% to 47.62% and 44.69% to 50.09% for the condensation temperature of  $40^{\circ}\text{C}$  and  $45^{\circ}\text{C}$ , respectively. Subsequently, the cooling capacity, COP, and global efficiency were compared for the system operating with R1234yf and R134a considering the same condensation temperature but varying the evaporation temperature used. The experimental results indicate that the system operating with R1234yf obtained a lower value of cooling capacity, COP, and global efficiency. These results occur because this system has lower enthalpy variation in the evaporator and greater electrical power consumption in the compressor.

Navarro Esbrí et al. (2013) performed an experimental study in a system operating with R134a and R1234yf, in order to compare the cooling capacity, COP, and the volumetric efficiency of the compressor. The plant consists of the following components: a shell-and-tube evaporator (refrigerant flows inside the tubes/water-propylene glycol mixture flows through along the shell), a shell-and-tube condenser (refrigerant flows along the shell/water flows inside the tubes), a reciprocating compressor, an internal tube-

in-tube heat exchanger (IHX) and a thermostatic expansion valve (TEV), as shown in FIG. 2.5.

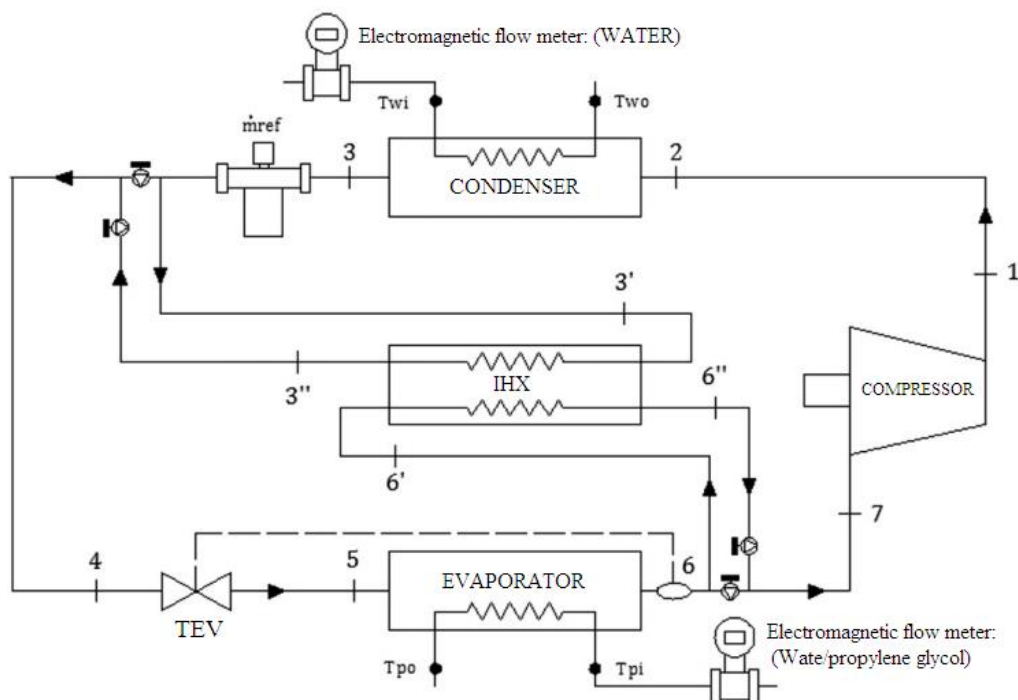


FIGURE 2.5 – Schematic plant diagram.  
SOURCE – Navarro Esbrí et al. (2013, p.872).

Experimental tests were performed varying the evaporation and condensation temperatures, the superheating degree, the rotation speed of the compressor, and the internal heat exchanger use. The results show that the cooling capacity of the system operating with R1234yf is about 9% lower than with R134a, this result may be related to lower enthalpy variation in the evaporator of the system with R1234yf. However, this percentage difference in cooling capacity decreased with the increase in the condensation temperature and with the use of the internal heat exchanger. It was also noted that the compressor operating with the R1234yf obtained a volumetric efficiency 5% lower compared to the value obtained with the R134a. Finally, the COP values for the system working with R1234yf were 5% to 30% lower than the values obtained with the system operating with R134a due to the higher electrical power consumption in the compressor of the system with R1234yf.

Sánchez et al. (2017) compared five low GWP refrigerants to replace the R134a for the same refrigeration facility and under the same conditions. The refrigerants were used without any change in the facility, and it consisted of the following components: a hermetic and reciprocating compressor with displacement volume of 12.11 cm<sup>3</sup>, an

evaporator, and a condenser, both brazed plate type, and an electronic expansion valve (EEV), as shown in FIG. 2.6.

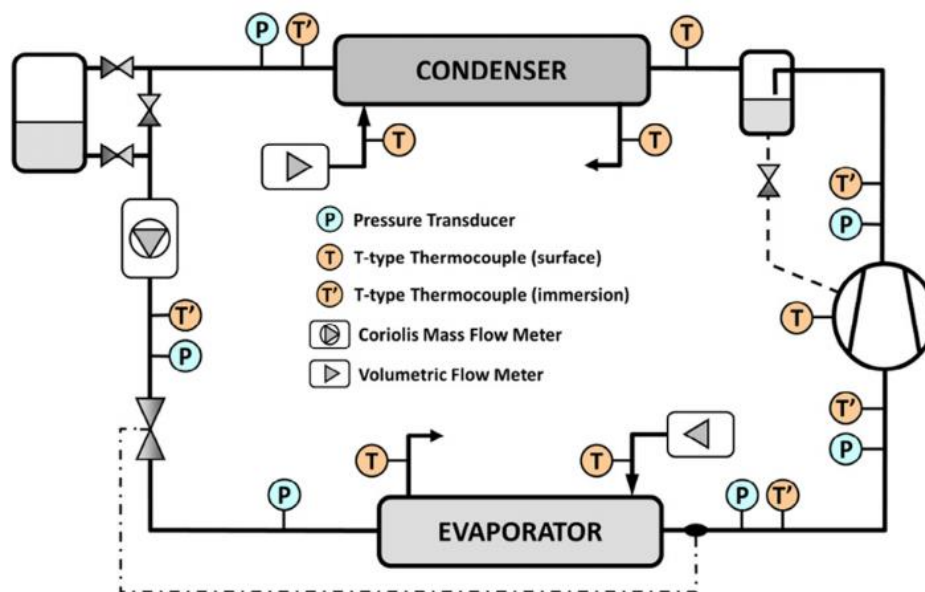


FIGURE 2.6 – Refrigeration facility diagram.  
SOURCE – Sánchez et al. (2017, p. 272).

The ecological refrigerants used were R290, R600a, R1234yf, R1234ze, and R152a. The experimental tests were carried out considering different operating conditions, two evaporation temperatures ( $0^{\circ}\text{C}$  and  $-10^{\circ}\text{C}$ ) and three condensation temperatures ( $25^{\circ}\text{C}$ ,  $35^{\circ}\text{C}$ , and  $45^{\circ}\text{C}$ ), and the mass introduced by each of the refrigerants in the system was 900g. Based on the experimental results and focusing only on the energy performance of the refrigeration cycle, the authors concluded that among the refrigerants tested, the most appropriate to perform the drop-in procedure in the studied installation were R1234yf and R152a because the system operating with these refrigerants did not need to make changes in its structure and the COP value in these situations did not present significant variations in relation to the COP value of the system operating with R1234yf.

Antunes and Bandarra Filho (2016) experimentally investigated the drop-in procedure for the following refrigerant fluids in a 5 TR refrigeration system: R438A, R404A, R410A, R32, R290, and R1270 to choose among the selected refrigerants the best substitute for R22. This experimental facility consists of a semi-hermetic reciprocating compressor, an evaporator, and a condenser, both heat exchangers of concentric-tube type, and an electronic expansion valve. A schematic diagram of this apparatus can be seen in FIG. 2.7.

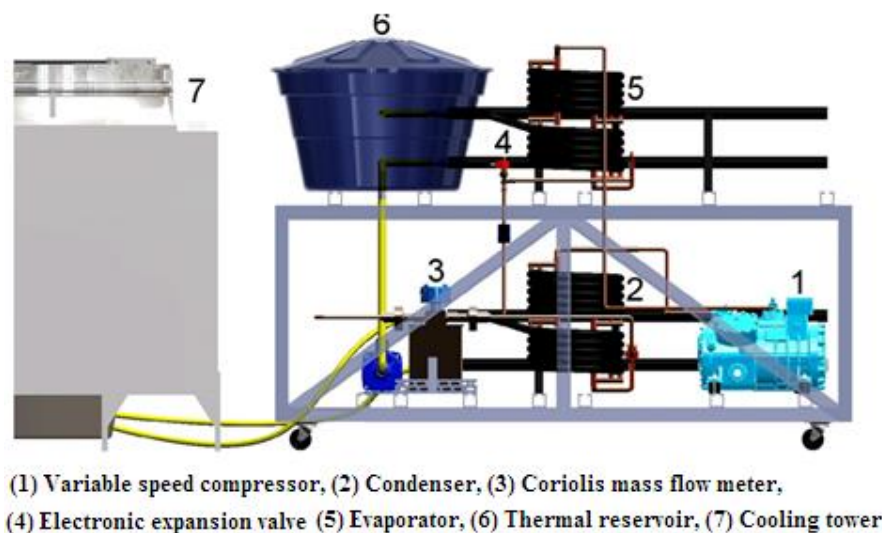


FIGURE 2.7 – Schematic diagram of the experimental facility.  
SOURCE – Antunes and Bandarra Filho (2016, p.121).

The tests were carried out in a steady-state regime, and the refrigerant fluids were replaced directly in the system, without causing any type of change in the system. The refrigerants were evaluated for three different evaporation temperatures ( $-15^{\circ}\text{C}$ ,  $-10^{\circ}\text{C}$  and  $-5^{\circ}\text{C}$ ), where the following parameters were determined: cooling capacity, power consumption, mass flow rate, COP and TEWI. Comparing the fluids for the same evaporation temperature and cooling capacity, the results show that the refrigerants (R290 and R1270) presented the highest values for the COP. The environmental impacts caused by these fluids in Brazil and in the United States were analyzed based on the TEWI parameter. This parameter is an environmental metric that has been applied in recent work on refrigeration systems. The function of TEWI is to indicate among a universe of tested fluids, which is the refrigerant that allows the system to produce the least possible environmental impact. The results show that R290 and R1270 are the most environmentally friendly fluids, with R1270 being the best.

Rigola et al. (2010) performed a numerical and experimental analysis of a vapor compression refrigeration system operating with carbon dioxide (R744). This system consists of an evaporator, a gas cooler and an internal heat exchanger of concentric-tube type, a thermostatic expansion valve and a semi-hermetic reciprocating compressor. This study evaluated the use of the internal heat exchanger (IHX) to improve the Coefficient of Performance (COP) and to verify the influence of the size of the IHE on the COP. The numerical results show that the system with an ambient temperature of  $35^{\circ}\text{C}$ , a pressure of 100 bar in the gas cooler and an IHX with 2 m, the COP obtained an increase of 23%

in relation to the system without IHX. The authors also noted that by increasing the IHX size from 2 m to 4.5 m, the COP increased by 3%. The main information described by these works is presented in Tab. 2.1.

TABLE 2.1: Some papers on VCRS operating with ecological refrigerants in recent years.

Paper	Refrigerant	T <sub>evap</sub> (°C)	T <sub>cond/gc</sub> (°C)	Q̇ <sub>evap</sub> (kW)	COP	Evap//Cond/gc Configuration	η <sub>v</sub> (%)	η <sub>global</sub> (%)	E.D
Jarall S. (2012)	R1234yf	- 7.3 to 14.7	45	0.91 to 2.08	1.86 to 3.95	Plate	---	45 to 50	TEV
	R134a	-5.4 to 15.3	45	1.04 to 2.47	2.01 to 4.64		---	45 to 56	
Navarro Esbrí et al. (2013)	R1234yf	-7.5 to 7.5	40 to 60	6.8 to 17	2.2 to 7.6	Shell and tube	58 to 77	---	TEV
	R134a	-7.5 to 7.5	40 to 60	8.0 to 18.1	2.7 to 7.3		58 to 82	---	
Sánchez et al. (2017)	R1234yf	0 to - 10	25 to 45	0.49 to 0.98	1.37 to 2.57	Brazen plate	66 to 75	28 to 42	EEV
	R1234ze(E)			0.40 to 0.77	1.41 to 2.63		66 to 76	28 to 39	
	R600a			0.29 to 0.60	1.31 to 2.69		71 to 80	28 to 37	
	R290			0.77 to 1.52	1.58 to 3.40		71 to 81	37 to 45	
	R152a			0.50 to 0.95	1.58 to 3.00		67 to 77	32 to 42	
	R134a			0.52 to 1.03	1.54 to 2.88		66 to 76	31 to 41	
Antunes and Bandarra filho (2016)	R22	-15 -10 -5	32.7 34.0 36.7	6.17 7.53 9.04	2.63 2.93 3.12	Concentric- tube	---	---	EEV
	R290		34.7 37.8 39.5	6.08 7.48 8.95	2.89 3.21 3.58		---	---	
	R1270		32.1 33.9 35.9	6.20 7.48 8.99	3.16 3.53 3.88		---	---	
	R438A		31.8 34.7 37.2	6.23 7.49 8.95	2.51 2.64 2.75		---	---	
	R404A		42.1 43.5 43.9	6.16 7.53 8.97	2.25 2.41 2.57		---	---	
	R410A		32.6 32.7 32.8	6.19 7.58 9.01	2.25 2.56 2.70		---	---	
	R32		31.3 31.6 31.7	6.24 7.61 8.86	2.46 2.71 2.89		---	---	
Rigola et al. (2010)	R744	-5	30	0.89 to 0.90	0.9 to 1.3	Concentric- tube	69 to 82	49 to 56	TEV

In general, the following factors can be observed: the condensation/gas cooling and evaporation temperature of most works is within the following range: 40°C to 60°C and -7.5°C to 15°C, respectively. Most of the vapor compression refrigeration systems analyzed have low cooling capacity. In addition, almost all of these systems use a thermostatic expansion valve (TEV).

In subsections 2.1 and 2.2, a series of information was presented regarding the VCRS studied in recent years. Among the components mentioned are the evaporator and the condenser/gas cooler, parts responsible for performing the thermal exchanges between the refrigerant and the secondary fluid in the low and high-pressure zone, respectively. An important parameter involved in thermal exchanges is the heat transfer coefficient by convection, whose behavior depends on the type of flow (single-phase or two-phase). In practice, the evaporator and the condenser have both types of flow. Thus, it is necessary to know the correlations for each specific situation, as presented in the next subsection.

### **2.3. Convective Heat Transfer Coefficients**

For each type of flow, there are many correlations available in the literature to calculate the convective heat transfer coefficient. However, it is not the focus of this thesis to present all these correlations. Thus, this subsection has as main objective to present the correlations used in the simulations to calculate the convective heat transfer coefficient for the single-phase and two-phase flow region.

#### **2.3.1. Internal single-phase flow in circular section ducts**

In horizontal circular section tubes, the critical Reynolds ( $Re_{crit}$ ) number is 2300 and the flow is considered fully turbulent for values above  $10^4$ . In this thesis, both for the laminar and turbulent flow regimes, the correlations used to determine the convective heat transfer coefficient for an internal single-phase flow are shown in Tab.2.2.



TABLE 2.2: Correlations used to determine convective heat transfer coefficient for an internal single-phase flow for the laminar and turbulent flow regimes.

	Correlation / Value	Conditions of use	Identification	Reference
Laminar	$Nu = 4.36$	Constant heat flow,	(2.1)	Bergman et al. (2011)
Turbulent	$Nu = 0.023 \cdot Re^{0.8} Pr^{0.4}$	Heating $0.7 \leq Pr \leq 160$ $Re \geq 10000$ $L/D \geq 10$	Dittus-Boelter (2.2)	Bergman et al. (2011)
	$Nu = 0.023 \cdot Re^{0.8} Pr^{0.3}$	Cooling $0.7 \leq Pr \leq 160$ $Re \geq 10000$ $L/D \geq 10$	Dittus-Boelter (2.3)	Bergman et al. (2011)
	$Nu = \frac{(f/8) \cdot (Re - 1000) Pr}{1 + 12.7(f/8)^{0.5} (Pr^{2/3} - 1)}$	$0.5 \leq Pr \leq 2000$ $3000 \leq Re \leq 5 \times 10^6$	Gnielinski (2.4)	Bergman et al. (2011)

Where L is the pipe length, h is the heat transfer coefficient by convection, D is the diameter, k is the thermal conductivity, Pr is the Prandlt number,  $\mu$  is the dynamic viscosity, and  $f$  is the friction factor. Duarte (2018) states that the correlation proposed by Churchill (1977), EQ. (2.5), has been the most used to calculate the factor  $f$ , both for laminar and turbulent flow. Where  $r$  represents the roughness.

$$f = 2 \left[ \left( \frac{8}{Re} \right)^{12} + \frac{1}{(A_0)^{1.5}} \right]^{1/12} \quad (2.5)$$

$$A_0 = \left\{ 2.2088 + 2.457 \cdot \ln \left[ \frac{r}{D} + \frac{42.683}{Re^{0.9}} \right] \right\}^{16} + \left( \frac{37530}{Re} \right)^{16} \quad (2.6)$$

### 2.3.2. Internal two-phase flow in circular section ducts

The transport mechanism in a two-phase flow depends on the flow pattern. In two-phase flows, the quality ( $x$ ) is defined by the ratio between the vapor mass flow rate ( $\dot{m}_v$ ) and the sum of the vapor mass flow rate and liquid mass flow rate ( $\dot{m}_L$ ), EQ. (2.7):

$$x = \frac{\dot{m}_v}{\dot{m}_L + \dot{m}_v} = \frac{\dot{m}_v}{\dot{m}} \quad (2.7)$$

The void fraction ( $\alpha$ ) is the ratio between the area through which the vapor flows ( $A_v$ ) and the area occupied by mixture (A), given by EQ. (2.8):

$$\alpha = \frac{A_v}{A_L + A_v} = \frac{A_v}{A} \quad (2.8)$$

The velocities of the vapor phase ( $V_v$ ) and the liquid phase ( $V_L$ ) are determined by EQ. (2.9), and the ratio between these velocities is called slip ( $\gamma$ ) and is given by EQ. (2.10).

$$V_v = \frac{\dot{m}_v}{\rho_v \cdot A_v} = \frac{\dot{V}_v}{A_v} \text{ and } V_L = \frac{\dot{m}_L}{\rho_L \cdot A_L} = \frac{\dot{V}_L}{A_L} \quad (2.9)$$

$$\gamma = \frac{V_v}{V_L} \quad (2.10)$$

Where ( $\rho_v$ ) is the vapor phase density, ( $\rho_L$ ) is the liquid phase density and ( $\dot{V}_L$ ) is the volumetric flow of the liquid phase. The Martinelli parameter ( $\chi$ ) relates the pressure variation in the direction of flow in each phase ( $\partial P/\partial z$ ), and is defined by Rohsenow, Hartnett, Cho, et al. (1998), as presented in EQ. (2.11):

$$\chi = \sqrt{\frac{(\partial P/\partial z)_L}{(\partial P/\partial z)_v}} \cong \left(\frac{1-x}{x}\right)^{0.9} \left(\frac{\rho_v}{\rho_L}\right)^{0.5} \left(\frac{\mu_L}{\mu_v}\right)^{0.1} \quad (2.11)$$

### 2.3.2.1. Boiling heat transfer coefficient

In this thesis, the evaporator used was a concentric tubes type, with the refrigerant flowing through the inner tube, and the water counterflowing through the annular space. The convective heat transfer coefficient of the refrigerant during boiling was determined by the correlation developed by Shah (2017). This correlation was evaluated by Duarte (2018). Shah (2017) corresponds to an update of Shah (1982) correlation. In Shah (2017), 4852 experimental data points from 81 sources for 30 different fluids were used, as can be seen in Tab. 2.3.

TABLE 2.3: Main information about Shah (2017) correlation.

Experimental data points	4852
Data sources	81
Number of fluids evaluated	30
Mass velocity (kg/m <sup>2</sup> s)	15-2437
Diameter (mm)	0.38-27.1

$$h = MAX \begin{cases} 1.8 \cdot B_1^{-0.8} B_3 h_L \\ 230 \cdot B_0^{0.5} B_3 h_L \\ B_2 B_0^{0.5} \exp(2.74 B_1^{-0.10}) B_3 h_L \\ B_2 B_0^{0.5} \exp(2.74 B_1^{-0.15}) B_3 h_L \end{cases} \quad (2.12)$$

$$B_1 = \begin{cases} C_o, & \text{If horizontal with tubes } Fr_L \geq 0.04 \text{ or vertical tubes} \\ 0.38 C_o Fr_L^{-0.3}, & \text{If horizontal tubes with } Fr_L < 0.04 \end{cases} \quad (2.13)$$

$$B_2 = \begin{cases} 14.7, & Bo \geq 0.0011 \\ 15.4, & Bo < 0.0011 \end{cases} \quad (2.14)$$

$$B_3 = \begin{cases} 2.1 - 0.008 \cdot W_{ev} - 110 \cdot Bo, & B_3 \geq 1 \\ 1, & B_3 < 1 \text{ or } Fr_L < 0.01 \end{cases} \quad (2.15)$$

Where  $h_L$  is the convective heat transfer coefficient of the liquid phase determined by EQ. (2.16),  $Fr_L$  is the Froud number given by EQ. (2.17),  $Co$  is the convection number given by EQ. (2.18),  $W_{ev}$  is the Weber number given by EQ. (2.19) and the  $Bo$  is the boiling number calculated by EQ. (2.20).

$$Nu = \frac{h D_i}{k} = 0.023 \cdot Re^{0.8} \cdot Pr^{0.4} \quad (2.16)$$

$$Fr_L = \frac{G^2}{\rho_L^2 \cdot g \cdot D_i} \quad (2.17)$$

$$Co = \left( \frac{1-x}{x} \right)^{0.8} \left( \frac{\rho_V}{\rho_L} \right)^{0.5} \quad (2.18)$$

$$W_{ev} = \frac{G^2 \cdot D_i}{\rho_V \cdot \sigma'} \quad (2.19)$$

$$Bo = \frac{q}{G \cdot i_{lv}} \quad (2.20)$$

The terms  $i_{lv}$ ,  $q$ ,  $\sigma'$  e  $G$  are vaporization enthalpy, heat flux, surface tension and mass velocity, respectively.

### 2.3.2.2. Condensation heat transfer coefficient

The condenser used was also a concentric tubes type, with the refrigerant flowing through the inner tube, and the water counterflowing through the annular space. The convective heat transfer coefficient of the refrigerant during condensation was determined using the relations proposed by Shah (2016), represented by EQ. (2.21) to EQ. (2.24), for

flow regimes I, II, and III. This correlation was also used by Duarte (2018). The ranges that occurs the regime I and III are presented in Tab. 2.4.

$$h_I = h_L \left( 1 + \frac{3.8}{B_1^{0.95}} \right) \left( \frac{\mu_L}{14 \cdot \mu_V} \right)^{0.0058 + 0.557 \cdot Pr} \quad (2.21)$$

$$h_{II} = h_I + h_{III} \quad (2.22)$$

$$h_{III} = 1.32 \cdot Re_L^{-1/3} \left[ \frac{\rho_L \cdot (\rho_L - \rho_V) \cdot g \cdot k_L^3}{\mu_L^2} \right]^{(1/3)} \quad (2.23)$$

$$B_1 = p_{red}^{0.4} \left( \frac{1}{1-x} \right)^{0.8} \quad (2.24)$$

In which  $h_L$  is the convective heat transfer coefficient of the liquid phase determined by EQ. (2.16) and  $Re_L$  is the Reynolds number of the liquid phase determined by EQ. (2.25).

$$Re_L = \frac{G \cdot (1-x) \cdot D_i}{\mu_L} \quad (2.25)$$

If the Regime is neither I nor III by the criteria bellow, it is Regime II. The number Weber ( $W_{ev}$ ) and dimensionless vapor velocity ( $v$ ) are calculated by EQ. (2.19) and EQ. (2.26), respectively.

$$v = \frac{x \cdot G}{(g \cdot D \cdot \rho_V \cdot (\rho_L - \rho_V))^{0.5}} \quad (2.26)$$

TABLE 2.4: Flow regimes of the correlation proposed by Shah (2016).

	Horizontal Flow	Vertical Flow
Regime I	$W_{ev} > 100$ and $v \geq 0.98(B_1 + 0.263)^{-0.62}$	$W_{ev} > 100$ and $v \geq (0.73 + 2.4B_1)^{-1}$
Regime III	$W_{ev} > 20$ and $v \leq 0.92(1.254 + 2.27B_1^{1.249})^{-1}$	$W_{ev} > 20$ and $v \leq 0.89 - 0.93 \exp(-0.087B_1^{-1.17})$

This correlation was compared with 4063 experimental data points from 67 different sources, and an absolute mean deviation from this correlation is 17%. In these experimental data, the range of available diameter is from 0.10 to 49 mm and the mass velocity from 1.1 to 1400 kg/(m<sup>2</sup>s).

### 2.3.2.3. Determination of void fraction

Machado, Haberschill, and Lallemand (1998) analyzed the behavior of the refrigerant charge inside an evaporator operating in both steady-state and transient regimes. The authors calculated the void fraction using three different correlations, and

the results indicated Hughmark (1962) correlation as the most appropriate to determine this parameter. Humia (2017) carried out a series of theoretical and experimental studies evaluating refrigeration systems operating with R134a and R1234yf. In these studies, the author used eight different correlations to determine the void fraction and also indicated Hughmark (1962) correlation as the most appropriate. Based on the results presented by these studies, the void fraction was determined by the correlation of Hughmark (1962) in this thesis. This correlation is defined by EQ. (2.27). Note that the  $K_H$  values are shown in Table 2.5 as a function of the  $Z_H$  parameter calculated by EQ. (2.28) iteratively.

$$\alpha = \frac{K_H}{1 + (1 + x) \frac{\rho_v}{\rho_L}} = K_H \alpha_{hom} \quad (2.27)$$

$$Z_H = \left[ \frac{D_i G}{\mu_L + \alpha(\mu_v - \mu_L)} \right]^{\frac{1}{6}} \left\{ \frac{1}{D_i g} \left[ \frac{Gx}{\rho_v \alpha_{hom} (1 - \alpha_{hom})} \right]^2 \right\}^{1/8} \quad (2.28)$$

TABLE 2.5: Hughmark correlation parameters.

$Z_H$	$K_H$	$Z_H$	$K_H$
1.3	0.185	8.0	0.767
1.5	0.225	10	0.780
2.0	0.325	15	0.808
3.0	0.490	20	0.830
4.0	0.605	40	0.880
5.0	0.675	70	0.930
6.0	0.720	130	0.980

SOURCE – Machado (1996, p. 36).

## 2.4. Environmental metrics for vapor compression refrigeration systems

To mitigate the environmental impact produced by old refrigeration facilities in recent decades, vapor compression refrigeration systems that operate with ecological refrigerants are being developed. The environmental metrics commonly used in the selection process of an ecological refrigerant are the global warming potential (GWP), total equivalent warming impact (TEWI), and the life cycle climate performance (LCCP), according to Makhnatch and Khodabandeh (2014).

GWP is an index whose value is established based on the comparison of the environmental impact produced by the emission of greenhouse gas for 100 years in relation to the effect produced by the emission of a similar amount of  $\text{CO}_2$  during the

same time. The lowest GWP value corresponds to the lowest the contribution of a substance to the global warming phenomenon.

LCCP is a metric that accounts for the environmental impacts produced by the refrigeration system due to direct and indirect emissions. Direct emission is related to refrigerant leakage over the lifespan of the system. However, the reference GWP used in this calculation is the sum of the refrigerant's GWP with an equivalent GWP related to the atmospheric degradation product of the refrigerant. Finally, indirect emission is related to the environmental impact due to emissions from energy consumption, manufacturing of materials, manufacturing of refrigerant and disposal of unit, according to Choi et al. (2017).

TEWI is an environmental metric similar to LCCP. It measures of the combined overall environmental impacts due to refrigerant losses to the atmosphere and CO<sub>2</sub> emissions from fossil fuels to generate power to run the refrigeration and air-conditioning systems (Fisher, 1993). Therefore, this parameter also considers both direct emissions (due to refrigerant leakage during the lifespan of the equipment) and indirect emissions (due to the compressor's electricity consumption over the lifespan of the equipment). Direct emission is intrinsically related to the GWP of the refrigerant while indirect emission is related to the electrical power consumption in the compressor ( $\dot{W}_{\text{comp}}$ ) and the electrical power consumption by the pump in the evaporator and condenser/gas cooler ( $\dot{W}_{\text{pump;evap}}$ ,  $\dot{W}_{\text{pump;cond/gc}}$ ) in this context of this thesis.

Based on Makhnatch and Khodabandeh (2014), GWP is a useful metric for comparing different refrigerants. Still, its main disadvantage is that it can overestimate the benefits of refrigerant with low GWP, since it does not consider other factors that also contribute to increasing the environmental impact of the system. The authors state that in practice the use of LCCP is complex due to the difficulty found in obtaining all information during the production and transport process of the refrigerant. Finally, TEWI is the most suitable metric because it is easier to apply than LCCP and more complete than GWP.

## 2.5. Concluding remarks

In this chapter, it was shown that ecological refrigerants have been gradually more studied over the years due to the high environmental impact produced by refrigeration systems operating with non-ecological refrigerants (high GWP). The ecological

refrigerants that have attracted the most interest are R744, R1234yf, R290, and R600a. However, it is noted that the thermo-economic and environmental performance of a refrigeration system operating with these refrigerants is still little examined.

In order to analyze and comparing the behavior of a refrigeration system operating with the mentioned refrigerants, some works were evaluated and their thermodynamic characteristics determined. The following aspects were observed: the condensation/gas cooling temperature ranges from 40°C to 60°C and evaporation temperature ranges from -7.5°C to 15°C. Most of the vapor compression refrigeration systems analyzed have low cooling capacity.

Subsequently, the environmental metrics commonly used in the selection of an ecological refrigerant were presented. These metrics are the global warming potential (GWP), total equivalent warming impact (TEWI), and the life cycle climate performance (LCCP). Where each of these metrics was described and the feasibility of their application in the practice discussed. In this thesis, the environmental metric chosen to assess the overall environmental impact produced by the system was TEWI because it is easier to apply, more sensitive to the system and more reliable than the others.

### 3. METHODOLOGY

In this chapter, the following information related to the mathematical modeling of the proposed refrigeration system is presented: the ecological refrigerants selected for analysis, the mathematical model of the main components of the refrigeration system, the commercial compressor selected for each refrigerant, the procedure for selecting the commercial diameters of the heat exchangers, the procedure for determining the commercial diameters of the heat exchangers, energy, exergy, environmental, economic analysis and the description of the simulation parameters used.

#### 3.1. Ecological refrigerants selected for analysis

The ecological refrigerants selected for analysis were R290 (propane), R600a (isobutane), R744 (dioxide of carbon), and R1234yf. The criteria used were described in detail in subsection 2.1. It is important to note that the mentioned refrigerants are classified as ecological because they have a low GWP value and Null ODP. In addition, R134a (non-ecological refrigerant) was also selected for analysis to compare the thermo-economic and environmental performance of the system operating with R134a against the thermo-economic and environmental performance of the system operating with the ecological refrigerants described above. Table 3.1 shows the most relevant properties of the selected refrigerants.

TABLE 3.1: Main properties of the selected refrigerants.

Refrigerant	R134a	R290	R600a	R1234yf	R744
Normal boiling point [°C]	-26	-42	-12	-29.4	-78
Critical temperature [°C]	101	96.68	134.7	94.7	30.98
Critical pressure [kPa]	4059	4247	3640	3382	7377
Liquid density at 25°C [kg/m <sup>3</sup> ]	1207	492.1	549.9	1092	705.1
Vapor density at 25°C [kg/m <sup>3</sup> ]	32.37	20.64	9.123	37.94	242.8
ODP	0	0	0	0	0
GWP 100 years	1370	20	20	<4.4	1
Atmospheric lifetime [years]	13.4	0.041	0.016	0.029	>50
ASHRAE 34-Safety code	A1	A3	A3	A2L	A1

SOURCE: Adapted from de Paula et. al (2020a, p.12)

#### 3.2. Mathematical modeling

The steady-state model was developed using the Engineering Equation Solver (EES) software. The input variables of the VCRS model are shown on the left, and the



output variables on the right, according to FIG. 3.1. FIG. 3.2 shows the refrigeration plant layout under study.

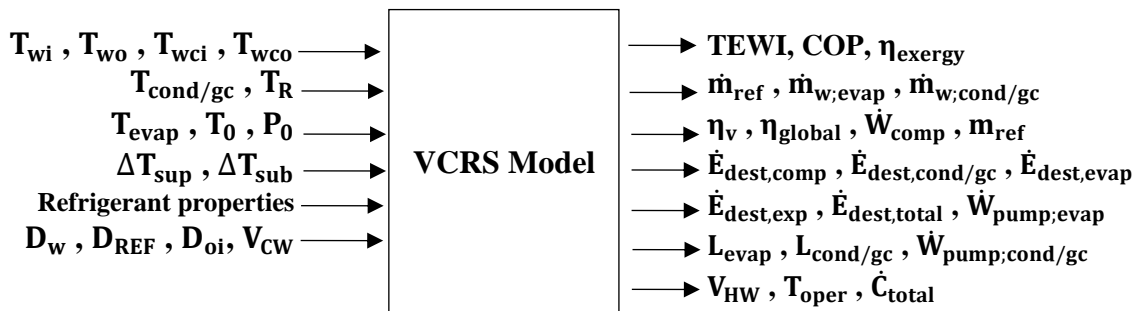


FIGURE 3.1 – Scheme of the input and output variables of the model  
SOURCE – Adapted from de Paula et al. (2020a)

During the development of the mathematical model, the following aspects were assumed:

- The pressure drop on the refrigerant side in the evaporator and condenser/gas cooler was not considered;
- The pressure drop on the waterside in the evaporator and condenser/gas cooler was considered;
- The contamination of the refrigerant by the compressor oil was not considered;
- The heat loss of heat exchangers to the environment was not considered;
- The expansion device chosen was a thermostatic expansion valve (TEV), and this device was modeled as adiabatic;
- The pipes between components were considered two meters long each;
- The refrigeration system under study operates in a steady-state regime.

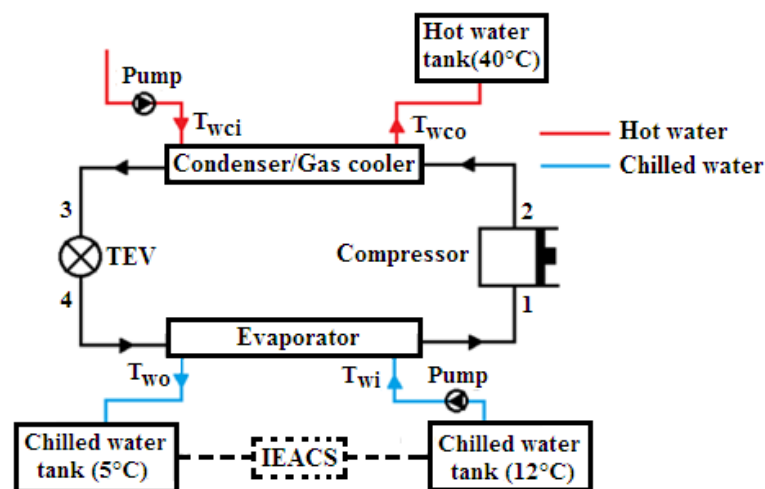


FIGURE 3.2 – Refrigerant plant layout under study.  
SOURCE – Adapted from de Paula et al. (2020a)

The refrigeration plant considered in this thesis was designed to produce and store chilled water (5°C) for an indirect expansion air-conditioning system (IEACS). The volume of chilled water produced and stored by the refrigeration plant under study is related to the cooling capacity adopted. The proposed layout was developed by de Paula et al. (2020a) and was designed to mitigate two important aspects. The first one is related to safety and maintenance features. Among the evaluated fluids, there are two fluids with a certain degree of flammability: propane (R290) and isobutane (R600a). The indirect expansion system restricts the area subject to refrigerant fluid leakage. The second aspect is related to the reduction in energy costs. The VCRS can operate when a reduced electricity tariff is applied and store the chilled water to be used at an appropriate moment.

This refrigeration plant was also designed to produce and store hot water (40°C) for a family's bath, focusing on energy cost reduction, taking advantage of the heat rejected by the condenser/gas cooler. The volume of hot water produced and stored by the refrigeration plant is also related to the size of the cooling capacity adopted. The systems proposed by Rabelo et al. (2019a) and Garcia et al. (2018) are concrete examples of experimental apparatus that make use of this application. Lastly, a real application of the proposed system in this thesis can be seen in some gyms, where the heat generated by the people in the weight room is used to help heat the pool water.

### 3.3. Evaporator model

The evaporator used was a concentric tube type, with the refrigerant flowing through the inner tube and the water counterflowing through the annular space, according to FIG. 3.3.

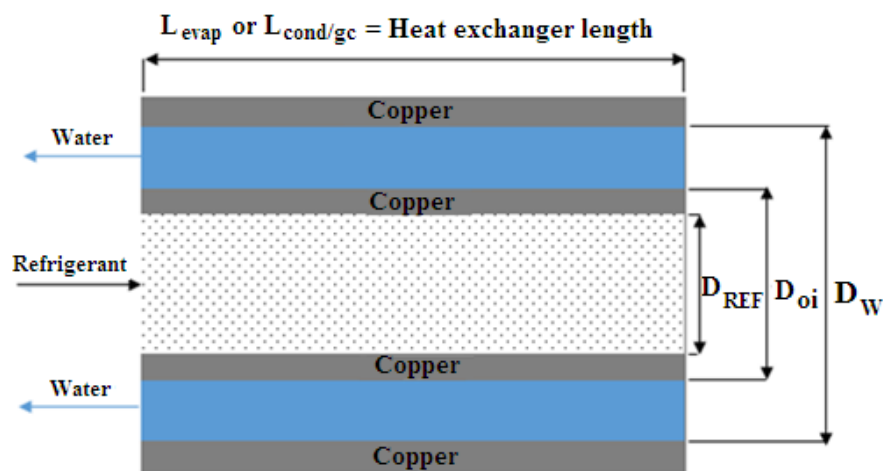


FIGURE 3.3 – Geometric characteristic of evaporator and condenser/gas cooler.

SOURCE – Adapted from de Paula et al. (2020b)

The cooling capacity ( $\dot{Q}_{\text{evap}}$ ) and water mass flow rate at the evaporator ( $\dot{m}_{\text{w;evap}}$ ) were obtained by the energy balance for steady-state condition and are given by EQ. (3.1).

$$\dot{Q}_{\text{evap}} = \dot{m}_{\text{ref}} \cdot (i_1 - i_4) = \dot{m}_{\text{w;evap}} \cdot C_{p_w} \cdot (T_{\text{wi}} - T_{\text{wo}}) \quad (3.1)$$

In this equation,  $\dot{m}_{\text{ref}}$  is the refrigerant mass flow rate,  $i_1$  is the refrigerant specific enthalpy at the evaporator outlet and  $i_4$  is the refrigerant specific enthalpy at the evaporator inlet,  $C_{p_w}$  is the specific heat of water at constant pressure,  $T_{\text{wi}}$  is the water temperature at the evaporator inlet and  $T_{\text{wo}}$  is the water temperature at the evaporator outlet.

The evaporator length ( $L_{\text{evap}}$ ) was calculated using the logarithmic mean temperature difference method ( $\Delta T_{\text{ml;evap}}$ ), as described by (BERGMAN et al., 2011).

$$\dot{Q}_{\text{evap}} = U_{\text{evap}} \cdot A_{\text{evap}} \cdot \Delta T_{\text{ml;evap}} \quad (3.2)$$

$$\Delta T_{\text{ml;evap}} = \frac{[(T_{\text{wi}} - T_1) - (T_{\text{wo}} - T_4)]}{\ln((T_{\text{wi}} - T_1)/(T_{\text{wo}} - T_4))} \quad (3.3)$$

$$U_{\text{evap}} = \left( \frac{1}{\bar{h}_{\text{ref}}} + \frac{1}{\bar{h}_{\text{w;evap}}} \right)^{-1} \quad (3.4)$$

$$A_{\text{evap}} = \pi \cdot D_{\text{REF}} \cdot L_{\text{evap}} \quad (3.5)$$

Where  $T_1$  is the refrigerant temperature at the evaporator outlet,  $T_4$  is the refrigerant temperature at the evaporator inlet,  $U_{\text{evap}}$  is the overall heat transfer coefficient of the evaporator,  $A_{\text{evap}}$  is the surface area of the evaporator,  $D_{\text{REF}}$  is the inner diameter of the inner tube (diameter for the refrigerant side),  $D_{\text{oi}}$  is the outer diameter of the inner tube,  $D_w$  is the inner diameter of the outer tube (diameter for the waterside).

The average convective heat transfer coefficient of the water flowing through the evaporator ( $\bar{h}_{\text{w;evap}}$ ) is determined by correlation 2.1 (constant heat flow), as shown in Tab. 2.2. This correlation is used because water has laminar flow in the annular region.

The average convective heat transfer coefficient of the refrigerant flowing through the inner tube ( $\bar{h}_{\text{ref}}$ ) is determined by discretizing the evaporator, according to the following procedure: Previously, the inlet ( $i_4$ ) and outlet ( $i_1$ ) enthalpy of the evaporator as well as the specific enthalpy of the saturated liquid ( $i_L$ ) and saturated vapor ( $i_V$ ) of this component are obtained. Subsequently, this component is divided into a set of points,

adopting a constant enthalpy step and considering that the enthalpy varies linearly with the evaporator length ( $L_{\text{evap}}$ ). Then, it is verified by means of the following test in which region (two-phase or single-phase) the local enthalpy ( $i_{\text{local}}$ ) of the point under analysis is located: If ( $i_{\text{local}} \leq i_L$  or  $i_{\text{local}} \geq i_V$ ), the point is in the single-phase region and local convective coefficient of the refrigerant ( $h_{\text{local}}$ ) is calculated by the Gnielinski (1976) correlation (Tab. 2.2). However, if ( $i_L < i_{\text{local}} < i_V$ ), the point is in the two-phase region and ( $h_{\text{local}}$ ) is determined by Shah (2017) correlation, according to EQ. (2.12). This procedure is repeated for the next points until the entire domain is reached. Finally, the average convective heat transfer coefficient ( $\bar{h}_{\text{ref}}$ ) is the arithmetic mean of the obtained local convective heat transfer coefficients.

### 3.4 Condenser/gas cooler model

The condenser/gas cooler used was also a concentric tube type, with the refrigerant flowing through the inner tube and water counterflowing through the annular space, according to FIG. 3.3. It was considered that the values adopted for  $D_{\text{REF}}$ ,  $D_{\text{oi}}$  and  $D_{\text{W}}$  are the same for both evaporator and condenser/gas cooler.

The heat transfer rate at the condenser/gas cooler ( $\dot{Q}_{\text{cond/gc}}$ ) and water mass flow rate at the condenser/gas cooler ( $\dot{m}_{\text{w,cond/gc}}$ ) were obtained by the energy balance for steady-state condition and are given by EQ. (3.6).

$$\dot{Q}_{\text{cond/gc}} = \dot{m}_{\text{ref}} \cdot (i_2 - i_3) = \dot{m}_{\text{w,cond/gc}} \cdot C_{p\text{w}} \cdot (T_{\text{wco}} - T_{\text{wci}}) \quad (3.6)$$

In this equation,  $i_2$  is the refrigerant specific enthalpy at the condenser/gas cooler inlet and  $i_3$  is the refrigerant specific enthalpy at the condenser/gas cooler outlet,  $T_{\text{wci}}$  is the water temperature at the condenser/gas cooler inlet and  $T_{\text{wco}}$  is the water temperature at the condenser/gas cooler outlet.

The condenser/gas cooler length ( $L_{\text{cond/gc}}$ ) is calculated using the logarithmic mean temperature difference method ( $\Delta T_{\text{ml,cond/gc}}$ ), as described by (BERGMAN et al., 2011).

$$\dot{Q}_{\text{cond/gc}} = U_{\text{cond/gc}} \cdot A_{\text{cond/gc}} \cdot \Delta T_{\text{ml,cond/gc}} \quad (3.7)$$

$$\Delta T_{\text{ml,cond/gc}} = \frac{[(T_2 - T_{\text{wco}}) - (T_3 - T_{\text{wci}})]}{\ln((T_2 - T_{\text{wco}})/(T_3 - T_{\text{wci}}))} \quad (3.8)$$

$$U_{\text{cond/gc}} = \left( \frac{1}{\bar{h}_{\text{ref}}} + \frac{1}{\bar{h}_{\text{w;cond/gc}}} \right)^{-1} \quad (3.9)$$

$$A_{\text{cond/gc}} = \pi \cdot D_{\text{REF}} \cdot L_{\text{cond/gc}} \quad (3.10)$$

Where  $T_2$  is the refrigerant temperature at the condenser/gas cooler inlet,  $T_3$  is the refrigerant temperature at the condenser/gas cooler outlet,  $U_{\text{cond/gc}}$  is the overall heat transfer coefficient of the condenser/gas cooler and  $A_{\text{cond/gc}}$  is the surface area of the condenser/gas cooler.

The average convective heat transfer coefficient of the water flowing through the condenser/gas cooler ( $\bar{h}_{\text{w;cond/gc}}$ ) is also determined by correlation 2.1 (Tab. 2.2). This correlation is used because water has laminar flow in the annular region of this heat exchanger.

The average convective heat transfer coefficient of the refrigerant flowing through the inner tube ( $\bar{h}_{\text{ref}}$ ) is also determined by discretizing the condenser/gas cooler, following the same methodology used in the evaporator. The only difference between the methodology applied to the current context in relation to the methodology applied to the evaporator was that the local convective heat transfer coefficient ( $h_{\text{local}}$ ) of the analyzed point was determined by the correlation of Shah (2016) in the two-phase region of the condenser/gas cooler.

### 3.5 Compressor model

The compressor model is based on the following assumptions:

- No refrigerant leakage;
- The rotation speed of the compressor is constant.

The refrigerant mass flow rate in the compressor ( $\dot{m}_{\text{ref}}$ ) is given by EQ. (3.11), according to (de Paula et al., 2020b).

$$\dot{m}_{\text{ref}} = \rho_1 \cdot \forall_{\text{cil}} \cdot N \cdot \eta_v \quad (3.11)$$

In which  $\forall_{\text{cil}}$  is the compressor displacement volume,  $N$  is the rotation speed of the compressor,  $\rho_1$  is the refrigerant density at the compressor inlet and  $\eta_v$  is the volumetric efficiency. The electrical power consumption in the compressor ( $\dot{W}_{\text{comp}}$ ) is given by EQ. (3.12), according to (Da Riva and Del Col., 2011).

$$W_{\text{comp}} = \frac{\dot{m}_{\text{ref}} \cdot (i_2 - i_1)}{\eta_{\text{global}}} \quad (3.12)$$

The volumetric ( $\eta_v$ ) and global ( $\eta_{\text{global}}$ ) efficiency curves of the compressor were represented by a polynomial regression regarding the pressure ratio ( $r_p = P_2/P_1$ ). All data required in this process were obtained from the manufacture's catalogs for commercial compressors, as described in topic 3.5.1.

### 3.5.1 Commercial compressor selection for each refrigerant

The selection of a specific commercial compressor for each refrigerant mentioned in topic 3.1 is an important step, because by using the data provided by the manufacturer, it is possible to obtain the volumetric ( $\eta_v$ ) and global ( $\eta_{\text{global}}$ ) efficiency curves. These curves are important to generate more realistic simulation data. This procedure allows the behavior of the simulated system to be closer to the real behavior of the system in practice. In addition, this consideration allows the modeled system for each refrigerant to operate within its own compression characteristics.

The most suitable commercial compressor for each refrigerant was selected according to the following criteria:

- I. For a reference cooling capacity of 0.5 kW,  $T_{\text{evap}} = -5^\circ\text{C}$  and  $T_{\text{cond}} = 50^\circ\text{C}$ .
- II. For a reference cooling capacity of 1.2 kW,  $T_{\text{evap}} = -5^\circ\text{C}$  and  $T_{\text{cond/gc}} = 50^\circ\text{C}$ .

The reference cooling capacity ( $\dot{Q}_{\text{evap.ref}}$ ) of 0.5 kW was adopted because this was the largest cooling capacity where it was possible to obtain a commercial compressor for the R600a. As noted in topic 2.1, the behavior of a system operating with R600a is still little explored in the literature. However, it was not possible to obtain a commercial compressor for the R744 in this first consideration. Thus, a commercial compressor for the R744 was selected considering  $\dot{Q}_{\text{evap.ref}} = 1.2$  kW. This reference refrigeration capacity was adopted because this was the smallest cooling capacity where it was possible to select a commercial compressor for the R744.

The thermodynamic condition was adopted based on the works presented in Tab. 2.1. Also, all selected compressors have a frequency of 50 Hz because manufacturers only supply this component with this frequency. The commercial compressors selected for  $\dot{Q}_{\text{evap.ref}} = 0.5$  kW and  $\dot{Q}_{\text{evap.ref}} = 1.2$  kW are presented in Tab. 3.2 and Tab. 3.3, respectively.

TABLE 3.2: Compressors selected for  $\dot{Q}_{\text{evap.ref}} = 0.5 \text{ kW}$ 

Refrigerant	Model	Type	Manufacturer	$V_{\text{cil}}$ ( $\text{cm}^3$ )	Rotation (rpm)	Frequency (Hz)	Voltage (V)
R134a	NEK1118Z	Hermetic and reciprocating	Embraco	8.39	2900	50	220
R1234yf	AE4440N-FZ1A	Hermetic and reciprocating	Tecumseh	10.33	2900	50	220
R290	EMC3121U	Hermetic and reciprocating	Embraco	5.19	2900	50	220
R600a	NEK6170Y	Hermetic and reciprocating	Embraco	14.28	2900	50	220

SOURCE – de Paula et al. (2020b).

TABLE 3.3: Compressors selected for  $\dot{Q}_{\text{evap.ref}} = 1.2 \text{ kW}$ 

Refrigerant	Model	Type	Manufacturer	$V_{\text{cil}}$ ( $\text{cm}^3$ )	Rotation (rpm)	Frequency (Hz)	Voltage (V)
R134a	NT6217ZV	Hermetic and reciprocating	Embraco	20.4	2900	50	220
R1234yf	CAJ4492N-FZ	Hermetic and reciprocating	Tecumseh	25.95	2900	50	220
R290	NEK6217U	Hermetic and reciprocating	Embraco	14.28	2900	50	220
R744	CD200/CD150M	Semi-hermetic and reciprocating	Dorin Innovation	6.44	1450	50	220

SOURCE – de Paula et al. (2020a).

The efficiency map data for each commercial compressor supplied by the manufacturer were collected. Thereafter, the volumetric and global efficiency curves were obtained utilizing polynomial regression as proposed by Minetto (2011). According to the manufacturer, the experimental data has an uncertainty of 5%. The equations for volumetric and global efficiency are presented in Tab. 3.4 and Tab. 3.5.

TABLE 3.4: Global and volumetric efficiency curves for  $\dot{Q}_{\text{evap.ref}} = 0.5 \text{ kW}$ 

Refrigerant	Volumetric efficiency	Global efficiency	$R^2$ of $\eta_v$ (%)	$R^2$ of $\eta_{\text{global}}$ (%)
R134a	$\eta_v = 0.8162 - 0.0131r_p$	$\eta_{\text{global}} = 0.1881 + 0.0916r_p + 0.0085r_p^2 + 0.0003r_p^3$	89.36	96.37
R1234yf	$\eta_v = 0.8957 - 0.0280r_p$	$\eta_{\text{global}} = 0.0499 + 0.2012r_p - 0.0342r_p^2 + 0.0018r_p^3$	95.66	75.92
R600a	$\eta_v = 0.9129 - 0.0219r_p$	$\eta_{\text{global}} = 0.0046 + 0.2649r_p - 0.0499r_p^2 + 0.0031r_p^3$	97.33	76.37
R290	$\eta_v = 0.9311 - 0.0276r_p$	$\eta_{\text{global}} = 0.3774 + 0.1405r_p - 0.0201r_p^2 + 0.0008r_p^3$	94.62	85.57

SOURCE – de Paula et al. (2020b).

TABLE 3.5: Global and volumetric efficiency curves for  $\dot{Q}_{\text{evap.ref}} = 1.2 \text{ kW}$ 

Refrigerant	Volumetric efficiency	Global efficiency	R <sup>2</sup> of $\eta_v$ (%)	R <sup>2</sup> of $\eta_{\text{global}}$ (%)
R134a	$\eta_v = 1.0368 - 0.1517r_p + 0.0243r_p^2 - 0.0014r_p^3$	$\eta_{\text{global}} = 0.2819 + 0.0766r_p - 0.0058r_p^2$	85.14	94.42
R1234yf	$\eta_v = 0.9041 - 0.0351r_p - 0.0013r_p^2$	$\eta_{\text{global}} = -0.6924 + 1.1139r_p - 0.4256r_p^2 + 0.0801r_p^3 - 0.0074r_p^4 + 0.0003r_p^5$	98.63	87.17
R744	$\eta_v = 1.0199 - 0.1390r_p + 0.0080r_p^2$	$\eta_{\text{global}} = 0.6038 + 0.0216r_p - 0.0075r_p^2$	99.32	96.34
R290	$\eta_v = 0.9361 - 0.0466r_p + 0.0022r_p^2$	$\eta_{\text{global}} = 0.2392 + 0.1256r_p - 0.0131r_p^2$	93.88	87.36

SOURCE – de Paula et al. (2020a).



### 3.6 Energy performance

The coefficient of performance (COP) of the refrigeration system is given by EQ. (3.13).

$$\text{COP} = \frac{\dot{Q}_{\text{evap}}}{\dot{W}_{\text{comp}} + \dot{W}_{\text{pump;evap}} + \dot{W}_{\text{pump;cond/gc}}} \quad (3.13)$$

In this equation,  $(\dot{W}_{\text{pump;evap}})$  and  $(\dot{W}_{\text{pump;cond/gc}})$  are respectively the electrical power consumption by the pump in the evaporator and condenser/gas cooler. These parameters are calculated by EQ. (3.14) and EQ. (3.15).

$$\dot{W}_{\text{pump;evap}} = \frac{\dot{m}_{\text{w;evap}} \cdot \Delta P_{\text{evap}}}{\rho_{\text{w}} \cdot \eta_{\text{pump}}} \quad (3.14)$$

$$\dot{W}_{\text{pump;cond/gc}} = \frac{\dot{m}_{\text{w;cond/gc}} \cdot \Delta P_{\text{cond/gc}}}{\rho_{\text{w}} \cdot \eta_{\text{pump}}} \quad (3.15)$$

Where  $\eta_{\text{pump}}$ ,  $\Delta P_{\text{cond/gc}}$  and  $\Delta P_{\text{evap}}$  are respectively the overall pump efficiency and the pressure drop on the waterside in the condenser/gas cooler and evaporator. The pressure drop on the waterside in the evaporator and condenser/gas cooler was calculated by EQ. (3.16) and EQ. (3.17). The pressure drop on the refrigerant side in the evaporator and condenser/gas cooler was not considered to facilitate the modeling of the system. Moreover, this consideration was also adopted in the following works: Roy and Mandal (2019), Shikalgar and Sapali (2019) and Ahamed et al. (2011).

$$\Delta P_{\text{evap}} = \frac{8 \cdot f \cdot L_{\text{total}} \cdot \dot{m}_{\text{w;evap}}^2}{\pi^2 (D_{\text{W}} - D_{\text{REF}})^5 \rho_{\text{w}}} \quad (3.16)$$

$$\Delta P_{\text{cond/gc}} = \frac{8 \cdot f \cdot L_{\text{total}} \cdot \dot{m}_{\text{w;cond/gc}}^2}{\pi^2 (D_{\text{W}} - D_{\text{REF}})^5 \rho_{\text{w}}} \quad (3.17)$$

The Darcy friction factor ( $f$ ) was calculated by Shah and London (2014) correlation for laminar flow in circular ducts and Li, Seem and Li (2011) correlation for turbulent flow in circular ducts. The following criterion was used to determine if the flow is laminar or turbulent: Laminar flow is assumed to occur for Reynold's numbers less

than 2300 and turbulent flow is adopted for Reynold's numbers greater than 2300. The total length of the pipe ( $L_{total}$ ) used to calculate the pressure drop on the waterside is the sum of the heat exchanger length with an equivalent length. Mathematically, this equivalent length is the sum of the straight lengths of the tubes that connect the tanks (chilled water or hot water) to the respective heat exchanger (evaporator or condenser/gas cooler), with the corresponding straight length related to the curves and connections. In this thesis, the total equivalent length due to curves, connections, as well as the straight lengths of the tubes, was defined to be seven meters long and  $\eta_{pump}$  equal to 0.5.

### 3.7 Environmental performance

Based on Makhnatch and Khodabandeh (2014), the environmental impact was evaluated by TEWI (Total Equivalent Warming Impact). This parameter was calculated by EQ. (3.18). The following studies also used the TEWI methodology to assess the environmental impact of the VCRS operating with different refrigerants: Belman-Flores et al. (2017), Tsamos et al. (2017), Mylona et al. (2017), Wu et al. (2020), Xião et al. (2020) and Antunes and Bandarra Filho (2016). This parameter takes into account both direct emissions ( $TEWI_{Direct}$ ) and indirect emissions ( $TEWI_{INDirect}$ ).

$$TEWI = TEWI_{Direct} + TEWI_{INDirect} \quad (3.18)$$

$$TEWI_{Direct} = GWP \cdot m_{ref;total} \cdot L_{rate} \cdot L_{time} + GWP \cdot m_{ref} \cdot (1 - \alpha_{recup}) \quad (3.19)$$

$$TEWI_{INDirect} = E_{annual} \cdot \beta \cdot L_{time} \quad (3.20)$$

In these equations,  $m_{ref;total}$  is the refrigerant charge of the VCRS,  $L_{rate}$  is the annual rate of refrigerant emitted (replacement and leaks) of the VCRS,  $L_{time}$  is the lifespan of the VCRS,  $\alpha_{recup}$  is the refrigerant life recovery rate,  $E_{annual}$  is the annual electricity consumption of the VCRS, EQ. (3.21), and  $\beta$  is the CO<sub>2</sub> emission factor for producing electricity.

$$E_{annual} = 365 \cdot T_{oper} \cdot [\dot{Q}_{evap}/COP] \quad (3.21)$$

In this equation,  $T_{oper}$  is the daily operating time of the system and it was calculated as follows: For the reference cooling capacity of 0.5 kW, this parameter is the required time for the system to produce 620 liters of chilled water (5°C) and at least 350 liters of hot water (40°C) for the bath of seven people. However, for the reference cooling

capacity of 1.2 kW, this parameter is the required time for the system to produce 1200 liters of chilled water (5°C) and at least 600 liters of hot water (40°C) for the bath of fourteen people. The refrigerant charge inside the pipe between components ( $m_{\text{ref,pipe}}$ ) is determined by the EQ. (3.22) while the refrigerant charge inside the heat exchanger ( $m_{\text{ref,HE}}$ ) is determined by the EQ. (3.23).

$$m_{\text{ref,pipe}} = \rho_{\text{ref}} \cdot \left( \frac{\pi \cdot D_{\text{REF}}^2}{4} \right) \cdot L_{\text{pipe}} \quad (3.22)$$

$$m_{\text{ref,HE}} = \bar{\rho}_{\text{ref}} \cdot \left( \frac{\pi \cdot D_{\text{REF}}^2}{4} \right) \cdot L_{\text{HE}} \quad (3.23)$$

Where ( $L_{\text{pipe}}$ ), ( $L_{\text{HE}}$ ), ( $\rho_{\text{ref}}$ ) and ( $\bar{\rho}_{\text{ref}}$ ) are the pipe length between components, the heat exchanger length, the density of the refrigerant inside the pipe and the average density of the refrigerant inside the heat exchanger (evaporator or condenser/gas cooler), respectively. As can be seen,  $L_{\text{HE}}$  refers to  $L_{\text{evap}}$  for the evaporator, but  $L_{\text{HE}}$  refers to  $L_{\text{cond/gc}}$  for the condenser/gas cooler.

The average density of the refrigerant is obtained by discretizing the heat exchanger following the same procedure described in subsection 3.3. As mentioned in this subsection, the heat exchanger is divided into a set of points, adopting a constant enthalpy step. Then, it is verified through the following test in which region (two-phase or single-phase) the local enthalpy ( $i_{\text{local}}$ ) of the point under analysis is located: If ( $i_{\text{local}} \leq i_{\text{L}}$  or  $i_{\text{local}} \geq i_{\text{V}}$ ), the point is in the single-phase region and the local density of the refrigerant ( $\rho_{\text{local}}$ ) is determined by the pressure acting in the component and local enthalpy of the point. However, if ( $i_{\text{L}} < i_{\text{local}} < i_{\text{V}}$ ), the point is in the two-phase region and ( $\rho_{\text{local}}$ ) is calculated by EQ. (3.24).

$$\rho_{\text{local}} = [\alpha_{\text{local}} \cdot \rho_{\text{V}} + (1 - \alpha_{\text{local}}) \cdot \rho_{\text{L}}] \quad (3.24)$$

Where ( $\alpha_{\text{local}}$ ), ( $\rho_{\text{L}}$ ) and ( $\rho_{\text{V}}$ ) are the void fraction, the density of the saturated liquid and the density of the saturated vapor, respectively. This procedure is also repeated for the next points until the entire domain is reached. Finally, the average density of the refrigerant ( $\bar{\rho}_{\text{ref}}$ ) is the arithmetic mean of the obtained local densities of the refrigerant.

The refrigerant charge inside the VCRS is the sum of the refrigerant charge inside the evaporator, condenser/gas cooler, and pipes that connect the following components: evaporator-compressor, compressor-condenser/gas cooler, condenser/gas cooler-thermostatic expansion valve, and thermostatic expansion valve/evaporator. As

previously mentioned, the pipes between components were considered two meters long each.

### 3.8 Exergy performance

The exergy efficiency ( $\eta_{\text{exergy}}$ ) is defined by EQ. (3.25), according to Shikalgar and Sapali (2019) and Roy and Mandal (2019). In this thesis, the electrical power consumption by the pumps was not considered in the calculation of ( $\eta_{\text{exergy}}$ ) to facilitate comparison with other works because the analyzed studies did not consider the electrical power consumption by the fans in the calculation of ( $\eta_{\text{exergy}}$ ). As noted in Tab. 4.4 (subsection 4.4), the electrical power consumption by the compressor corresponds to more than 99.3% of the total electrical power consumption by the system ( $\dot{W}_{\text{total}}$ ).

$$\eta_{\text{exergy}} = 1 - \frac{\dot{E}_{\text{dest,total}}}{\dot{W}_{\text{comp}}} \quad (3.25)$$

Where ( $\dot{E}_{\text{dest,total}}$ ) is the total exergy destruction of the system. The total exergy destruction is the sum of exergy destruction of the compressor ( $\dot{E}_{\text{dest,comp}}$ ), condenser/gas cooler ( $\dot{E}_{\text{dest,cond/gc}}$ ), evaporator ( $\dot{E}_{\text{dest,evap}}$ ) and expansion valve ( $\dot{E}_{\text{dest,exp}}$ ). The exergy destruction of each component can be determined by EQ. (3.26-29), according to Altinkaynak et al. (2019), Roy and Mandal (2019), and Ahamed et al. (2011).

$$\dot{E}_{\text{dest,comp}} = \dot{E}x_1 - \dot{E}x_2 + \dot{W}_{\text{comp}} \quad (3.26)$$

$$\dot{E}_{\text{dest,cond/gc}} = \dot{E}x_2 - \dot{E}x_3 - \dot{Q}_{\text{cond/gc}} \cdot \left(1 - \frac{T_0}{T_R}\right) \quad (3.27)$$

$$\dot{E}_{\text{dest,evap}} = \dot{E}x_4 - \dot{E}x_1 + \dot{Q}_{\text{evap}} \cdot \left(1 - \frac{T_0}{T_{\text{evap}}}\right) \quad (3.28)$$

$$\dot{E}_{\text{dest,exp}} = \dot{E}x_3 - \dot{E}x_4 \quad (3.29)$$

The exergy of the refrigerant circulating in the VCRS is calculated by EQ. (3.30).

$$\dot{E}x = \dot{m}_{\text{ref}} \cdot [(h - h_0) - T_0(s - s_0)] \quad (3.30)$$

Where  $h_0$  and  $s_0$  are the enthalpy and entropy values of the dead state of the refrigerant at the pressure ( $P_0$ ) and temperature ( $T_0$ ). In Eq. (3.27),  $T_R$  is the reference temperature adopted to calculate ( $\dot{E}_{\text{dest,cond/gc}}$ ), according to two considerations: ( $T_R =$

$T_{\text{cond/gc}}$ ) for refrigeration system with subcritical cycle and ( $T_R = 45^\circ\text{C}$ ) for refrigeration system with transcritical cycle. The first consideration is based on the works of Altinkaynak et al. (2019) and Roy and Mandal (2019). The second consideration is related to the selected reference temperature to minimize the exergy destruction in the gas cooler. The reference temperature was chosen based on the temperature distribution profile of the gas cooler, according to de Paula et al. (2020a).

### 3.9 Economic performance

The economic performance of the VCRS under study was evaluated using the total plant cost rate. The total plant cost rate ( $\dot{C}_{\text{total}}$ ) is given by EQ. (3.31), according to Roy and Mandal (2019) and Aminyavari et al. (2014).

$$\dot{C}_{\text{total}} = \dot{C}_{\text{CM}} + \dot{C}_{\text{op}} + \dot{C}_{\text{env}} \quad (3.31)$$

Where ( $\dot{C}_{\text{CM}}$ ) is the capital and maintenance cost rate, ( $\dot{C}_{\text{op}}$ ) is the operational cost rate and ( $\dot{C}_{\text{env}}$ ) is the penalty cost rate due to  $\text{CO}_2$  emission. The capital and maintenance cost rate of the VCRS is calculated by EQ. (3.32).

$$\dot{C}_{\text{CM}} = (C_{\text{evap}} + C_{\text{cond/gc}} + C_{\text{comp}} + C_{\text{TEV}} + C_{\text{p;evap}} + C_{\text{p;cond/gc}}) \cdot \varphi \cdot \text{CRF} \quad (3.32)$$

Where  $C_{\text{evap}}$ ,  $C_{\text{cond/gc}}$ ,  $C_{\text{comp}}$ ,  $C_{\text{TEV}}$ ,  $C_{\text{p;evap}}$  and  $C_{\text{p;cond/gc}}$  are the capital cost function of the evaporator, condenser/gas cooler, compressor, thermostatic expansion valve, pump related to the evaporator circuit, and pump related to the condenser/gas cooler circuit, respectively. These capital cost functions are listed in Tab. 3.6.

TABLE 3.6: Capital cost function of the main components

Component	Capital cost (R\$/year)	Reference
Evaporator	$C_{\text{evap}} = 516.62 \cdot A_{\text{evap}} + 268.45$	Tontu et al. (2019), Mosaffa and Farshi (2016)
Condenser/gas cooler	$C_{\text{cond/gc}} = 516.62 \cdot A_{\text{cond/gc}} + 268.45$	Tontu et al. (2019), Mosaffa and Farshi (2016)
Compressor	$C_{\text{comp}} = \frac{39.5 \cdot \dot{m}_{\text{ref}}}{(0.9 - \eta_{\text{global}})} \cdot r_p \cdot \ln(r_p)$	Mosaffa and Farshi (2016), Mansuriya et al. (2020)
TEV	$C_{\text{TEV}} = 114.5 \cdot \dot{m}_{\text{ref}}$	Roy and Mandal (2019), Mansuriya et al. (2020)
Pump-evap	$C_{\text{p;evap}} = 2100 \cdot (\dot{W}_{\text{evap}})^{0.26} \left( \frac{1 - \eta_{\text{pump}}}{\eta_{\text{pump}}} \right)^{0.5}$	Mansuriya et al. (2020)
Pump-cond/gas cooler	$C_{\text{p;cond/gc}} = 2100 \cdot (\dot{W}_{\text{cond/gc}})^{0.26} \left( \frac{1 - \eta_{\text{pump}}}{\eta_{\text{pump}}} \right)^{0.5}$	Mansuriya et al. (2020)

SOURCE – de Paula et al. (2020b).

In this thesis, it was considered that the capital cost function of the evaporator is equal to the capital cost function of the condenser. The parameter ( $\varphi$ ) represents the maintenance factor and (CRF) is the capital recovery factor, which can be calculated by EQ. (3.33).

$$\text{CRF} = \frac{iR(1 + iR)^n}{(1 + iR)^n - 1} \quad (3.33)$$

Where ( $iR$ ) corresponds to the interest rate and ( $n$ ) is the refrigeration plant lifetime. The operational cost rate of the VCRS is given by EQ. (3.34).

$$\dot{C}_{\text{op}} = \dot{W}_{\text{comp}} \cdot 365 \cdot T_{\text{oper}} \cdot C_{\text{ele}} \quad (3.34)$$

In which  $C_{\text{ele}}$  is the electricity unit cost. The penalty cost rate due to  $\text{CO}_2$  emission of the VCRS is given by EQ. (3.35).

$$\dot{C}_{\text{env}} = \beta \cdot E_{\text{annual}} \cdot C_{\text{CO}_2} \quad (3.35)$$

Where  $C_{\text{CO}_2}$  is the unit damage cost of carbon dioxide emission.

### 3.10 Selection process of the commercial diameters

As mentioned in subsections 3.3 and 3.4, both the evaporator and condenser/gas cooler are concentric tube type heat exchangers. According to FIG. 3.3, the main geometric parameters of this type of heat exchanger are the heat exchanger length ( $L_{\text{evap}}$  or  $L_{\text{cond/gc}}$ ), the diameter for the refrigerant side ( $D_{\text{REF}}$ ) and the diameter for the waterside ( $D_{\text{W}}$ ). In this thesis, it was adopted that both the evaporator and condenser/gas cooler have the same values for ( $D_{\text{REF}}$ ) and ( $D_{\text{W}}$ ). For all the refrigerants analyzed, these diameters were selected according to the following steps:

\*First step, the following values were selected for the mentioned diameters, according to Appendix F:

$$\begin{cases} D_{\text{REF}} = 6.36 \text{ mm}, 7.94 \text{ mm}, 11.12 \text{ mm} \\ D_{\text{W}} = 26.8 \text{ mm}, 20.8 \text{ mm}, 14 \text{ mm} \end{cases}$$

\*Second step, the following arrangements were developed between  $D_{\text{REF}}$  and  $D_{\text{W}}$ :

$$D_{\text{REF}} = 6.36 \text{ mm} \begin{cases} D_{\text{W}} = 26.8 \text{ mm} \\ D_{\text{W}} = 20.8 \text{ mm} \\ D_{\text{W}} = 14 \text{ mm} \end{cases} \quad D_{\text{REF}} = 7.94 \text{ mm} \begin{cases} D_{\text{W}} = 26.8 \text{ mm} \\ D_{\text{W}} = 20.8 \text{ mm} \\ D_{\text{W}} = 14 \text{ mm} \end{cases}$$

$$D_{\text{REF}} = 11.12 \text{ mm} \begin{cases} D_{\text{W}} = 26.8 \text{ mm} \\ D_{\text{W}} = 20.8 \text{ mm} \\ D_{\text{W}} = 14 \text{ mm} \end{cases}$$

\*Third step, these combinations were evaluated considering the following thermodynamic conditions:

$$T_{\text{evap}} = -5^{\circ}\text{C} \begin{cases} T_{\text{cond/gc}} = 45^{\circ}\text{C} \\ T_{\text{cond/gc}} = 50^{\circ}\text{C} \end{cases} \quad T_{\text{evap}} = -4^{\circ}\text{C} \begin{cases} T_{\text{cond/gc}} = 45^{\circ}\text{C} \\ T_{\text{cond/gc}} = 50^{\circ}\text{C} \end{cases}$$

$$T_{\text{evap}} = -3^{\circ}\text{C} \begin{cases} T_{\text{cond/gc}} = 45^{\circ}\text{C} \\ T_{\text{cond/gc}} = 50^{\circ}\text{C} \end{cases}$$

\*Fourth step, for each thermodynamic condition above, the arrangement that presented the highest environmental (lowest TEWI value) and energy (highest COP value) performance was selected. At this stage, it was observed that the same arrangement was obtained in the three evaluated thermodynamic conditions.

\*Fifth step, among the thermodynamic conditions analyzed, the thermodynamic condition that obtained the best environmental and energy performance in global terms was selected.

For the reference cooling capacity of 0.5 kW and 1.2 kW, the results for each evaluated system are presented in Appendix G.

### 3.11 Simulation parameters

The thermodynamic considerations adopted to perform the simulation are presented in Tab. 3.7. These parameters were chosen based on the studies shown in Tab. 2.1.

TABLE 3.7: Thermodynamic considerations adopted to perform the simulation

PARAMETER	VALUE
Evaporation temperature ( $T_{\text{evap}}$ )	-5 °C, -4°C, -3°C
Condensation/gas cooling temperature ( $T_{\text{cond/gc}}$ )	45°C, 50°C
Superheating degree ( $\Delta T_{\text{sup}}$ )	7°C
Subcooling degree ( $\Delta T_{\text{sub}}$ )	5°C
Water temperature in the evaporator inlet ( $T_{\text{wi}}$ )	12°C
Water temperature in the evaporator outlet ( $T_{\text{wo}}$ )	5°C
Water temperature in the condenser inlet ( $T_{\text{wci}}$ )	25°C
Water temperature in the condenser outlet ( $T_{\text{wco}}$ )	40°C
inner diameter of the outer tube ( $D_{\text{w}}$ )	26.8mm, 20.8mm, 14mm
outer diameter of the inner tube ( $D_{\text{oi}}$ )	7.94mm, 9.52mm, 12.7mm
inner diameter of the inner tube ( $D_{\text{REF}}$ )	6.36mm, 7.94mm, 11.12mm
Dead state temperature ( $T_0$ ) and pressure ( $P_0$ )	25°C, 101.3 kPa

SOURCE – de Paula et al. (2020b).

Due to the established thermodynamic conditions, the following refrigerants have a subcritical refrigeration cycle: R290, R600a, R1234yf, and R134a, as shown in FIG. 3.4. Notice that the evaporator consists of a single-phase region (1'-1) and a two-phase region

(4-1'). The condenser consists of two single-phase regions (2-2' and 3'-3) and a two-phase region (2'-3').

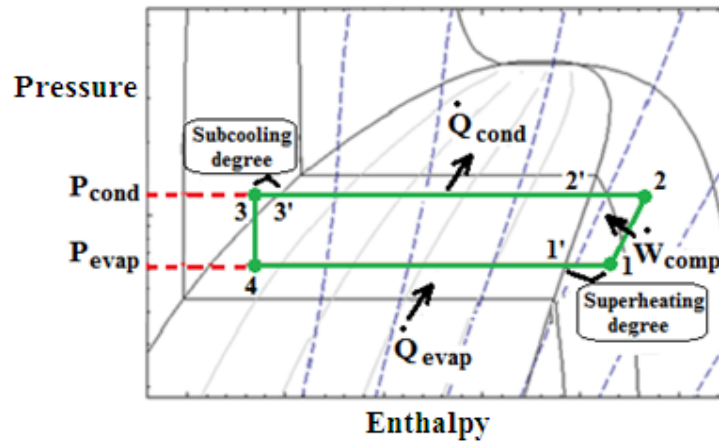


FIGURE 3.4-Subcritical refrigeration cycle: R290, R600a, R134a, R1234yf  
SOURCE – de Paula et al. (2020b).

The R744 has a transcritical refrigeration cycle, as shown in FIG. 3.5. In this cycle, the evaporator is also composed of a single-phase region (1'-1) and a two-phase region (4-1').

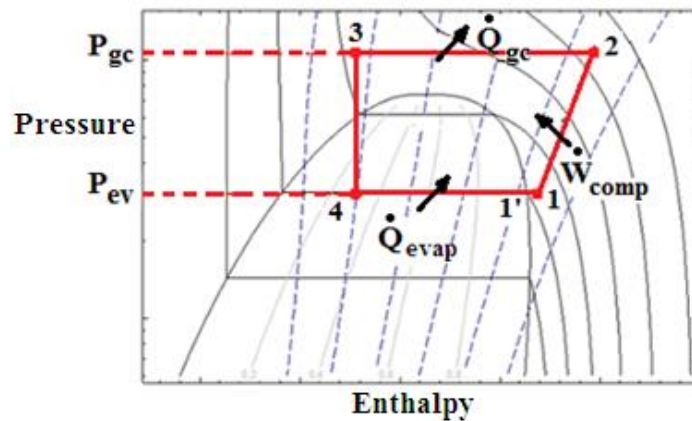


FIGURE 3.5-Transcritical refrigeration cycle: R744.  
SOURCE – Adapted from de Paula et al. (2020a).

The pressure in the gas cooler ( $P_{gc}$ ) was calculated using the correlation proposed by Kim et al. (2009). This correlation was adapted to the proposed thesis and is given by Eq. (3.36).

$$P_{gc} = 1.938 \cdot T_{cond/gc} + 9.872 \text{ [bar]} \quad (3.36)$$

The environmental performance of the refrigeration system is given by TEWI parameter. This parameter was calculated by Eq. (3.18) and it serves to guide the selection of the most suitable ecological refrigerant for the VCERS from the selected refrigerants to replace the R134a. The principal considerations are presented in Tab. 3.8.



TABLE 3.8: Considerations for calculating of the TEWI parameter

Parameter analyzed	Adopted consideration	Reference
$L_{\text{time}} = 15$ [years]	Equipment operating with an economic lifespan	Makhnatch and Khodabandeh (2014), de Paula et al. (2020a)
$\alpha_{\text{recup}} = 70\%$ .	Refrigerant mass less than 100 kg	AIRAH (2012), de Paula et al. (2020a), de Paula et al. (2020b)
$\beta = 0.082$ [kgCO <sub>2</sub> /kWh]	A reference value for Brazil	Rees (2016), de Paula et al. (2020a), de Paula et al. (2020b)
$L_{\text{rate}} = 12.5\%$	A centralized system, normal operation, catastrophic losses during service and maintenance	AIRAH (2012), de Paula et al. (2020a), de Paula et al. (2020b)

SOURCE – de Paula et al. (2020b).

Finally, the economic performance of the vapor compression refrigeration system is given by Total plant cost rate ( $\dot{C}_{\text{total}}$ ). The values considered for the input parameters to calculate the  $\dot{C}_{\text{total}}$  are presented in Tab. 3.9.

TABLE 3.9: Input parameters to calculate the Total plant cost rate

Parameter	Adopted value	Reference
$\Phi$	1.06	Roy and Mandal (2019), Tontu et al. (2019), Mosaffa and Farshi (2016), Mansuriya et al. (2020)
iR	14%	Mosaffa and Farshi (2016), Roy and Mandal (2019)
N	15 [years]	Mosaffa and Farshi (2016), Mansuriya et al. (2020), Roy and Mandal (2019)
$C_{\text{ele}}$	0.956 [R\$/kWh]	Duarte et al. (2019b), de Paula et al. (2020b)
$C_{\text{CO}_2}$	0.09 [USD/kgCO <sub>2</sub> ]	Mosaffa and Farshi (2016), Roy and Mandal (2019)

SOURCE – de Paula et al. (2020b).

### 3.12 Model solution path

As mentioned in subsection 3.2, the mathematical model was developed using the Engineering Equation Solver (EES) software. On this platform, the lines of a program can be written without the need to follow an established order. In other words, to determine the output variables of the program, this platform only requires that the number of variables is equal to the number of equations. However, an overview of the procedure performed by the software to determine the output variables in the program is described in FIG. 3.6. This figure has as main objective to provide a global idea of the steps performed by the software to calculate the following parameters: COP, TEWI,  $\eta_{\text{exergy}}$  and  $\dot{C}_{\text{total}}$ .

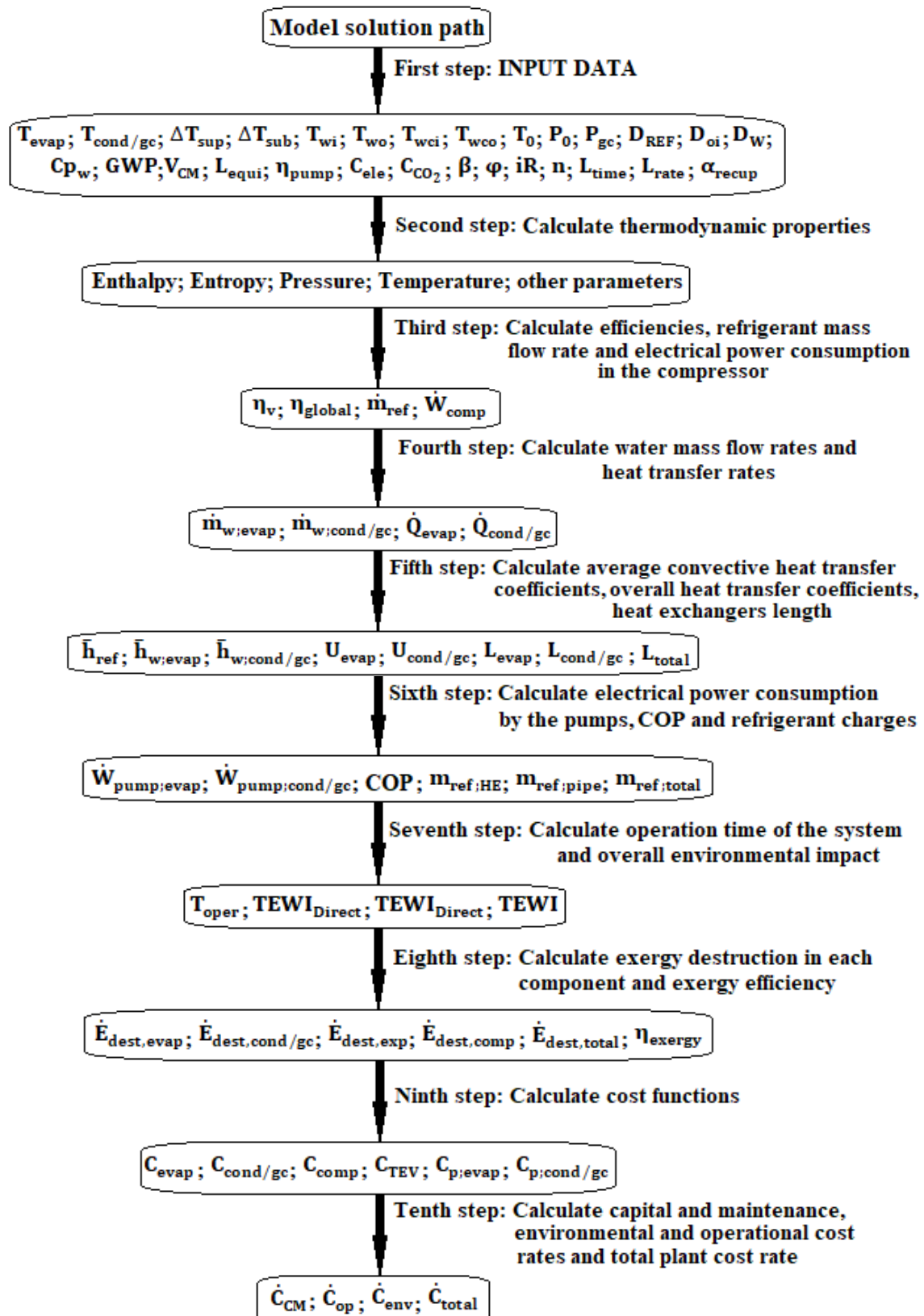


FIGURE 3.6- Steps performed by the program to calculate the output variables.  
 SOURCE – Elaborated by the author.

All input data required for the operation of the program are provided in the first step. These input data are information related to the thermodynamic condition of the system, refrigerant used, geometric characteristics of the heat exchangers and information related to environmental, cost, and operation issues of the system.

In steps two through eight, the program calculates all the output parameters that are necessary to determine the energy, environmental, and exergy performance of the system. Finally, in the ninth and tenth, the program calculates the capital and maintenance cost rate, the operational cost rate, the environmental cost rate and the total plant cost rate of the system.

## 4 RESULTS AND DISCUSSION

In this chapter, energy, exergy, environmental, and economic analysis was carried out for different evaporation and condensation/gas cooling temperatures. The purpose of this analysis was to determine two main aspects: the most suitable system with ecological refrigerant to replacing the system with R134a and the thermodynamic condition in which the selected system operates with the highest performance. In addition, this analysis was carried out considering different commercial diameters to select the best combination between the diameter for the refrigerant side ( $D_{REF}$ ) and diameter for the waterside ( $D_w$ ) for both heat exchangers. The use of commercial diameters in the design of heat exchangers is important to design a component that takes into account what is available in the market.

### 4.1 Energy analysis

The energy performance was evaluate based on the COP. This parameter was calculated for each system under study considering different evaporation and condensation/gas cooling temperatures. For the reference cooling capacity ( $\dot{Q}_{evap.ref}$ ) of 0.5 kW, the results are shown in FIG. 4.1.

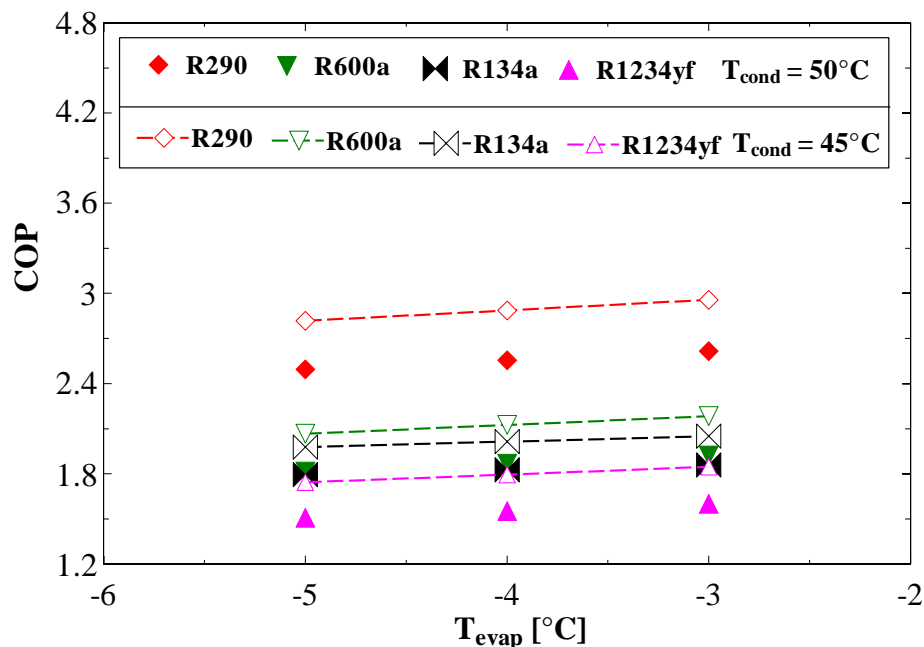


FIGURE 4.1 – COP behavior for the VCRES as a function of  $T_{evap}$  and  $T_{cond}$  for  $\dot{Q}_{evap.ref} = 0.5kW$   
SOURCE – de Paula et al. (2020b).

As noted in FIG. 4.1, all systems achieved the highest energy performance in the following thermodynamic condition:  $T_{evap} = -3^{\circ}C$  and  $T_{cond} = 45^{\circ}C$ . Only the system

with R1234yf does not have a higher energy performance than the system with R134a. Moreover, the system with R290 has the highest COP value. This result occurs because this system has the lowest electrical power consumption in the compressor ( $\dot{W}_{\text{comp}}$ ) due to the higher global efficiency ( $\eta_{\text{global}}$ ) and the lower refrigerant mass flow rate ( $\dot{m}_{\text{ref}}$ ) among the analyzed refrigerants. The mass flow rate of the R290 is the lowest because it has the smallest compressor displacement volume ( $V_{\text{cil}}$ ) and one of the lowest densities ( $\rho$ ).

The energy performance of the systems with R290, R1234yf, and R134a was again determined for the reference cooling capacity ( $\dot{Q}_{\text{evap.ref}}$ ) of 1.2 kW, but with the system operating with R744 in place of the system with R600a. The results are shown in FIG. 4.2.

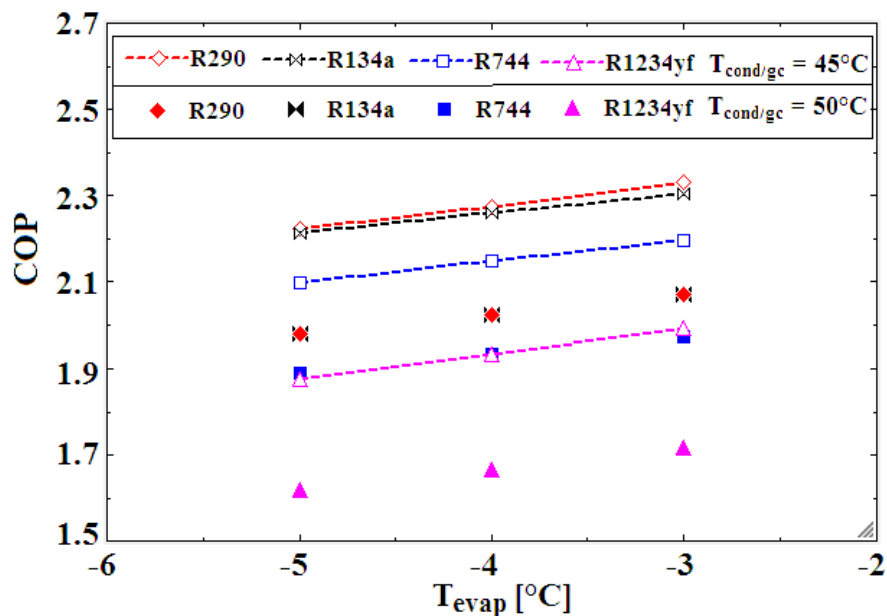


FIGURE 4.2 – COP behavior for the VCRES as a function of  $T_{\text{evap}}$  and  $T_{\text{cond/gc}}$  for  $\dot{Q}_{\text{evap.ref}} = 1.2\text{ kW}$   
SOURCE – Elaborated by the author.

Looking at FIG. 4.2 it is noted that also in this case all systems obtained the highest energy performance for condensation/gas cooling temperature of 45°C and evaporation temperature of -3°C. This time, only the COP of the system with R290 is greater than the COP of the system with R134a, although it was observed that the electrical power consumption in the compressor of the system with R290 is slightly higher than the electrical power consumption in the compressor of the system with R134a. The reason for the COP of the system with R290 is higher than the COP of the system with R134a is

because the system with R290 has greater cooling capacity. This fact can be explained by the greater variation of enthalpy in the evaporator of the system with R290.

Concerning other refrigerants, the COP of the system with R290 is higher mainly due to its lower electrical power consumption in the compressor because this system has the lowest mass flow rate and one of the highest global efficiency. In this context, the mass flow rate of the R290 is the lowest due to its lower density ( $\rho$ ) and one of the lowest compressor displacement volume ( $V_{cil}$ ).

In this thesis, all systems were modeled using for each analyzed refrigerant its specific volumetric and global efficiency curve. This procedure was performed to make the behavior of the modeled systems closer to their real behavior. Thus, in order to understand the relevance of using the procedure described. The COP of the systems with R290, R1234yf, R744, and R134a was calculated considering condensation/gas cooling temperature of 45°C and three different compression procedures: isentropic compression process, isentropic efficiency of 80%, and global efficiency curve for each refrigerant. The results are shown in FIG. 4.3.

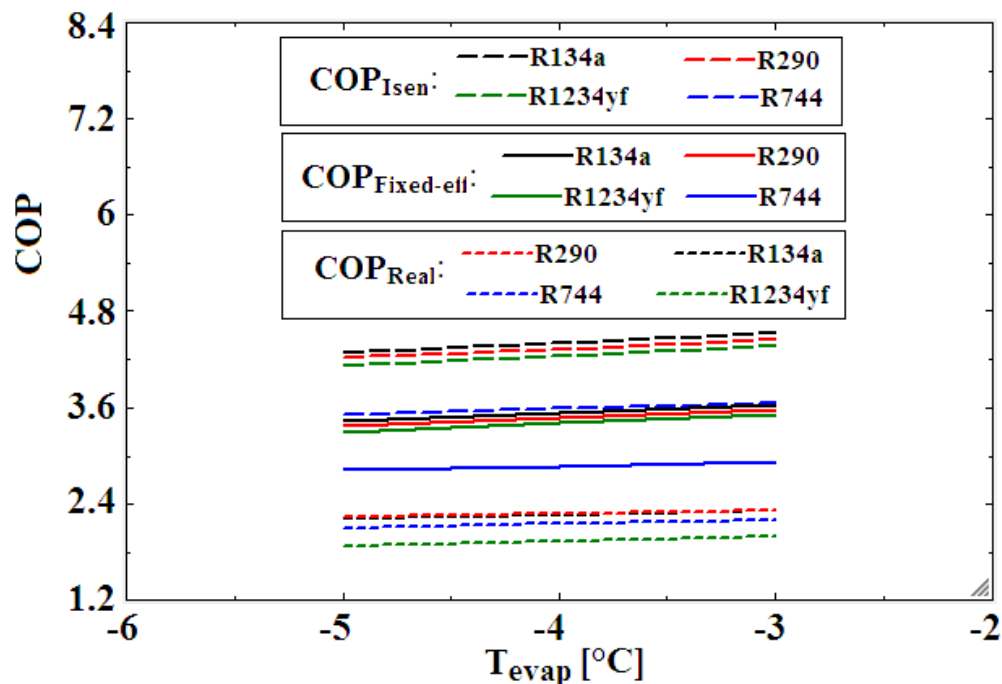


FIGURE 4.3 – COP behavior for three different compression procedures as a function of  $T_{evap}$   
SOURCE – Elaborated by the author.

As noted in FIG. 4.3, the isentropic compression process and the procedure of adopting a fixed value of isentropic efficiency caused distortions in the COP behavior. According to these procedures, the system with R134a has the highest performance, while

the system with R744 has the worse. However, when using for each refrigerant its global efficiency curve obtained from its compressor, it is observed that the system with R290 has the highest energy performance and the system operating with R1234yf has the worse. When analyzing FIG. 4.3 for the isentropic compression process and isentropic efficiency of 80%, it is observed that the COP values were overestimated for all systems compared to the COP values taking into account the real compression process (global efficiency curve). For example, for  $T_{\text{evap}} = -3^{\circ}\text{C}$  and  $T_{\text{cond/gc}} = 45^{\circ}\text{C}$ , the system with R290 has a real COP value approximately 53% lower than the COP value considering an isentropic efficiency of 80%. In addition, this real COP value is about 91% lower than the COP value considering an isentropic compression process.

Therefore, the observations above demonstrate that it is important to use the global and volumetric efficiency curve for each specific refrigerant to model the refrigeration system with a behavior similar to its behavior in practice.

Finally, after evaluating several possible combinations for  $D_{\text{REF}}$  and  $D_{\text{W}}$ , it was observed that the best combination for all studied systems in this thesis is  $D_{\text{REF}} = 6.36$  mm and  $D_{\text{W}} = 14$  mm for both evaporator and condenser/gas cooler, as illustrated in Appendix G.

## 4.2 Exergy analysis

The exergy performance ( $\eta_{\text{exergy}}$ ) of each system was also determined for different evaporation and condensation/gas cooling temperatures. For the reference cooling capacity of 0.5 kW, the results are shown in FIG. 4.4.

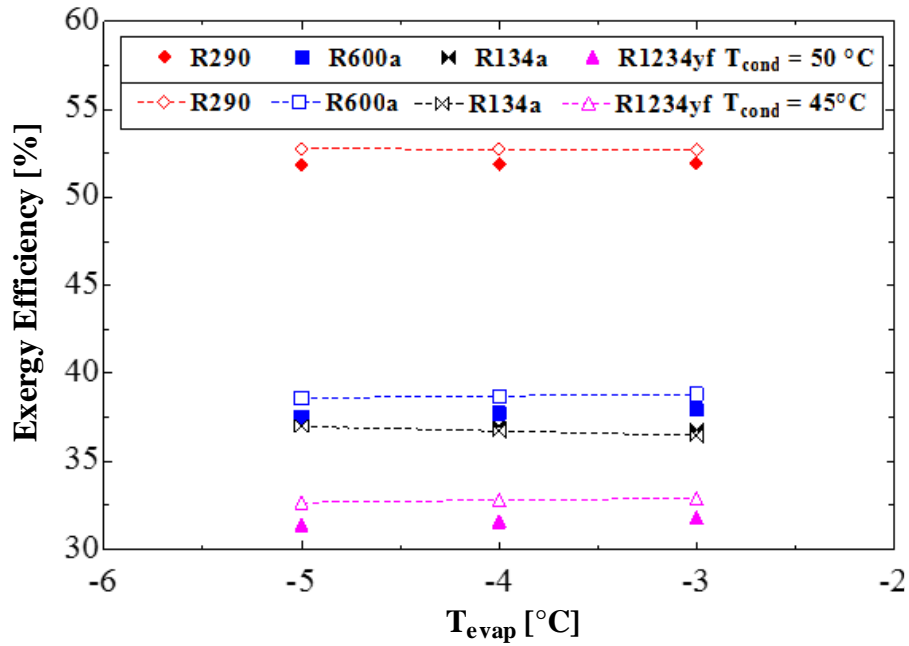


FIGURE 4.4 –  $\eta_{\text{exergy}}$  behavior for the VCRES as a function of  $T_{\text{evap}}$  and  $T_{\text{cond}}$  for  $\dot{Q}_{\text{evap,ref}} = 0.5\text{kW}$   
SOURCE – de Paula et al. (2020b).

In FIG. 4.4, the systems with R290 and R600a presented higher exergy performance than the system with R134a. The exergy efficiency of the system with R1234yf was the lowest. In addition, most of the evaluated systems achieved higher exergy performance for evaporation temperature of  $-3^{\circ}\text{C}$  and condensation temperature of  $45^{\circ}\text{C}$ , while almost all systems achieved lower exergy performance in the following thermodynamic condition:  $T_{\text{evap}} = -5^{\circ}\text{C}$  and  $T_{\text{cond}} = 50^{\circ}\text{C}$ .

To better understand the reason for these results presented in FIG. 4.4, the exergy destruction in each component as well as the total exergy destruction ( $\dot{E}_{\text{dest,total}}$ ) for each system were evaluated for the thermodynamic conditions mentioned. The results are shown in FIG. 4.5 and FIG. 4.6.



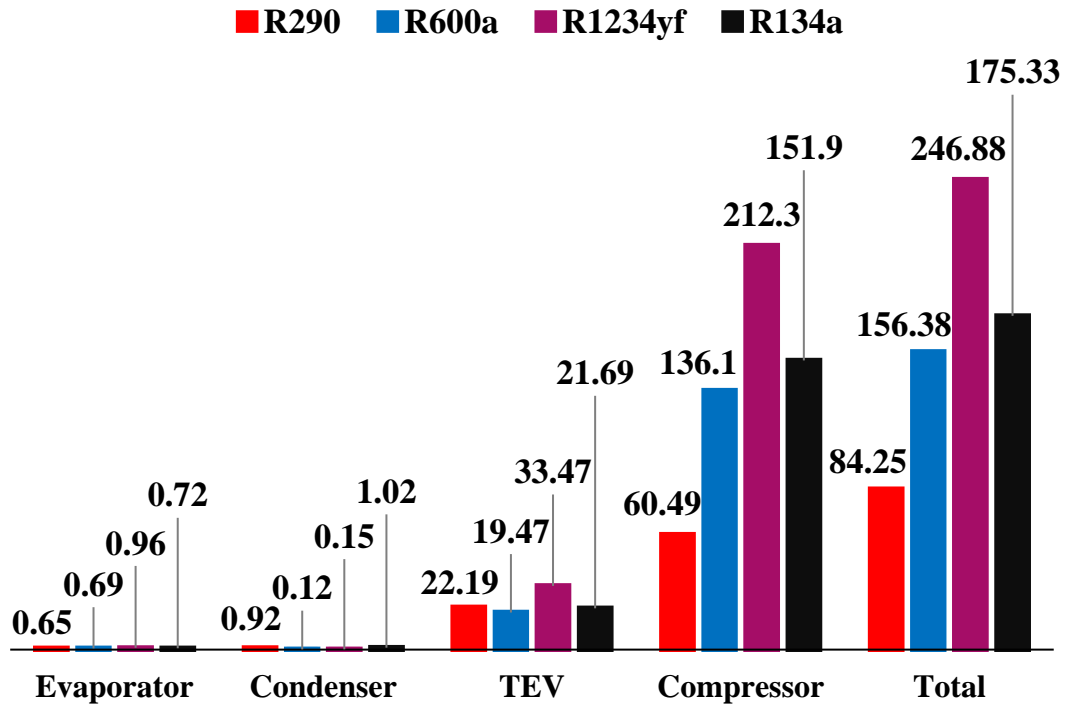


FIGURE 4.5 – Exergy destruction (W) in each component of the VCRS and  $\dot{E}_{dest,total}$  (W) for  $\dot{Q}_{evap,ref} = 0.5\text{kW}$ ,  $T_{evap} = -3^{\circ}\text{C}$  and  $T_{cond} = 45^{\circ}\text{C}$ .

SOURCE – de Paula et al. (2020b).

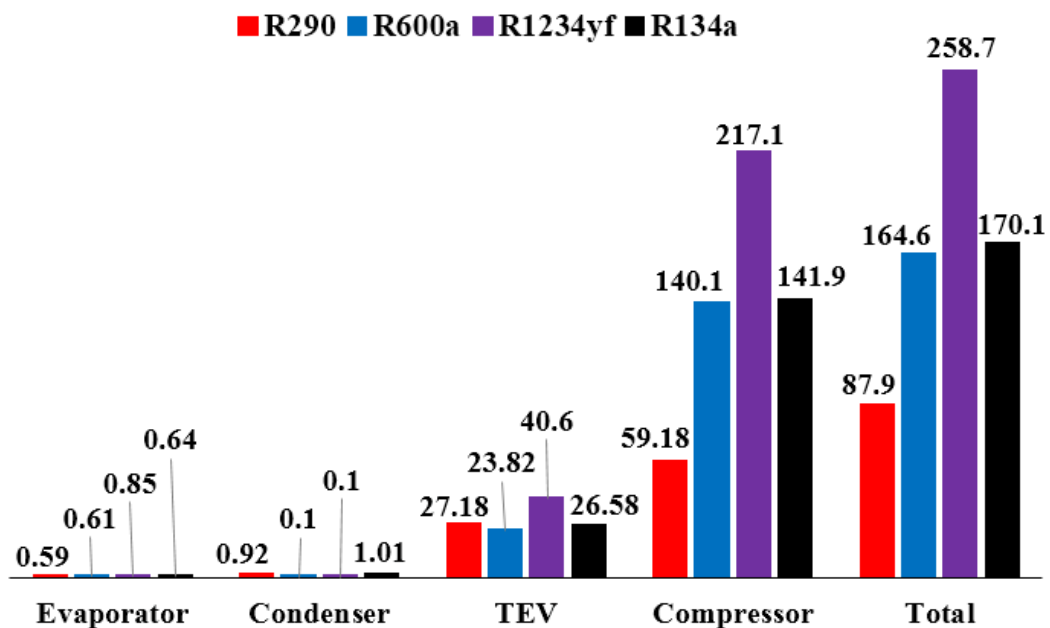


FIGURE 4.6 – Exergy destruction (W) in each component of the VCRS and  $\dot{E}_{dest,total}$  (W) for  $\dot{Q}_{evap,ref} = 0.5\text{kW}$ ,  $T_{evap} = -5^{\circ}\text{C}$  and  $T_{cond} = 50^{\circ}\text{C}$ .

SOURCE – Elaborated by the author.

Looking at FIG. 4.5 and FIG. 4.6, it is noted that almost all systems (except R134a) have higher total exergy destruction ( $\dot{E}_{dest,total}$ ) in the following thermodynamic

condition:  $T_{\text{evap}} = -5^{\circ}\text{C}$  and  $T_{\text{cond}} = 50^{\circ}\text{C}$ . Examining EQ. (3.24), it is clear that this parameter is one of the main factors that contributes to the reduction of exergy efficiency. For this reason, most systems have higher performance for the thermodynamic condition described in FIG. 4.5.

Based on the results presented in FIG. 4.5, the total exergy destruction in the system with R600a, R134a, and R1234yf is 85.6%, 108.1%, and 193% respectively higher than in the system with R290. The most significant amount of exergy destruction occurs in the compressor, and it corresponds to about 71.8%, 87%, 86% and 86.6% of the ( $\dot{E}_{\text{dest,total}}$ ) value in the system with R290, R600a, R1234yf and R134a, respectively. In the works of Shikalgar and Sapali (2019) and Altinkaynak et al. (2019), it was also observed that the greatest amount of exergy destruction occurs in the compressor. The difference between the values of exergy efficiency is mainly due to the exergy destruction in the compressor and it is related to the electrical power consumption in this component.

The behavior of the exergy efficiency of the systems operating with R290, R1234yf, R134a, and R744 for the reference cooling capacity of 1.2 kW was also evaluated considering different condensation/gas cooling and evaporation temperatures. The results are illustrated in FIG. 4.7.

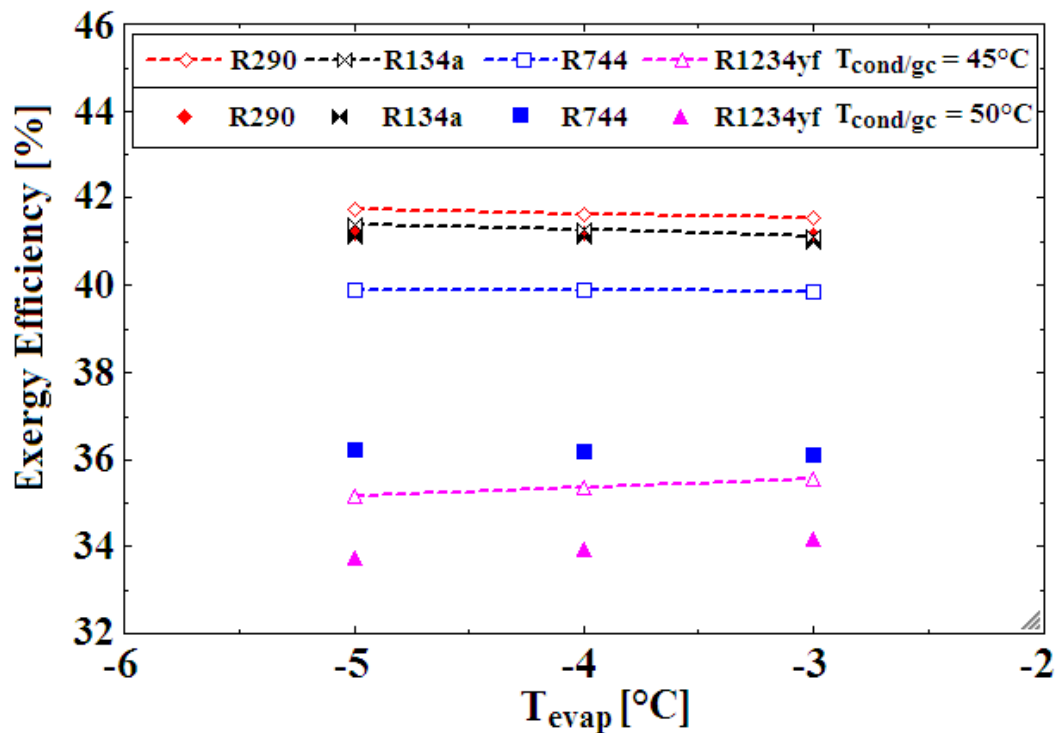


FIGURE 4.7 –  $\eta_{\text{exergy}}$  behavior for the VCRES as a function of  $T_{\text{evap}}$  and  $T_{\text{cond/gc}}$  for  $\dot{Q}_{\text{evap,ref}} = 1.2\text{kW}$   
SOURCE – Elaborated by the author.

Analyzing the FIG. 4.7, it is noted that almost all systems obtained higher exergy performance in the following thermodynamic condition:  $T_{\text{evap}} = -5^{\circ}\text{C}$  and  $T_{\text{cond/gc}} = 45^{\circ}\text{C}$ , while almost all systems achieved lower exergy performance in the following thermodynamic condition:  $T_{\text{evap}} = -3^{\circ}\text{C}$  and  $T_{\text{cond/gc}} = 50^{\circ}\text{C}$ .

In order to understand the reason for these results shown in FIG. 4.7, the exergy destruction in each component and the total exergy destruction for each system were evaluated and compared for the thermodynamic conditions described above. The results are shown in FIG. 4.8 and FIG. 4.9. After evaluating these results, it is noted that all systems have higher total exergy destruction for  $T_{\text{evap}} = -3^{\circ}\text{C}$  and  $T_{\text{cond/gc}} = 50^{\circ}\text{C}$ .

As explained earlier, this parameter is one of the main factors that contributes to the reduction of exergy efficiency. For this reason, the systems under study have higher exergy performance for the thermodynamic condition described in FIG. 4.8.

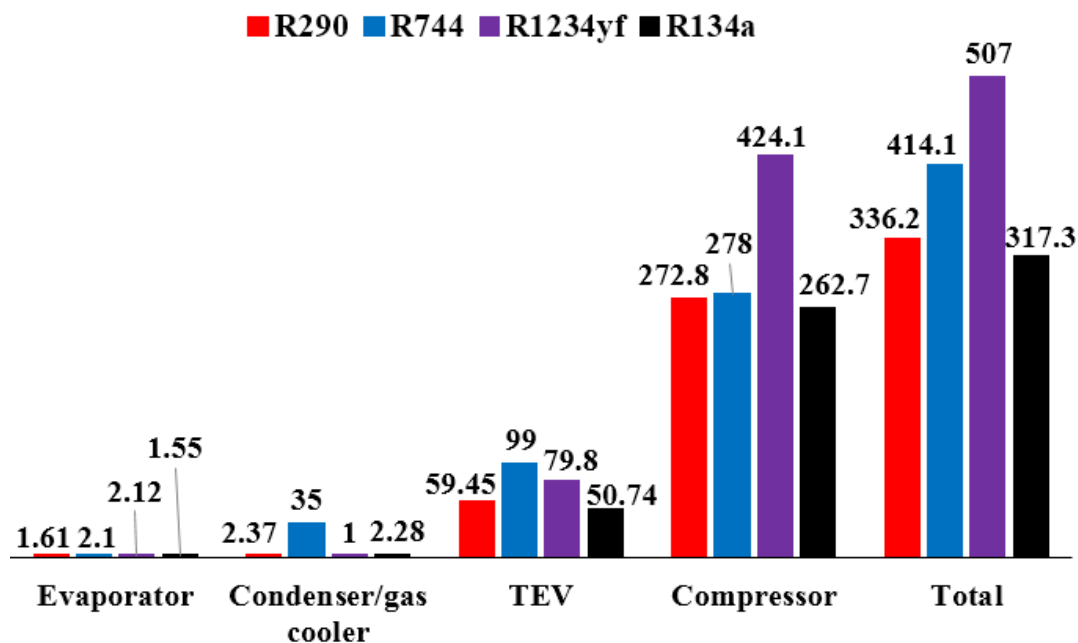


FIGURE 4.8 – Exergy destruction (W) in each component of the VCRS and  $\dot{E}_{\text{dest,total}}$  (W) for  $\dot{Q}_{\text{evap.ref}} = 1.2\text{kW}$ ,  $T_{\text{evap}} = -5^{\circ}\text{C}$  and  $T_{\text{cond/gc}} = 45^{\circ}\text{C}$ .

SOURCE – Elaborated by the author.

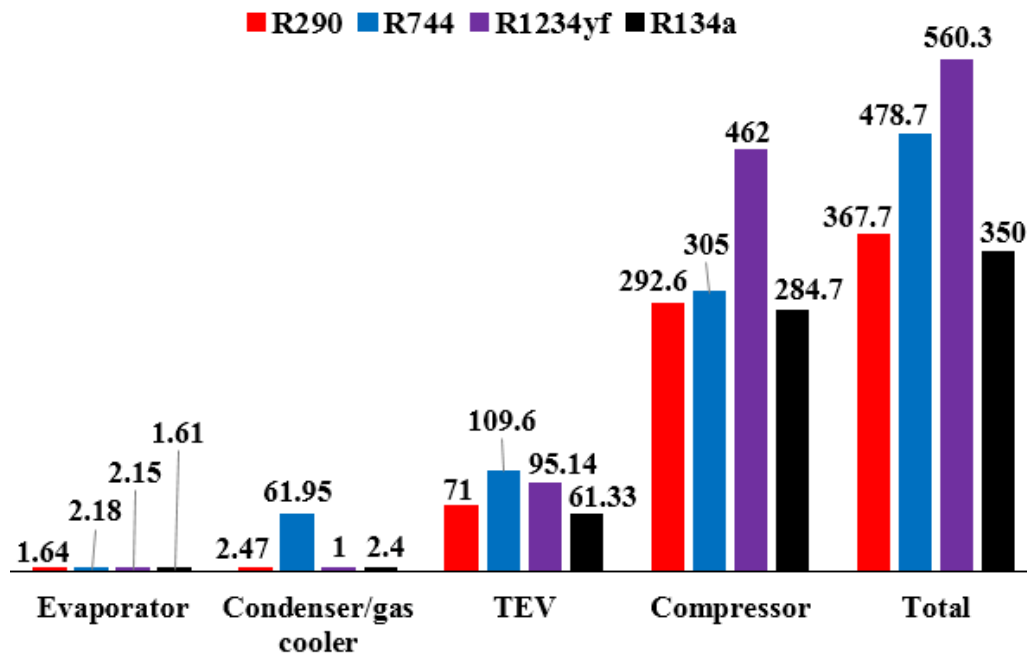


FIGURE 4.9 – Exergy destruction (W) in each component of the VCRS and  $\dot{E}_{dest,total}$  (W) for  $\dot{Q}_{evap,ref} = 1.2\text{kW}$ ,  $T_{evap} = -3^{\circ}\text{C}$  and  $T_{cond/gc} = 50^{\circ}\text{C}$ .

SOURCE – Elaborated by the author.

Among the systems analyzed, the system with R290 has the highest exergy performance. Most of the time, the exergy efficiency of the system with R290 is greater than the exergy efficiency of the other systems due to its lower total exergy destruction, as noted in FIG. 4.8 and FIG. 4.9. As noted earlier, the most significant amount of exergy destruction occurs in the compressor, and this corresponds to more than 80% of the  $\dot{E}_{dest,total}$  value in almost all systems.

However, the system with R290 has a higher exergy performance than the system with R134a, although the total exergy destruction in the system with R134a is less. According to EQ. (3.24), exergy performance ( $\eta_{exergy}$ ) takes into account the contribution of the following factors: total exergy destruction ( $\dot{E}_{dest,total}$ ) and electrical power consumption in the compressor ( $\dot{W}_{comp}$ ). As the  $\dot{E}_{dest,total}$  increases, the  $\eta_{exergy}$  decreases. However, as the  $\dot{W}_{comp}$  increases, the  $\eta_{exergy}$  increases. The reason that the  $\eta_{exergy}$  of the system with R290 is greater than the  $\eta_{exergy}$  of the system with R134a is due to the effect caused by  $\dot{W}_{comp}$  on  $\eta_{exergy}$  is greater than the effect caused by  $\dot{E}_{dest,total}$  on  $\eta_{exergy}$ . For the thermodynamic condition described in FIG. 4.8, the system with R290 has an  $\dot{E}_{dest,total}$  approximately 6% greater than the system with R134a. However, the system with R290 has a  $\dot{W}_{comp}$  approximately 6.5% higher than the system with R134a.

Another important aspect that can be observed in FIG. 4.8 and FIG. 4.9 is that the exergy destruction in the gas cooler of the system with R744 is markedly higher than the exergy destruction in the condenser of the other systems. Analyzing the EQ. (3.26), it was observed that this parameter is strongly influenced by the following variables: mass flow rate of the refrigerant, variation of enthalpy and variation of entropy. Thus, this system with R744 has greater exergy destruction in related to the other systems due to the better combined effect of these properties with its mass flow. This combined effect is largely obtained due to the large variation of enthalpy and entropy in the gas cooler because the system with R744 has a transcritical cycle.

Similar to the analysis carried out with the COP, the  $\eta_{\text{exergy}}$  the behavior of the systems with R290, R1234yf, R744, and R134a was analyzed considering condensation/gas cooling temperature of 45°C and two different compression procedures: isentropic efficiency of 80% and global efficiency curve for each refrigerant, obtained from the manufacturer. The results are shown in FIG. 4.10.

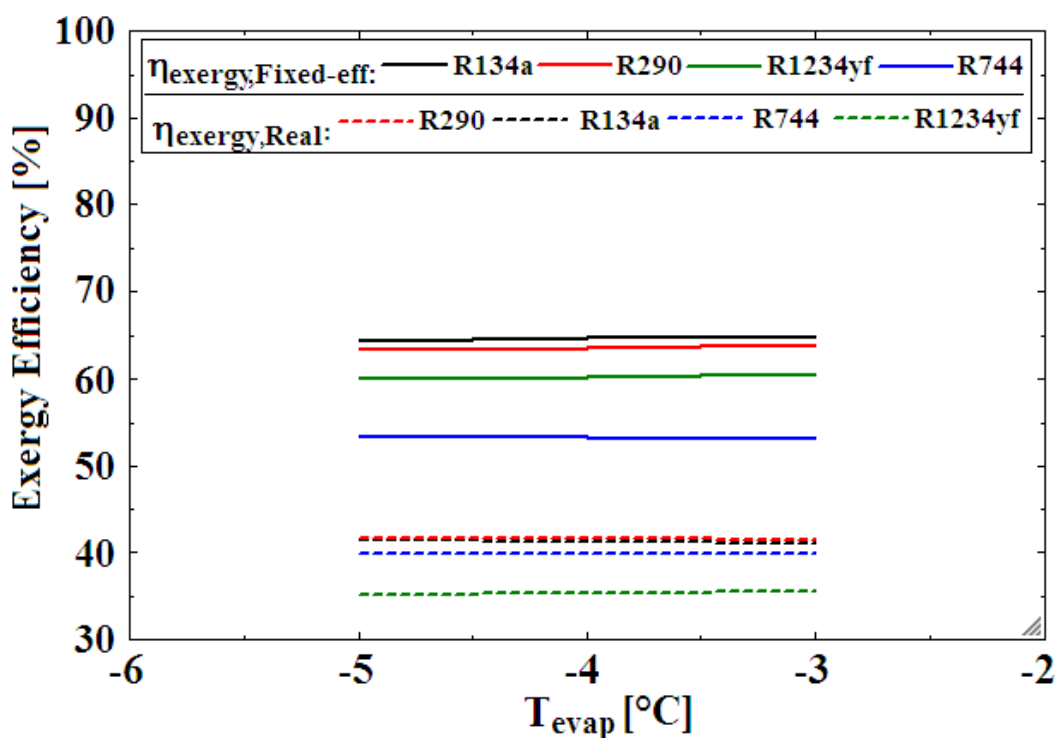


FIGURE 4.10 –  $\eta_{\text{exergy}}$  behavior for two different compression procedures as a function of  $T_{\text{evap}}$   
SOURCE – Elaborated by the author.

As noted in FIG. 4.10, the procedure of adopting a fixed value of isentropic efficiency also proved to be an inadequate approach again due to the same aspects mentioned in topic 4.1. For example, the system with R290 has a real  $\eta_{\text{exergy}}$  value

approximately 51.7% lower than the  $\eta_{\text{exergy}}$  value considering an isentropic efficiency of 80% for the following thermodynamic condition:  $T_{\text{evap}} = -5^{\circ}\text{C}$  and  $T_{\text{cond/gc}} = 45^{\circ}\text{C}$ .

Therefore, these observations again demonstrate the importance of using global and volumetric efficiency curves for each refrigerant to adapt the modeled system closer to its real behavior. In this topic, the best possible combination for  $D_{\text{REF}}$  and  $D_{\text{W}}$  on all systems was also  $D_{\text{REF}} = 6.36 \text{ mm}$  and  $D_{\text{W}} = 14 \text{ mm}$  for both evaporator and condenser/gas cooler, as illustrated in Appendix G.

### 4.3 Environmental analysis

The TEWI parameter was the environmental metric chosen to assess the environmental performance of the systems. This parameter was calculated considering different evaporation and condensation/gas cooling temperatures. For the reference cooling capacity of 0.5 kW and 1.2 kW, the results are shown in FIG. 4.11 and FIG. 4.12, respectively.

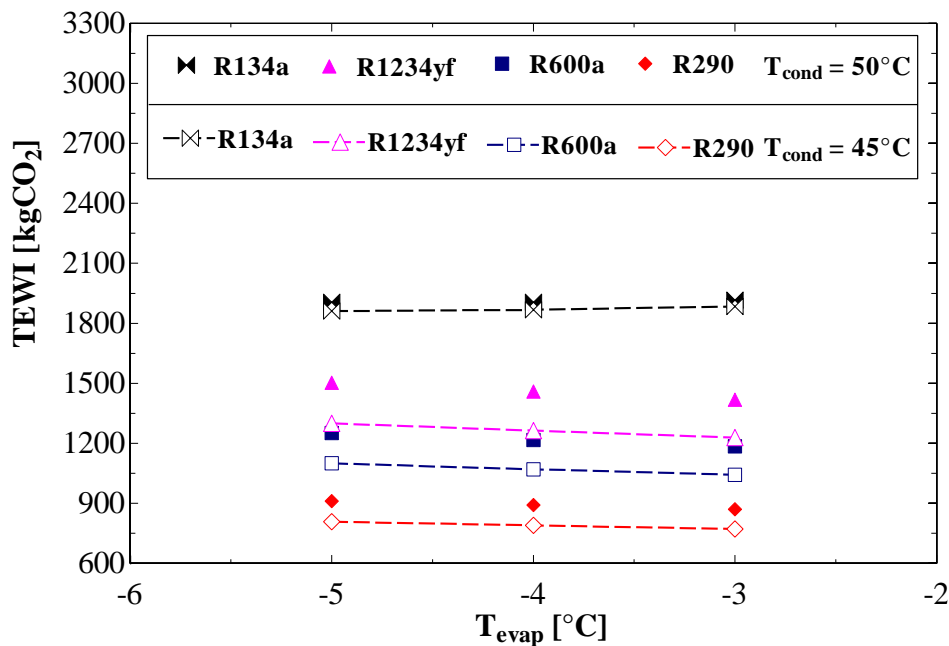


FIGURE 4.11 – TEWI behavior for the VCRS as a function of  $T_{\text{evap}}$  and  $T_{\text{cond}}$  for  $\dot{Q}_{\text{evap.ref}} = 0.5\text{kW}$   
SOURCE – de Paula et al. (2020b).

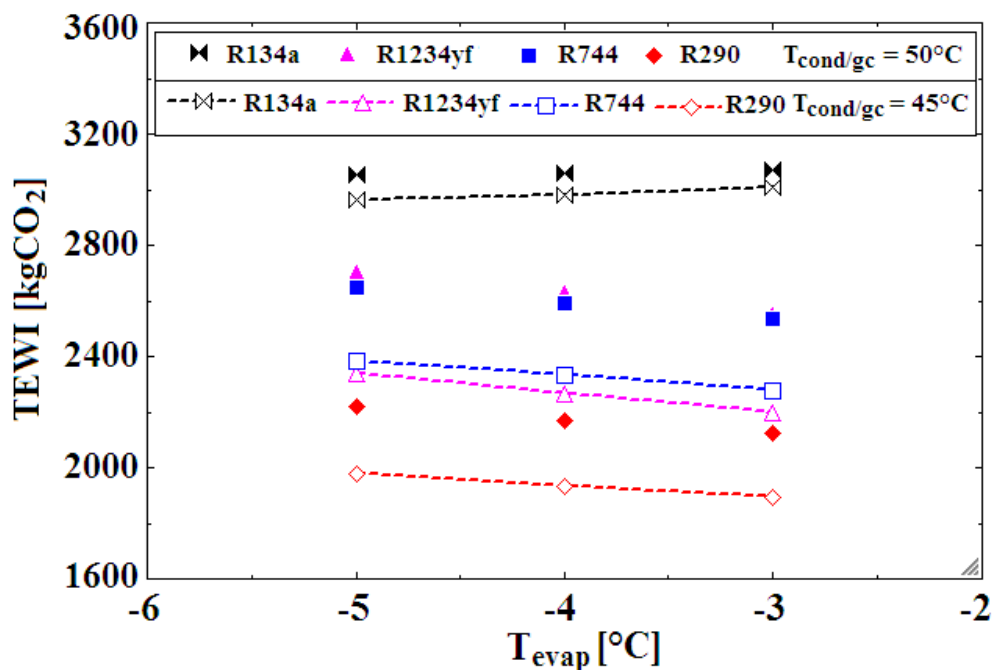


FIGURE 4.12 – TEWI behavior for the VCRS as a function of  $T_{\text{evap}}$  and  $T_{\text{cond/gc}}$  for  $\dot{Q}_{\text{evap,ref}} = 1.2\text{kW}$   
SOURCE – Elaborated by the author.

Analyzing the TEWI behavior in FIG. 4.11 and FIG. 4.12, all systems with ecological refrigerant have higher environmental performance (lower TEWI value) than the system with R134a, and the performance reached its maximum value for  $T_{\text{evap}} = -3^{\circ}\text{C}$  and  $T_{\text{cond/gc}} = 45^{\circ}\text{C}$ . For this thermodynamic condition, the system with R290 presented the highest environmental performance for both reference cooling capacities.

This fact was also obtained in Duarte et al. (2019a), where the system with R290 also achieved the highest energy and environmental performance for the following thermodynamic condition: solar radiation of  $500\text{ W/m}^2$ , the ambient temperature of  $25^{\circ}\text{C}$ , wind speed of  $0\text{ m/s}$ .

To obtain more information about the results presented in FIG. 4.11 and FIG. 4.12, the direct ( $\text{TEWI}_{\text{Direct}}$ ) and indirect ( $\text{TEWI}_{\text{INDirect}}$ ) emissions were determined for each system considering the thermodynamic condition where the systems achieved the highest performance. In addition, the refrigerant charge inside of the system was also calculated for each analyzed system. The results are illustrated in Tab. 4.1 for both the reference cooling capacity of  $0.5\text{ kW}$  and  $1.2\text{ kW}$ .

TABLE 4.1: TEWI values related to direct and indirect emissions.

$\dot{Q}_{\text{evap.ref}} = 0.5 \text{ kW}, T_{\text{evap}} = -3^\circ\text{C}, T_{\text{cond}} = 45^\circ\text{C}$				
Refrigerant	$m_{\text{ref,total}}$ [g]	TEWI [kgCO <sub>2</sub> ]	TEWI <sub>Direct</sub> [kgCO <sub>2</sub> ]	TEWI <sub>INDirect</sub> [kgCO <sub>2</sub> ]
R134a	261.8	1884	780	1104
R1234yf	302.3	1228	2.63	1225.37
R290	119.9	770.4	5.22	765.18
R600a	135.2	1042	5.88	1036.12
$\dot{Q}_{\text{evap.ref}} = 1.2 \text{ kW}, T_{\text{evap}} = -3^\circ\text{C}, T_{\text{cond/gc}} = 45^\circ\text{C}$				
Refrigerant	$m_{\text{ref,total}}$ [g]	TEWI [kgCO <sub>2</sub> ]	TEWI <sub>Direct</sub> [kgCO <sub>2</sub> ]	TEWI <sub>INDirect</sub> [kgCO <sub>2</sub> ]
R134a	372.6	3009	1110	1899
R1234yf	193.8	2198	1.69	2196.31
R290	187.1	1891	8.14	1882.86
R744	220.4	2277	0.48	2276.52

As noted in Tab. 4.1, the environmental impact due to indirect emissions (TEWI<sub>INDirect</sub>) is the most significant contribution, and it corresponds to 58.6% and 63.1% of TEWI value for the system with R134a for the reference cooling capacities of 0.5 kW and 1.2 kW, and more than 99% of TEWI value for other systems with ecological refrigerant in both situations. All tested refrigerants have a small GWP except R134a, as shown in Tab. 3.1. As can be observed in Tab. 4.1, the TEWI part linked to GWP (TEWI<sub>Direct</sub>) of the ecological refrigerants presented small values. The other part of TEWI (TEWI<sub>INDirect</sub>) has a strong relationship with the electrical power consumption in the compressor ( $\dot{W}_{\text{comp}}$ ).

In general, the systems with higher  $\dot{W}_{\text{comp}}$  values presented a higher contribution of TEWI<sub>INDirect</sub>. However, a notable exception can be observed for the reference cooling capacity of 1.2 kW, where the system with R290 has a lower TEWI<sub>INDirect</sub> value compared to the system with R134a, even the system with R290 having a higher  $\dot{W}_{\text{comp}}$  value. In this context, the operating time of the system ( $T_{\text{oper}}$ ) had more influence on TEWI<sub>INDirect</sub> compared to  $\dot{W}_{\text{comp}}$ . The operating time of the system with R134a is 6.1% higher, while the electrical power consumption in the compressor of the system with R290 é 5.3% higher.

Therefore, based on the results shown in Tab. 4.1 to reduce the environmental impact of a refrigeration system, it is not enough to choose a refrigerant based only on GWP, because this parameter does not evaluate the environmental impact related to indirect emissions as TEWI does. Thus, the TEWI parameter has proven to be a useful tool in the selection of the most suitable refrigerant.



Finally, the best possible combination for  $D_{REF}$  and  $D_W$  on all systems was also  $D_{REF} = 6.36$  mm and  $D_W = 14$  mm for both evaporator and condenser/gas cooler, as illustrated in Appendix G.

#### 4.4 Economic analysis

The economic performance is given by the total plant cost rate ( $\dot{C}_{total}$ ). This parameter was determined for three evaporation temperatures and two condensation/gas cooling temperatures. For the reference cooling capacity of 0.5 kW and 1.2 kW, the results are shown in FIG. 4.13 and FIG. 4.14, respectively. As explained earlier, for the  $\dot{Q}_{evap.ref} = 0.5$  kW, R744 was not analyzed because it does not have a commercial compressor in this capacity. For the same reason, R600a was not analyzed for  $\dot{Q}_{evap.ref} = 1.2$  kW.

Finally, it was observed that the best combination for all studied systems is  $D_{REF} = 6.36$  mm and  $D_W = 14$  mm for both evaporator and condenser/gas cooler, according to Appendix G.

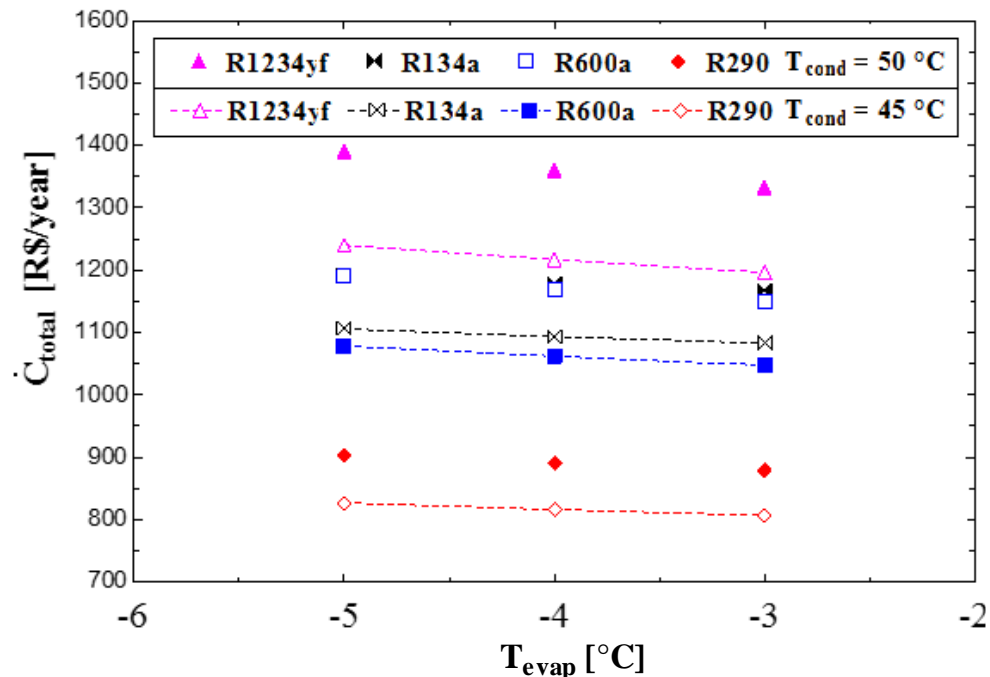


FIGURE 4.13 –  $\dot{C}_{total}$  behavior for the VCRCs as a function of  $T_{evap}$  and  $T_{cond}$  for  $\dot{Q}_{evap.ref} = 0.5$  kW  
SOURCE – de Paula et al. (2020b).

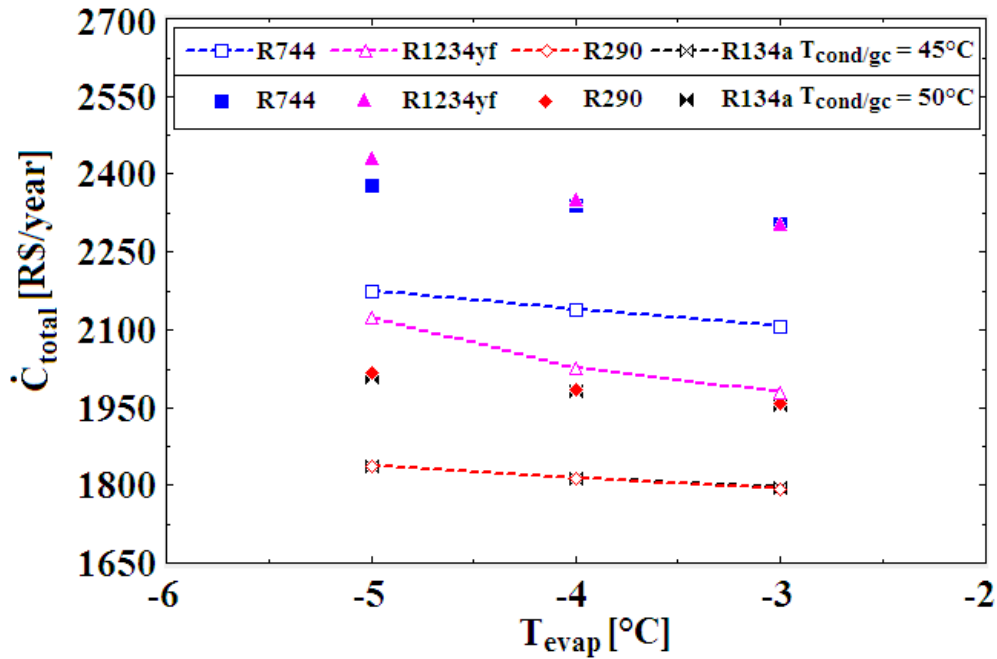


FIGURE 4.14 –  $\dot{C}_{\text{total}}$  behavior for the VCRES as a function of  $T_{\text{evap}}$  and  $T_{\text{cond/gc}}$  for  $\dot{Q}_{\text{evap.ref}} = 1.2\text{kW}$   
SOURCE – Elaborated by the author.

All evaluated systems have the lowest total plant cost rate (greater economic performance) for evaporation temperature of  $-3^{\circ}\text{C}$  and condensation/gas cooling temperature of  $45^{\circ}\text{C}$ . For reference cooling capacity of  $0.5\text{ kW}$ , only the systems with R290 and R600a have higher economic performance than the system with R134a, according to FIG. 4.13. However, for reference cooling capacity of  $1.2\text{ kW}$ , only the system with R290 has higher economic performance than the system with R134a, according to FIG. 4.14. These results occurred due to the  $\dot{C}_{\text{total}}$  value of these systems is lower than the  $\dot{C}_{\text{total}}$  value of the system with R134a.

To better understand the results presented in FIG. 4.13 and FIG. 4.14, the capital and maintenance cost rate ( $\dot{C}_{\text{CM}}$ ), the operational cost rate ( $\dot{C}_{\text{op}}$ ), the penalty cost rate due to  $\text{CO}_2$  emission ( $\dot{C}_{\text{env}}$ ) and the total plant cost rate ( $\dot{C}_{\text{total}}$ ) related to each system in the reference cooling capacities of  $0.5\text{ kW}$  and  $1.2\text{ kW}$  for  $T_{\text{evap}} = -3^{\circ}\text{C}$  and  $T_{\text{cond/gc}} = 45^{\circ}\text{C}$  are shown in FIG. 4.15 and FIG. 4.16, respectively.

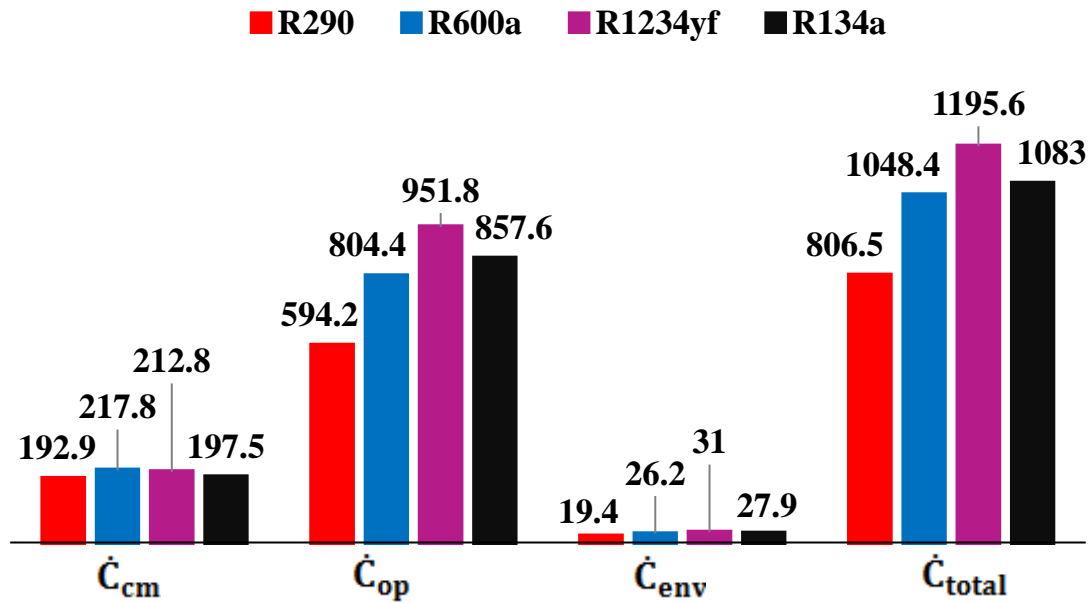


FIGURE 4.15 –  $\dot{C}_{total}$ ,  $\dot{C}_{cm}$ ,  $\dot{C}_{op}$ ,  $\dot{C}_{env}$  (R\$/year) related to each system for  $\dot{Q}_{evap.ref} = 0.5$  kW,  $T_{evap} = -3^{\circ}\text{C}$  and  $T_{cond} = 45^{\circ}\text{C}$   
SOURCE – de Paula et al. (2020b).

Analyzing the contribution of each of the three cost rates in  $\dot{C}_{total}$ , it is clear that the  $\dot{C}_{op}$  is the most relevant, and it corresponds to 73.7%, 76.7%, 79.6%, and 79.2% of the  $\dot{C}_{total}$  value for system with R290, R600a, R1234yf, and R134a, respectively, as noted in FIG. 4.15. The system with R1234yf has the highest  $\dot{C}_{op}$  value, while the system with R290 has the lowest. In this case, this result is exclusively due to the electrical power consumption ( $\dot{W}_{comp}$ ) because the operational cost rate has a direct relationship with this variable, according to Eq. (3.33). On the other hand, the  $\dot{C}_{env}$  is the least relevant cost rate, and it corresponds to 2.4%, 2.5%, 2.6%, and 2.6% of the  $\dot{C}_{total}$  value for the system with R290, R600a, R1234yf, and R134a, respectively. Finally, the  $\dot{C}_{CM}$  corresponds to 23.9%, 20.8%, 17.8%, and 18.2% of the  $\dot{C}_{total}$  value for the system with R290, R600a, R1234yf, and R134a, respectively. The contribution in percentage terms of the evaporator, condenser, compressor, TEV (thermostatic expansion valve), and pumps on the  $\dot{C}_{CM}$  value was evaluated for each system and it was observed that the evaporator and condenser are the components that most contribute, while the contribution of TEV is practically negligible compared to the other components. In this way, the contribution of the evaporator and condenser together corresponds to 69.8%, 70.5%, 71.5%, and 68.4% for the system with R134a, R290, R600a, and R1234yf, respectively.

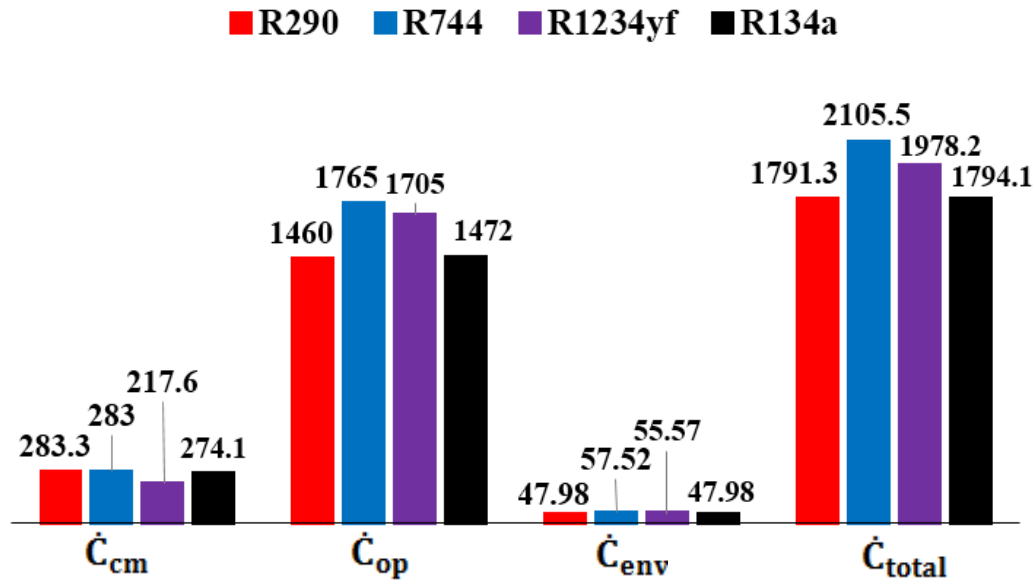


FIGURE 4.16 –  $\dot{C}_{total}$ ,  $\dot{C}_{cm}$ ,  $\dot{C}_{op}$ ,  $\dot{C}_{env}$  (R\$/year) related to each system for  $\dot{Q}_{evap.ref} = 1.2$  kW,  $T_{evap} = -3^{\circ}\text{C}$  and  $T_{cond/gc} = 45^{\circ}\text{C}$   
SOURCE – Elaborated by the author.

As noted in FIG. 4.16, it is also clear that the  $\dot{C}_{op}$  is the most relevant, corresponding to 81.5%, 83.8%, 86.2%, and 82% of the  $\dot{C}_{total}$  value for the system with R290, R744, R1234yf, and R134a, respectively. In this situation, the system with R744 has the highest  $\dot{C}_{op}$  value, while the system with R290 has the lowest. In most cases, this result is related to the electrical power consumption. However, the system with R744 has a higher  $\dot{C}_{op}$  value compared to the system with R1234yf due to the operating time of the system ( $T_{oper}$ ). This variable also has a direct relationship with the  $\dot{C}_{op}$  as well as the electrical power consumption, according to EQ. (3.34). The operating time of the system with R744 is 19.7% higher than the operating time of the system with R1234yf, while the electrical power consumption in the compressor of the system with R744 is 15.6% smaller than the electrical power consumption in the compressor of the system with R1234yf. Therefore, the effect caused by  $T_{oper}$  on  $\dot{C}_{op}$  value is greater than the effect caused by  $\dot{W}_{comp}$  on  $\dot{C}_{op}$  value for this case.

The  $\dot{C}_{env}$  is the least relevant cost rate, and it corresponds to 2.7%, 2.8%, 2.8%, and 2.7% of the  $\dot{C}_{total}$  value for the system with R290, R744, R1234yf, and R134a, respectively. Finally, the  $\dot{C}_{CM}$  corresponds to 15.8%, 13.4%, 11%, and 15.3% of the  $\dot{C}_{total}$  value for system with R290, R744, R1234yf, and R134a, respectively. The contribution in percentage terms of the evaporator, condenser/gas cooler, compressor, TEV (thermostatic expansion valve), and pumps on the  $\dot{C}_{CM}$  value was evaluated for each

individual system and it was observed that the evaporator and condenser/gas cooler are the components that most contribute, while the contribution of TEV is practically negligible compared to the other components. In this way, the contribution of the evaporator and condenser/gas cooler together corresponds to 63.1%, 62.9%, 62.3%, and 56.2% for the system with R134a, R290, R744, and R1234yf, respectively.

As observed in the results presented in topics 4.1 to 4.4, for evaporation temperature of  $-3^{\circ}\text{C}$  and condensation/gas cooling temperature of  $45^{\circ}\text{C}$ , it was the thermodynamic condition where almost all systems predominantly achieved higher energy, exergy, environmental, and economic performance. Moreover, for both evaporator and condenser/gas cooler, the best combination between  $D_{\text{REF}}$  and  $D_{\text{W}}$  on all systems was  $D_{\text{REF}} = 6.36$  mm and  $D_{\text{W}} = 14$  mm. Thus, the mathematical model was used to detail the geometric, energy, exergy, economic and environmental characteristics of each evaluated system for the mentioned thermodynamic condition, as shown in Tab. 4.2 and Tab. 4.3 for  $\dot{Q}_{\text{evap.ref}} = 0.5$  kW and  $\dot{Q}_{\text{evap.ref}} = 1.2$  kW, respectively. The values of the total plant cost rate of each system in (R\$/year) were converted in (USD/year), considering the CENTRAL BANK OF BRAZIL quotation on 06/24/2020. On this date, the US dollar had the following purchase price: 1 USD was equal to 5.2429 R\$.

TABLE 4.2: Geometric, energy, exergy, economic and environmental characteristics of each evaluated system for  $\dot{Q}_{\text{evap.ref}} = 0.5$  kW,  $T_{\text{evap}} = -3^{\circ}\text{C}$  and  $T_{\text{cond}} = 45^{\circ}\text{C}$

Vapor Compression Refrigeration Systems: Brazil ( $\beta = 0.082[\text{kgCO}_2/\text{kWh}]$ )											
Refrigerant	$\eta_{\text{global}}$ (%)	$\eta_{\text{v}}$ (%)	$L_{\text{cond}}$ (m)	$L_{\text{evap}}$ (m)	COP	TEWI ( $\text{kgCO}_2$ )	$\eta_{\text{exergy}}$ (%)	$\dot{C}_{\text{total}}$ (USD/year)	$\dot{E}_{\text{dest,total}}$ (W)	$T_{\text{oper}}$ (h/day)	V <sub>HW</sub> (liters)
R134a	44.9	75.8	7.58	17.84	2.05	1884	36.45	206.7	175	8.9	355
R1234yf	42.3	78.2	13.71	16.06	1.85	1228	32.91	228.2	247	7.4	357
<b>R290</b>	<b>66.1</b>	<b>83.3</b>	<b>7.54</b>	<b>16.84</b>	<b>2.96</b>	<b>770.4</b>	<b>52.71</b>	<b>153.9</b>	<b>84</b>	<b>9.6</b>	<b>356</b>
R600a	46.7	81.9	11.57	23.66	2.18	1042	38.81	200	156	9.0	353

TABLE 4.3: Geometric, energy, exergy, economic and environmental characteristics of each evaluated system for  $\dot{Q}_{\text{evap.ref}} = 1.2$  kW,  $T_{\text{evap}} = -3^{\circ}\text{C}$  and  $T_{\text{cond/gc}} = 45^{\circ}\text{C}$

Vapor Compression Refrigeration Systems: Brazil ( $\beta = 0.082[\text{kgCO}_2/\text{kWh}]$ )											
Refrigerant	$\eta_{\text{global}}$ (%)	$\eta_{\text{v}}$ (%)	$L_{\text{cond/gc}}$ (m)	$L_{\text{evap}}$ (m)	COP	TEWI ( $\text{kgCO}_2$ )	$\eta_{\text{exergy}}$ (%)	$\dot{C}_{\text{total}}$ (USD/year)	$\dot{E}_{\text{dest,total}}$ (W)	$T_{\text{oper}}$ (h/day)	V <sub>HW</sub> (liters)
R134a	50.7	72.2	16.98	28.18	2.31	3009	41.11	342.4	334	7.4	686
R1234yf	45.7	74.1	8.58	8.06	1.99	2198	35.56	377.5	523	6.0	692
<b>R290</b>	<b>52.0</b>	<b>79.9</b>	<b>18.34</b>	<b>29.77</b>	<b>2.33</b>	<b>1891</b>	<b>41.53</b>	<b>341.9</b>	<b>349</b>	<b>7.0</b>	<b>688</b>
R744	60.1	67.3	9.13	37.95	2.20	2277	39.84	401.8	422	7.2	819

Evaluating the results presented in Tab. 4.2 and Tab. 4.3 from a purely environmental point of view, all systems with ecological refrigerant can replace the

system with R134a, because these systems have a lower TEWI value. However, when analyzing the other parameters addressed in this thesis, the results clearly show in Tab. 4.2 that only the systems with R290 and R600a can replace the system with R134a for  $\dot{Q}_{\text{evap.ref}} = 0.5 \text{ kW}$ , whereas only the system com R290 can replace the system with R134a for  $\dot{Q}_{\text{evap.ref}} = 1.2 \text{ kW}$ , according to Tab. 4.3. In general, the most suitable candidate to replace old installations with R134a is the system with R290 in both situations. In addition, the values obtained for other variables are presented in Tab. 4.4 for each system evaluated for the reference cooling capacities of 0.5 kW and 1.2 kW.

TABLE 4.4: Values obtained for other variables for each evaluated system

$\dot{Q}_{\text{evap.ref}} = 0.5 \text{ kW}, T_{\text{evap}} = -3^{\circ}\text{C}, T_{\text{cond}} = 45^{\circ}\text{C}$										
VCRS	$\dot{m}_{\text{ref}}$ [kg/h]	$\dot{m}_{\text{w;evap}}$ [kg/h]	$\dot{m}_{\text{w;cond/gc}}$ [kg/h]	$U_{\text{evap}}$ [W/m <sup>2</sup> ]	$U_{\text{cond/gc}}$ [W/m <sup>2</sup> ]	$\dot{W}_{\text{comp}}$ [kW]	$\dot{W}_{\text{total}}$ [kW]	$\dot{Q}_{\text{evap}}$ [kW]	$A_{\text{evap}}$ [m <sup>2</sup> ]	$A_{\text{cond/gc}}$ [m <sup>2</sup> ]
R134a	13.88	69.58	39.58	198.3	285.5	0.2758	0.2761	0.566	0.357	0.152
R1234yf	21.68	84.10	48.20	266.3	271.2	0.3680	0.3703	0.684	0.321	0.274
R290	6.88	64.89	37.05	195.9	271.9	0.1781	0.1782	0.527	0.337	0.151
R600a	7.71	67.88	38.54	147.5	281.1	0.2555	0.2560	0.558	0.473	0.231
$\dot{Q}_{\text{evap.ref}} = 1.2 \text{ kW}, T_{\text{evap}} = -3^{\circ}\text{C}, T_{\text{cond/gc}} = 45^{\circ}\text{C}$										
VCRS	$\dot{m}_{\text{ref}}$ [kg/h]	$\dot{m}_{\text{w;evap}}$ [kg/h]	$\dot{m}_{\text{w;cond/gc}}$ [kg/h]	$U_{\text{evap}}$ [W/m <sup>2</sup> ]	$U_{\text{cond/gc}}$ [W/m <sup>2</sup> ]	$\dot{W}_{\text{comp}}$ [kW]	$\dot{W}_{\text{total}}$ [kW]	$\dot{Q}_{\text{evap}}$ [kW]	$A_{\text{evap}}$ [m <sup>2</sup> ]	$A_{\text{cond/gc}}$ [m <sup>2</sup> ]
R134a	32.15	161.2	91.68	290.9	295.3	0.567	0.568	1.31	0.563	0.339
R1234yf	51.47	199.60	114.40	1259	1029	0.810	0.814	1.63	0.161	0.171
R290	18.14	171.1	97.65	292.2	294.7	0.596	0.598	1.39	0.595	0.366
R744	31.03	166.1	112.8	239.7	670	0.701	0.702	1.54	0.758	0.182

To qualitatively verify if the results generated by the proposed mathematical model are consistent, the data presented in Tab. 4.2 and Tab. 4.3 were compared with the results of experimental (Jarall S. (2012), Sánchez et al. (2017), Navarro-Esbrí et al. (2013)) and numerical (Baakeem et al. (2018)) works found in the literature for similar systems (systems operating with the same refrigerant and similar thermodynamic condition). This procedure was used to verify if the tendency and the order of magnitude of the parameters evaluated are consistent. The data found in the literature were not suitable to validate the mathematical model presented in this thesis, because although the compared systems are similar, they have different characteristics, such as type of heat exchangers and compressor.

The results of COP presented in Tab. 4.3 for the systems with R134a and R1234yf were compared with the results provided by Jarall S. (2012), for systems with the same refrigerants and in the same thermodynamic conditions. The COP obtained by Jarall S. (2012) for the system with R134a was 2.23, while the COP for the system with R1234yf was 2.14. As can be seen, the COP values shown in Tab. 4.3 for the systems

with R134a and R1234yf have an order of magnitude similar to the COP values described by Jarall S. (2012).

The COP values shown in Tab. 4.2 for the systems with R134a, R1234yf, R600a, and R290 were compared with the values presented by Sánchez et al. (2017) for systems with the same refrigerant and in the following thermodynamic condition:  $T_{\text{evap}} = 0^{\circ}\text{C}$  and  $T_{\text{cond}} = 45^{\circ}\text{C}$ . The COP values obtained by Sánchez et al. (2017) for the system with R134a, R1234yf, R600a, and R290 were 2.05, 1.85, 1.86, and 2.15, respectively. As noted, the COP values of the systems shown in Tab. 4.2 have an order of magnitude similar to the COP values described by Sánchez et al. (2017).

The COP shown in Tab. 4.3 for the systems with R134a and R1234yf were compared with the values presented by Navarro-Esbrí et al. (2013) for system with R134a and R1234yf in the following condition:  $T_{\text{evap}} = -7.5^{\circ}\text{C}$  and  $T_{\text{cond}} = 50^{\circ}\text{C}$ . The COP value obtained by Navarro-Esbrí et al. (2013) for the system with R134a was 2.3, while the COP value for the system with R1234yf was 1.7. Analyzing the results, the COP values shown in Tab. 4.3 for the systems with R134a and R1234yf have an order of magnitude similar to the COP values for the systems described by Navarro-Esbrí et al. (2013).

Analyzing the comparisons above, it is observed that the proposed model is consistent, because the difference between the results obtained for the modeled systems concerning the results presented by Jarall S. (2012), Sánchez et al. (2017) and Navarro-Esbrí et al. (2013) is small. This difference may be related to the difference between the compared systems and mainly due to the modeling of the compression process. In this thesis, the compression process was modeled using volumetric and global efficiency curves obtained from the specific compressor for each refrigerant, while in the works of Jarall S. (2012), Sánchez et al. (2017) and Navarro-Esbrí et al. (2013) were adopted an isentropic compression process. In addition, the authors used the same compressor for all tested refrigerants.

The results of  $\eta_{\text{exergy}}$  and  $\dot{C}_{\text{total}}$  presented in Tab. 4.2 for the system with R1234yf were compared to the results provided by Baakeem et al. (2018), for a system operating with R1234yf in the following thermodynamic condition:  $T_{\text{evap}} = 0^{\circ}\text{C}$  and  $T_{\text{cond}} = 45^{\circ}\text{C}$ . The  $\eta_{\text{exergy}}$  and  $\dot{C}_{\text{total}}$  values for the system described by Baakeem et al. (2018) were 31.7% and 625 USD for the reference the year considered. Analyzing the results, the  $\eta_{\text{exergy}}$  value shown in Tab. 4.2 for the system with R1234yf has an order of magnitude

similar to the  $\eta_{\text{exergy}}$  value for the system with R1234yf described by Baakeem et al. (2018), whereas the  $\dot{C}_{\text{total}}$  value shown in Tab. 4.2 for the system with R1234yf is much lower. This difference in the  $\dot{C}_{\text{total}}$  values between the systems occurs because the system studied by Baakeem et al. (2018) has more components and consumes more electrical power during the compression process (system composed of two compressors). As noted in Eqs. (3.32) and (3.34), these factors increase the cost rates due to  $\dot{C}_{\text{CM}}$  and  $\dot{C}_{\text{op}}$ . Thus, the total plant cost rate ( $\dot{C}_{\text{total}}$ ) increases.

Finally, Tab. 4.5 summarizes the parameters compared above for each refrigeration system analyzed.

TABLE 4.5: Summary of the parameters compared in each refrigeration system analyzed.

<b>SYSTEMS OPERATING WITH R1234yf</b>					
<b>Compared results</b>	<b>T<sub>evap</sub> [°C]</b>	<b>T<sub>cond/gc</sub> [°C]</b>	<b>COP</b>	<b><math>\eta_{\text{exergy}}</math> [%]</b>	<b><math>\dot{C}_{\text{total}}</math> [USD/year]</b>
Jarall S. (2012)	-3	45	2.14		
Table 4.3	-3	45	1.99		
Sánchez et al. (2017)	0	45	1.85		
Table 4.2	-3	45	1.85		
Navarro-Esbrí et al. (2013)	-7.5	50	1.70		
Table 4.3	-3	45	1.99		
Baakeem et al. (2018)	0	45		31.7	625
Table 4.2	-3	45		32.9	228.1
<b>SYSTEMS OPERATING WITH R134a</b>					
<b>Compared results</b>	<b>T<sub>evap</sub> [°C]</b>	<b>T<sub>cond/gc</sub> [°C]</b>	<b>COP</b>	<b><math>\eta_{\text{exergy}}</math> [%]</b>	<b><math>\dot{C}_{\text{total}}</math> [USD/year]</b>
Jarall S. (2012)	-3	45	2.23		
Table 4.3	-3	45	2.31		
Sánchez et al. (2017)	0	45	2.05		
Table 4.2	-3	45	2.05		
Navarro-Esbrí et al. (2013)	-7.5	50	2.30		
Table 4.3	-3	45	2.31		
<b>SYSTEMS OPERATING WITH R600a</b>					
<b>Compared results</b>	<b>T<sub>evap</sub> [°C]</b>	<b>T<sub>cond/gc</sub> [°C]</b>	<b>COP</b>	<b><math>\eta_{\text{exergy}}</math> [%]</b>	<b><math>\dot{C}_{\text{total}}</math> [USD/year]</b>
Sánchez et al. (2017)	0	45	1.86		
Table 4.2	-3	45	2.18		
<b>SYSTEMS OPERATING WITH R290</b>					
<b>Compared results</b>	<b>T<sub>evap</sub> [°C]</b>	<b>T<sub>cond/gc</sub> [°C]</b>	<b>COP</b>	<b><math>\eta_{\text{exergy}}</math> [%]</b>	<b><math>\dot{C}_{\text{total}}</math> [USD/year]</b>
Sánchez et al. (2017)	0	45	2.15		
Table 4.2	-3	45	2.96		



## 5 CONCLUSIONS

In this thesis, a thermo-economic and environmental analysis of a vapor compression refrigeration system operating with different ecological refrigerants was performed. The parameters used to compare the energy, exergy, environmental, and economic performance were COP,  $\eta_{\text{exergy}}$ , TEWI and  $\dot{C}_{\text{total}}$ , respectively. For both reference cooling capacities of 0.5 kW and 1.2 kW, the analysis of these parameters indicates that the system operating with R290 is the most suitable to replace old systems with R134a. Moreover, this system operated with higher thermo-economic and environmental performance in the following thermodynamic condition:  $T_{\text{evap}} = -3^{\circ}\text{C}$  and  $T_{\text{cond/gc}} = 45^{\circ}\text{C}$ .

Investigating the contribution of cost rates related to the  $\dot{C}_{\text{total}}$  value in each evaluated system, it was observed that the operational cost rate ( $\dot{C}_{\text{op}}$ ) was the most relevant cost, whereas the penalty due to CO<sub>2</sub> emission ( $\dot{C}_{\text{env}}$ ) was the least relevant cost. For the system operating with R290 and reference cooling capacity of 0.5 kW, the  $\dot{C}_{\text{op}}$ ,  $\dot{C}_{\text{cm}}$  and  $\dot{C}_{\text{env}}$  were respectively 73.7%, 23.9% and 2.4% of the  $\dot{C}_{\text{total}}$  value, while the  $\dot{C}_{\text{op}}$ ,  $\dot{C}_{\text{cm}}$  and  $\dot{C}_{\text{env}}$  of this system are respectively 81.5%, 15.8% and 2.7% of the  $\dot{C}_{\text{total}}$  value for reference cooling capacity of 1.2 kW.

The COP and  $\eta_{\text{exergy}}$  of each system were calculated considering different compression procedures: isentropic efficiency of 80% and global efficiency curve for each refrigerant. The results showed that the procedure of adopting a fixed value of isentropic efficiency caused distortions in the behavior of the COP and  $\eta_{\text{exergy}}$ . For  $\dot{Q}_{\text{evap.ref}} = 1.2 \text{ kW}$ ,  $T_{\text{evap}} = -3^{\circ}\text{C}$  and  $T_{\text{cond/gc}} = 45^{\circ}\text{C}$ , the system with R290 has a real COP value approximately 53% lower than the COP value considering an isentropic efficiency of 80% while the real  $\eta_{\text{exergy}}$  value is 51.7% lower than the  $\eta_{\text{exergy}}$  value considering an isentropic efficiency of 80%. Therefore, the results described above show that the methodology of using volumetric and global efficiency curve is an interesting procedure to be applied in modeling work of a refrigeration system because this method makes the behavior of the modeled system close to its real behavior.

One feature of this thesis was the use of commercial diameters in the modeling of the heat exchangers. In this way, a series of possible combinations between  $D_{\text{REF}}$  (diameter for the refrigerant side) and  $D_w$  (diameter for the waterside) were analyzed,

where it was observed that the best combination in all studied systems is  $D_{REF} = 6.36$  mm and  $D_W = 14$  mm.

Finally, the results obtained by the model developed in this thesis were compared with the results obtained by different experimental and numerical works considering similar refrigeration systems. The simulation data produced by the proposed mathematical model were consistent with the results presented by the experimental and numerical works analyzed in this study.

## REFERENCES

- Ahamed J.U., Saidur R., Masjuki H. H. A review on exergy analysis of vapor compression refrigeration system. **Renewable and Sustainable Energy Reviews**, v. 15, n. 3, p. 1593-1600, 2011.
- Altinkaynak M., Olgun E., Şahin A. Ş. Comparative Evaluation of Energy and 24 Exergy Performances of R22 and its Alternative R407C, R410A and R448A Refrigerants in Vapor Compression Refrigeration Systems. **El-Cezeri Journal of Science and Engineering**, v. 6, n. 3, p. 659-667, 2019.
- Aminyavari, M., Najafi, B., Shirazi, A., Rinaldi, F. Exergetic, economic and environmental (3E) analyses, and multi-objective optimization of a CO<sub>2</sub>/NH<sub>3</sub> cascade refrigeration system. **Applied Thermal Engineering**, v. 65, n. 1-2, p. 45-50, 2014.
- Antunes, A. H. P., Bandarra F., E. P. Experimental investigation on the performance and global environmental impact of a refrigeration system retrofitted with alternative refrigerants. **International Journal of Refrigeration**, v.70, p.119-127, 2016.
- ARIAH. The Australian Institute of Refrigeration, Air Conditioning and Heating Methods of calculating Total Equivalent Warning Impact (TEWI), 2012.
- Baakeem, S. S., Orfi, J., Alabdulkarem, A. Optimization of a multistage vapor-compression refrigeration system for various refrigerants. **Applied Thermal Engineering**, v. 136, p. 84-96, 2018.
- BANCO CENTRAL DO BRASIL, Home Page <<https://www.bcb.gov.br/estabilidadefinanceira/historicocotacoes>>Accessed on:06/21/2021.
- Baroczy, C. Correlation of liquid fraction in two-phase flow with application to liquid metals. **Atomics international**, 1963.
- Belman-Flores J. M., Rodríguez-Muñoz A. P., Pérez-Reguera C. G., Mota-Babiloni A. Experimental study of R1234yf as drop-in replacement for R134a in a domestic refrigerator. **International Journal of Refrigeration**, v. 81, p. 1-11, 2017.
- Bergman, T. L., Incropera, F. P., Dewitt, D. P., Lavine, A. S. **Fundamentals of heat and mass transfer**. 7. ed. Hoboken: John Wiley & Sons, 2011.
- Çengel, Y. A., Boles, M. A. Thermodynamics: An engineering approach. 6. ed (SI Units). The McGraw-Hill Companies, Inc., New York, 2007.
- Choi S., Oh J. H. Y., Lee H. Life cycle climate performance evaluation (LCCP) on cooling and heating systems in South Korea. **Applied thermal engineering**, v. 120, p. 88-98, 2017.
- Churchill, S. W. Friction-factor equation spans all fluid flow regimes. **Chemical engineering**, MCGRAW HILL INC, NEW YORK, v.84, n.24, p.91-92, 1977.
- Collier, John G.; Thome, John R. **Convective boiling and condensation**. Clarendon Press, 1994.

Da Riva, E., Del Col, D. Performance of a semi-hermetic reciprocating compressor with propane and mineral oil. **International Journal of Refrigeration**, v. 34, n. 3, p. 752-763, 2011.

de Paula, C. H., Duarte, W. M., Rocha, T. T. M., de Oliveira, R. N., Maia, A. A. T. Environmental and energy performance evaluation of the R1234yf as an environmentally friendly alternative to R134a. **In: 25<sup>th</sup> ABCM International Congress of Mechanical Engineering**, 2019.

de Paula, C. H., Duarte, W. M., Rocha, T. T. M., de Oliveira, R. N., Maia, A. A. T. Optimal design and environmental, energy and exergy analysis of a vapor compression refrigeration system using R290, R1234yf, and R744 as alternatives to replace R134a. **International Journal of Refrigeration**, v. 113, p. 10-20, 2020a.

de Paula, C. H.; Duarte, W. M.; Rocha, T. T. M.; de Oliveira, R. N.; de Paoli Mendes, R.; Maia, A. A. T. Thermo-economic and environmental analysis of a small capacity vapor compression refrigeration system using R290, R1234yf, and R600a. **International Journal of Refrigeration**, 2020b.

Duarte, W. M. **Numeric model of a direct expansion solar assisted heat pump water heater operating with low GWP refrigerants (R1234yf, R290, R600a and R744) for replacement of R134a**. 2018. PhD thesis-UFGM.

Duarte W. M., Paulino T. F., Pabon J. J. G., Sawalha S., Machado L. Refrigerants selection for a direct expansion solar assisted heat pump for domestic hot water. **Solar Energy**, v. 184, p. 527-538, 2019a.

Duarte, W. M., Tavares, S. G., Paulino, T. F., Machado, L., Maia, A. A. T. Feasibility of solar geothermal hybrid source heat pump for producing domestic hot water in Brazilian climates. **In: 25<sup>th</sup> ABCM International Congress of Mechanical Engineering**, 2019b.

Faria, R. N., Nunes, R. O., Koury, R. N. N., Machado, L. Dynamic modeling study for a solar evaporator with expansion valve assembly of a transcritical CO<sub>2</sub> heat pump. **International Journal of Refrigeration**, v. 64, p. 203-213, 2016.

Fazelpour F., Morosuk T. Exergoeconomic analysis of carbon dioxide transcritical refrigeration machines. **International Journal of Refrigeration**, v. 38, p. 128-139, 2014.

Fischer, S. K. Total equivalent warming impact: a measure of the global warming impact of CFC alternatives in refrigerating equipment. **International Journal of Refrigeration**, v. 16, n. 6, p. 423-428, 1993.

Garcia, J., Ali, T., Duarte, W. M., Khosravi, A., Machado, L. Comparison of transient response of an evaporator model for water refrigeration system working with R1234yf as a drop-in replacement for R134a. **International Journal of Refrigeration**, v. 91, p. 211-222, 2018.

Gill, J., Singh, J., Ohunakin, O. S., Adelekan, D. S. Exergy analysis of vapor compression

refrigeration system using R450A as a replacement of R134a. **Journal of Thermal Analysis and Calorimetry**, v. 136, n. 2, p. 857-872, 2019.

Gnielinski, V. New equations for heat and mass transfer in turbulent pipe and channel flow. **Int. Chem. Eng.**, v. 16, n. 2, p. 359-368, 1976.

Hughmark, G. A. Holdup in gas-liquid flow. **Chemical Engineering Progress**, v. 58, n. 4, p. 62-65, 1962.

Humia, G. M. **Estudo experimental e modelo de simulação para a determinação do inventário em sistemas de refrigeração carregados com os fluidos R134a e HFO-1234yf**. 2017. MA thesis-UFMG.

Jarall, S. Study of refrigeration system with HFO-1234yf as a working fluid. **International Journal of Refrigeration**, v. 35, n. 6, p. 1668-1677, 2012.

Karakurt, A. S., Gunes, U., Ust, Y. Exergetic and economic analysis of subcooling & superheating effect on vapor compression refrigeration system. **In: Proceedings of the ASME 2016 Power Conference collocated with the ASME 2016 10<sup>th</sup> International conference on energy sustainability and the ASME 2016 14<sup>th</sup> International conference on fuel cell science, engineering and technology**. American Society of Mechanical Engineers Digital Collection, 2016.

Keshtkar, M. M., Talebizadeh, P. Multi-Objective Optimization of a R744/R134a Cascade Refrigeration System: Exergetic, Economic, Environmental, and Sensitive Analysis (3ES). **Journal of Thermal Engineering**, v. 5, n.4, p. 237-250, 2019.

Kim, S. C., Won, J. P., Kim, M. S. Effects of operating parameters on the performance of a CO<sub>2</sub> air conditioning system for vehicles. **Applied Thermal Engineering**, v. 29, n.11-12, p. 2408-2416, 2009.

Li, P., Seem, J. E., Li, Y. A new explicit equation for accurate friction factor calculation of smooth pipes. **International Journal of Refrigeration**, v. 34, n.6, p. 1535-1541, 2011.

Lockhart, R.; Martinelli, R. Proposed correlation of data for isothermal two-phase, two-component flow in pipes. **Chem. Eng. Prog.**, v.45, n. 1, p. 39-48, 1949.

Machado, L. **Modèle de simulation et étude expérimentale d'un évaporateur de machine frigorifique en régime transitoire**. 1996. PhD thesis - INSA, Lyon.

Machado, L.; Haberschill, P.; Lallemand, M. Masse du fluide frigorigène dans un évaporateur em fonctionnement permanent ou transitoire: Refrigerant mass inside an evaporator in a steady or non-steady state. **International Journal of Refrigeration**, v. 21, n. 6, p. 430-439, 1998.

Makhnatch, P., Khodabandeh, R. Selection of low GWP refrigerant for heat pumps by assessing the life Cycle Climate Performance (LCCP) **In: 11<sup>TH</sup> International Energy Agency Heat Pump Conference**. Montreal: International Energy Agency, 2014.

Mansuriya, K., Patel, V. K., Raja, B. D., Mudgal, A. Assessment of liquid desiccant dehumidification aided vapor-compression refrigeration system based on thermo-economic approach. **Applied Thermal Engineering**, v.164, p. 114542, 2020.

Minetto, S. Theoretical and experimental analysis of a CO<sub>2</sub> heat pump for domestic hot water. **International Journal of Refrigeration**, v. 34, n. 3, p. 742-751, 2011.

Mosaffa, A. H., Farshi, L. G. Exergoeconomic and environmental analyses of an air conditioning system using thermal energy storage. **Applied Energy**, v. 162, p. 515-526, 2016.

Mylona, Z., Kolokotroni, M., Tsamos, K. M., Tassou, S. A. Comparative analysis on the energy use and environmental impact of different refrigeration systems for frozen food supermarket application. **Energy Procedia**, v. 123, p. 121-130, 2017.

Navarro-Esbrí, J., Mendoza-Miranda, J. M., Mota-Babiloni, A., Barragán-Cervera, A., Belman-Flores, J. M. Experimental analysis of R1234yf as drop-in replacement for R134a in a vapor compression system. **International Journal of Refrigeration**, v. 36, p. 870-880, 2013.

Nunes, R. O., Faria, R. N., Bouzidi, N., Machado, L., Koury, R. N. N. Adiabatic Capillary Tube Model for a Carbon Dioxide Transcritical Cycle. **International Journal of Air-Conditioning and Refrigeration**, v. 23, n.2, p. 1550011, 2015.

Paulino, T. F., de Oliveira, R. N., Maia, A. A. T., Palm, B., Machado, L. Modeling and experimental analysis of the solar radiation in a CO<sub>2</sub> direct-expansion solar-assisted heat pump. **Applied Thermal Engineering**, v. 148, p. 160-172, 2019.

Rabelo, S. N., Paulino, T. F., Machado, L., Duarte, W. M., Maia, A. A. T., Machado, L. Experimental analysis of the influence of the expansion valve opening on the performance of the small size CO<sub>2</sub> solar assisted heat pump. **Solar Energy**, v. 190, p. 255-263, 2019a.

Rabelo, S. N., Paulino, T. F., Machado, L., Duarte, W. M. Economic analysis and design optimization of a direct expansion solar assisted heat pump. **Solar Energy**, v. 188, p. 164-174, 2019b.

Rees, S. J. An introduction to ground-source heat pump technology. **In: Advances in Ground-Source Heat Pump Systems**. Woodhead Publishing, p. 1-25, 2016.

Rigola, J., Ablanque, N., Pérez-Segarra, C. D., Oliva, A. Numerical simulation and experimental validation of internal heat exchanger influence on CO<sub>2</sub> trans-critical cycle performance. **International Journal of Refrigeration** 33 (2010) 664-674.

Rohsenow, W. M.; Hartnett, J. P.; Cho, Y. I. **Handbook of heat transfer**. New York: MCGRAW-HILL, v.3, p. 4.1-99, 1998.

Roy, R., Mandal, B. K. Thermo-economic assessment and multi-objective optimization of vapour compression refrigeration system using low gwp refrigerants. **8<sup>th</sup> International Conference on Modeling Simulation and Applied Optimization**, 2019.

Sánchez, D., Cabello, R., Llopis, R., Arauzo, I., Catalán-Gil, J., Torella, E. Energy performance evaluation of R1234yf, R1234ze (E), R600a, R290 and R152a as low-GWP R134a alternatives. **International Journal of Refrigeration**, v. 74, p. 269-282, 2017.

Shah, M. M. Chart correlation for saturated boiling heat transfer: equation and further study. **ASHRAE Trans.**; (United States), v.88, CONF-820112, 1982.

Shah, R. K., London, A. L. **Laminar flow forced convection in ducts: a source book for compact heat exchanger analytical data**. Academic press, 2014.

Shah, M. M. Comprehensive correlation for heat transfer during condensation in conventional and mini/micro channels in all orientations. **International Journal of Refrigeration**, v. 67, p. 22 - 41, 2016.

Shah, M. M. Unified correlation for heat transfer during boiling in plain mini/micro and conventional channels. **International Journal of Refrigeration**, v. 74, p. 606-624, 2017.

Shikalgar, N. D., Sapali, S. N. Energy and exergy analysis of a domestic refrigerator: Approaching a sustainable refrigerator. **Journal of Thermal Engineering**, v. 5, n. 5, p. 469-481, 2019.

Sun, J., Li, W., Cui, B. Energy and exergy analyses of R513a as a R134a drop-in replacement in a vapor compression refrigeration system. **International Journal of Refrigeration**, v. 112, p. 348-356, 2020.

Thom, J. Prediction of pressure drop during forced circulation boiling of water. **International journal of heat and mass transfer**, v. 7, n. 7, p. 709-724, 1964.

Tontu, M., Sahin, B., Bilgili, M. Exergoeconomic analysis of steam turbine driving vapor compression refrigeration system in an existing coal-fired power plant. **Arabian Journal for Science and Engineering**, v. 44, n. 9, p. 7553-7566, 2019.

Tsamos, K. M., Ge, Y. T., Santosa, I., Tassou, S. A., Bianchi, G., Mylona, Z. Energy analysis of alternative CO<sub>2</sub> refrigeration system configurations for retail food applications in moderate and warm climates. **Energy Conversion and Management**, v. 150, p. 822-829, 2017.

Turner, J.; Wallis, G. The separate-cylinders model of two-phase flow. Paper no. **NYO-3114-6, Thayer's School Eng., Dartmouth College, Hanover, NH, USA**, 1965.

Xiao, B., Chang, H., He, L., Zhao, S., Shu, S. Annual performance analysis of an air source heat pump water heater using a new eco-friendly refrigerant mixture as an alternative to R134a. **Renewable Energy**, v. 147, p. 2013-2023, 2020.

Zivi, S. M. Estimation of Steady-state Steam Void-fraction by Means of the Principle of Minimum Entropy Production. **Journal of Heat Transfer**, v. 86, n. 2, p. 247-251, 1964.

Wu, J., Zhou, G., Wang, M. A comprehensive assessment of refrigerants for cabin heating and cooling on electric vehicles. **Applied Thermal Engineering**, p. 115258, 2020.





## APPENDIX A - R290 COMPRESSOR EFFICIENCY MAP DATA


Model	<b>EMC3121U</b>	Code	51330169099.Q	<b>embraco</b>	POWER IN. CHANGE ON.
-------	-----------------	------	---------------	----------------	-------------------------

220-240V 50 1~



### GENERAL DATA

**Application:** L/MBP  
**Refrigerant:** R290  
**Compressor Cooling:** Fan  
**Type:** Hermetic reciprocating  
**Technology Type:** On-Off  
**Expansion Device:** Capillary Tube  
**Packing Quantity:** 80  
**Displacement:** 5.19 cm<sup>3</sup>  
**Horse power:** 1/4 hp

Approvals: 



### MECHANICAL DATA

**Bore:** 21 mm  
**Stroke:** 15 mm  
**Oil Charge:** 150ml  
**Oil Type Configuration:** ESTER  
**Oil Type Viscosity:** ISO10  
**Weight:** 6.8 kg

### MOUNTING ACCESSORIES

	Description	Code
Anchorage:	no	-
Overload Protector Bracket:	no	-
Capacitor Bracket:	no	-
Washer:	no	-
Pin:	no	-
Clip:	no	-
Cover:	no	-
Grommets:	no	-
Sleeves:	no	-
Terminal:	no	-

### ELECTRICAL DATA

**Motor Type:** RSCR  
**Starting Torque:** LST  
**Voltage working range at 60 Hz:** 198-264 V  
**Maximum Motor Temperature:** 130 °C  
**Start Winding Resistance:** 20.76 Ω (± 10%) at 25°C  
**Run Winding Resistance:** 16.4 Ω (± 10%) at 25°C  
**Locked Rotor Amperage (LRA):** 6 A

### ELECTRICAL COMPONENTS

	Component type	Description	Code
CSR / CSIR Box:	No		
Starting Device:	PTC	8EA17C3 QPS2-A22MD3	
Motor Protection:		4TM232KFBYY-53	13634047
Run Capacitor:		5UF - 350V	513556030

### EXTERNAL CHARACTERISTICS

**Base Plate:** UNI  
**Tray Holder:** No  
**Height:** mm

	Internal Diameter (mm)	Material	Shape
Suction Connector	6.5	Copper	Straight
Discharge Connector	6.5	Copper	Straight
Process Connector	6.5	Copper	Straight

 [mktembraco@embraco.com](mailto:mktembraco@embraco.com)

Date of printing: 27.03.2019

Model	<b>EMC3121U</b>	Code	51330169099.Q	<b>embraco</b>	POWER IN. CHANGE ON.
-------	-----------------	------	---------------	----------------	-------------------------

**RATED POINT DATA**

Cooling Capacity (W)	Power Consumption (W)	Current Consumption (A)	Gas Flow Rate (kg/h)	Efficiency (W/W)
±5%	±5%	±5%	±5%	±7%
234	134	0.61	2.38	1.75


Test condition: ASHRAE, Fan, Return Gas 32.2°C, Evaporating: -23.3°C, Condensing: 54°C, Ambient: 32.2°C, Liquid: 32.2°C

**PERFORMANCE CURVE DATA****220V 50Hz**

Condensing Temperature (°C)	Evaporating Temperature (°C)	Cooling Capacity (W)	Power Consumption (W)	Current Consumption (A)	Gas Flow Rate (kg/h)	Efficiency (W/W)
		±5%	±5%	±5%	±5%	±7%
<b>35°C</b>	0	670	165	0.75	6.96	4.07
	-5	568	153	0.70	5.86	3.71
	-10	475	143	0.65	4.88	3.33
	-15	391	133	0.60	4.00	2.94
	-20	317	124	0.56	3.23	2.56
	-25	253	115	0.51	2.56	2.21
	-30	198	104	0.47	2.00	1.90
	-35	154	93	0.43	1.55	1.66


Condensing Temperature (°C)	Evaporating Temperature (°C)	Cooling Capacity (W)	Power Consumption (W)	Current Consumption (A)	Gas Flow Rate (kg/h)	Efficiency (W/W)
		±5%	±5%	±5%	±5%	±7%
<b>45°C</b>	0	642	186	0.84	6.66	3.45
	-5	542	173	0.79	5.60	3.14
	-10	452	160	0.73	4.64	2.82
	-15	370	148	0.68	3.79	2.50
	-20	298	136	0.62	3.04	2.19
	-25	236	124	0.56	2.39	1.90
	-30	183	111	0.50	1.85	1.65
	-35	140	97	0.44	1.42	1.45

Condensing Temperature (°C)	Evaporating Temperature (°C)	Cooling Capacity (W)	Power Consumption (W)	Current Consumption (A)	Gas Flow Rate (kg/h)	Efficiency (W/W)
		±5%	±5%	±5%	±5%	±7%
<b>55°C</b>	0	610	206	0.93	6.32	2.96
	-5	512	190	0.87	5.28	2.70
	-10	423	174	0.81	4.34	2.43
	-15	343	159	0.74	3.51	2.16
	-20	273	144	0.67	2.78	1.89
	-25	211	129	0.59	2.15	1.64

Model	<b>EMC3121U</b>	Code	51330169099.Q	 POWER IN. CHANGE ON.		
-------	-----------------	------	---------------	---	--	--


Condensing Temperature (°C)	Evaporating Temperature (°C)	Cooling Capacity (W)	Power Consumption (W)	Current Consumption (A)	Gas Flow Rate (kg/h)	Efficiency (W/W)
		±5%	±5%	±5%	±5%	±7%
<b>55°C</b>	-30	160	112	0.51	1.62	1.42

Test condition: ASHRAE, Fan, Return Gas 32.2°C, Ambient: 32.2°C, Liquid: 32.2°C

Model	<b>EMC3121U</b>	Code	51330169099.Q	 POWER IN. CHANGE ON.		
-------	-----------------	------	---------------	---	--	--

#### CUSTOM POINT

Condensing Temperature (°C)	Evaporating Temperature (°C)	Cooling Capacity (W)	Power Consumption (W)	Current Consumption (A)	Gas Flow Rate (kg/h)	Efficiency (W/W)
		±5%	±5%	±5%	±5%	±7%
<b>50°C / 122°F</b>	-5°C	528	181	0.83	5.44	2.91

 [mktembraco@embraco.com](mailto:mktembraco@embraco.com)

Date of printing: 27.03.2019

## APPENDIX B – R134a COMPRESSOR EFFICIENCY MAP DATA

Model	<b>NEK1118Z</b>	Code	268FA4294PO	<b>embraco</b> POWER IN. CHANGE ON.
-------	-----------------	------	-------------	-------------------------------------

220-240V 50 1~



### GENERAL DATA

**Application:** LBP  
**Refrigerant:** R134a  
**Evaporating Temperature Range:** -30°C to -5°C  
**Compressor Cooling:** Static  
**Type:** Hermetic reciprocating  
**Technology Type:** On-Off  
**Expansion Device:** Capillary Tube  
**Packing Quantity:** Multi - 74 pcs  
**Displacement:** 8.39 cm<sup>3</sup>  
**Horse power:** 1.4 hp

Approvals:   

### MECHANICAL DATA

**Bore:** 24.28 mm  
**Stroke:** 18.12 mm  
**Oil Charge:** 350ml +/-15ml  
**Free Internal Volume:** 2.1 cm<sup>3</sup>  
**Maximum Recommended Refrigerant Charge:** 350 g  
**Oil Type Configuration:** Polyolester  
**Oil Type Viscosity:** ISO22  
**Compressor pressurization:** Dry air charge  
**Weight:** 10.7 kg

### ELECTRICAL DATA

**Motor Type:** RSIR  
**Starting Torque:** LST  
**Voltage working range at 50 Hz:** 198-254 V  
**Maximum Motor Temperature:** 130 °C  
**Start Winding Resistance:** 14.1 Ω (± 10%) at 25°C  
**Run Winding Resistance:** 13 Ω (± 10%) at 25°C  
**Locked Rotor Amperage (LRA):** 7 A

### MOUNTING ACCESSORIES

	Description	Code
<b>Terminal Board:</b>	no	-
<b>Overload Protector Bracket:</b>	no	-
<b>Capacitor Bracket:</b>	no	-
<b>Rotolock valve:</b>	no	-
<b>Sleeves:</b>	no	-
<b>Cover:</b>	yes	2075282
<b>Anchorage:</b>	yes	1027058
<b>Grommets:</b>	yes	2221011
<b>Washer:</b>	yes	2211047
<b>Pin:</b>	yes	2037140
<b>Clip:</b>	yes	2220020

### ELECTRICAL COMPONENTS

	Component type	Description	Code
<b>Starting Device:</b>	PTC	PTC 230V	1260011
<b>Motor Protection:</b>	External 3/4"	T0503/07   MRP357JZ-3166	2288072   2288306

### EXTERNAL CHARACTERISTICS

**Base Plate:** European  
**Tray Holder:** No  
**Height:** 200 mm

	Internal Diameter (mm)	Material	Shape
<b>Suction Connector</b>	6.1	Copper	Slanted 42Å°
<b>Discharge Connector</b>	4.86	Copper	Straight
<b>Process Connector</b>	6.1	Copper	Slanted 42Å°

 [mktembraco@embraco.com](mailto:mktembraco@embraco.com)

Date of printing: 27.03.2019

Model **NEK1118Z** | Code 268FA4294PO**embraco** POWER IN.  
CHANGE ON.**RATED POINT DATA**

Cooling Capacity (W)	Power Consumption (W)	Current Consumption (A)	Gas Flow Rate (kg/h)	Efficiency (W/W)
±5%	±5%	±5%	±5%	±7%
228	160	0.96	4.41	1.42

Test condition: ASHRAE, Static, Return Gas 32.2°C, Evaporating: -23.3°C, Condensing: 54°C, Ambient: 32.2°C, Liquid: 32.2°C

**PERFORMANCE CURVE DATA****220V 50Hz**

Condensing Temperature (°C)	Evaporating Temperature (°C)	Cooling Capacity (W)	Power Consumption (W)	Current Consumption (A)	Gas Flow Rate (kg/h)	Efficiency (W/W)
		±5%	±5%	±5%	±5%	±7%
<b>35°C</b>	-5	592	247	1.48	11.62	2.40
	-10	482	215	1.26	9.43	2.25
	-15	386	186	1.09	7.53	2.07
	-20	305	162	0.96	5.92	1.89
	-25	237	141	0.88	4.60	1.69
	-30	184	124	0.83	3.56	1.49

Condensing Temperature (°C)	Evaporating Temperature (°C)	Cooling Capacity (W)	Power Consumption (W)	Current Consumption (A)	Gas Flow Rate (kg/h)	Efficiency (W/W)
		±5%	±5%	±5%	±5%	±7%
<b>45°C</b>	-5	567	262	1.49	11.12	2.16
	-10	461	229	1.29	9.00	2.02
	-15	368	198	1.13	7.16	1.86
	-20	288	171	1.00	5.59	1.69
	-25	221	146	0.90	4.28	1.51
	-30	167	124	0.83	3.24	1.35

Condensing Temperature (°C)	Evaporating Temperature (°C)	Cooling Capacity (W)	Power Consumption (W)	Current Consumption (A)	Gas Flow Rate (kg/h)	Efficiency (W/W)
		±5%	±5%	±5%	±5%	±7%
<b>55°C</b>	-5	541	277	1.50	10.62	1.95
	-10	439	242	1.32	8.58	1.81
	-15	349	210	1.17	6.80	1.66
	-20	271	179	1.04	5.26	1.51
	-25	205	151	0.92	3.97	1.36

Test condition: ASHRAE, Static, Return Gas 32.2°C, Ambient: 32.2°C, Liquid: 32.2°C

**CUSTOM POINT**

Condensing Temperature (°C)	Evaporating Temperature (°C)	Cooling Capacity (W)	Power Consumption (W)	Current Consumption (A)	Gas Flow Rate (kg/h)	Efficiency (W/W)
		±5%	±5%	±5%	±5%	±7%
<b>50°C / 122°F</b>	-5°C	554	270	1.49	10.87	2.05

✉ [mktembraco@embraco.com](mailto:mktembraco@embraco.com)

Date of printing: 27.03.2019

## APPENDIX C – R600a COMPRESSOR EFFICIENCY MAP DATA

Model **NEK6170Y** | Code **861LA41N1AM**

**embraco** POWER IN.  
CHANGE ON.

220-240V 50 1~



### GENERAL DATA

**Application:** HBP  
**Refrigerant:** R600a  
**Evaporating Temperature Range:** -15°C to 10°C  
**Compressor Cooling:** Fan  
**Fan air flow:** 520 m<sup>3</sup>/h  
**Type:** Hermetic reciprocating  
**Technology Type:** On-Off  
**Expansion Device:** Capillary Tube or Expansion Valve  
**Packing Quantity:** Multi - 80 pcs  
**Displacement:** 14.28 cm<sup>3</sup>  
**Horse power:** 1.4 hp

Approvals:   

### MECHANICAL DATA

**Bore:** 30.16 mm  
**Stroke:** 20 mm  
**Oil Charge:** 350ml +/-15ml  
**Free Internal Volume:** 2.1 cm<sup>3</sup>  
**Maximum Recommended Refrigerant Charge:** 150 g  
**Oil Type Configuration:** Polyolester  
**Oil Type Viscosity:** ISO22  
**Compressor pressurization:** Without dry air charge  
**Weight:** 10.3 kg

### MOUNTING ACCESSORIES

	Description	Code
<b>Anchorage:</b>	no	-
<b>Capacitor Bracket:</b>	no	-
<b>Washer:</b>	no	-
<b>Pin:</b>	no	-
<b>Clip:</b>	no	-
<b>Rotolock valve:</b>	no	-
<b>Cover:</b>	yes	2075282
<b>Grommets:</b>	yes	2221011
<b>Sleeves:</b>	yes	2222018
<b>Terminal Board:</b>	yes	1027060
<b>Overload Protector Bracket:</b>	yes	2075299

### ELECTRICAL DATA

**Motor Type:** CSIR  
**Starting Torque:** HST  
**Voltage working range at 50 Hz:** 198-254 V  
**Maximum Motor Temperature:** 130 °C  
**Start Winding Resistance:** 29.57 Ω (± 10%) at 25°C  
**Run Winding Resistance:** 7.96 Ω (± 10%) at 25°C  
**Locked Rotor Amperage (LRA):** 13 A

### ELECTRICAL COMPONENTS

	Component type	Description	Code
<b>Start Capacitor:</b>	43-53 MFD	330V	2252347
<b>Motor Protection:</b>	External 3/4"	T0186/G6	2319069
<b>Starting Device:</b>	Current relay	MTRPH-0026-65	2334117

### EXTERNAL CHARACTERISTICS

**Base Plate:** European  
**Tray Holder:** No  
**Height:** 188 mm

	Internal Diameter (mm)	Material	Shape
<b>Suction Connector</b>	8.1	Copper	Slanted 42°
<b>Discharge Connector</b>	6.1	Copper	Straight
<b>Process Connector</b>	6.1	Copper	Slanted 42°

 [mktembraco@embraco.com](mailto:mktembraco@embraco.com)

Date of printing: 26.03.2019

Model **NEK6170Y** | Code **861LA41N1AM****embraco** POWER IN.  
CHANGE ON.**RATED POINT DATA**

Cooling Capacity (W)	Power Consumption (W)	Current Consumption (A)	Gas Flow Rate (kg/h)	Efficiency (W/W)
±5%	±5%	±5%	±5%	±7%
817	324	2.05	9.79	2.52

Test condition: ASHRAE, Fan, Return Gas 35°C, Subcooling 8.3K, Evaporating: 7.2°C, Condensing: 54°C, Ambient: 35°C

**PERFORMANCE CURVE DATA****220V 50Hz**

Condensing Temperature (°C)	Evaporating Temperature (°C)	Cooling Capacity (W)	Power Consumption (W)	Current Consumption (A)	Gas Flow Rate (kg/h)	Efficiency (W/W)
		±5%	±5%	±5%	±5%	±7%
<b>35°C</b>	10	1 099	271	1.87	11.37	4.06
	5	921	258	1.82	9.49	3.57
	0	763	244	1.77	7.84	3.13
	-5	624	229	1.72	6.39	2.73
	-10	504	213	1.67	5.16	2.37
	-15	404	196	1.62	4.12	2.06

Condensing Temperature (°C)	Evaporating Temperature (°C)	Cooling Capacity (W)	Power Consumption (W)	Current Consumption (A)	Gas Flow Rate (kg/h)	Efficiency (W/W)
		±5%	±5%	±5%	±5%	±7%
<b>45°C</b>	10	995	307	1.99	11.09	3.24
	5	832	288	1.92	9.23	2.89
	0	686	268	1.85	7.59	2.56
	-5	558	248	1.78	6.16	2.25
	-10	448	227	1.71	4.93	1.97
	-15	355	206	1.64	3.90	1.73

Condensing Temperature (°C)	Evaporating Temperature (°C)	Cooling Capacity (W)	Power Consumption (W)	Current Consumption (A)	Gas Flow Rate (kg/h)	Efficiency (W/W)
		±5%	±5%	±5%	±5%	±7%
<b>55°C</b>	10	893	340	2.12	10.81	2.63
	5	745	316	2.02	8.98	2.36
	0	613	292	1.93	7.36	2.10
	-5	496	267	1.84	5.94	1.86
	-10	395	241	1.75	4.72	1.64

Test condition: ASHRAE, Fan, Return Gas 35°C, Subcooling 8.3K, Ambient: 35°C

✉ [mktembraco@embraco.com](mailto:mktembraco@embraco.com)

Date of printing: 26.03.2019

Model **NEK6170Y** | Code **861LA41N1AM****embraco** POWER IN.  
CHANGE ON.**CUSTOM POINT**

Condensing Temperature (°C)	Evaporating Temperature (°C)	Cooling Capacity (W)	Power Consumption (W)	Current Consumption (A)	Gas Flow Rate (kg/h)	Efficiency (W/W)
		±5%	±5%	±5%	±5%	±7%
<b>50°C / 122°F</b>	-5°C	527	257	1.81	6.05	2.05

✉ [mktembraco@embraco.com](mailto:mktembraco@embraco.com)

Date of printing: 26.03.2019

## APPENDIX D – R1234yf COMPRESSOR EFFICIENCY MAP DATA



Compressor  
Voltage Code : FZ

# AE4440N-FZ1A

High Temp. Commercial (HP)

220 - 240V 1~ 50 Hz

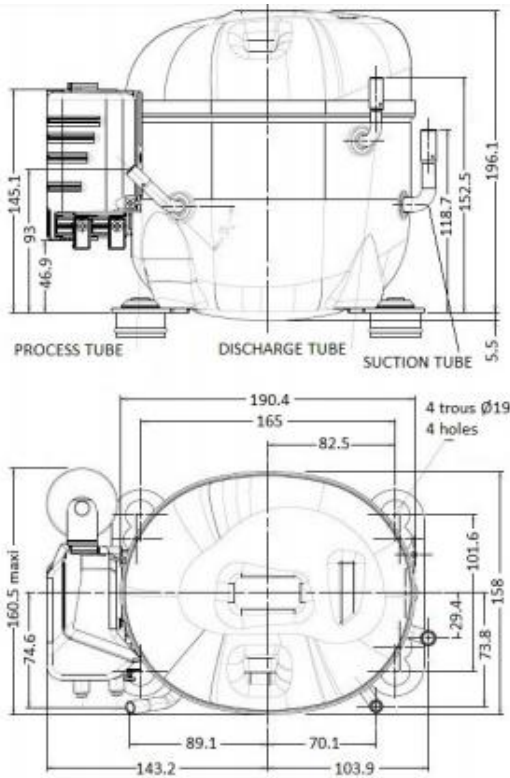
R1234yf

AE4440N-FZ1A\_BR

Conditions	Frequency	Nominal Cooling Capacity		Sound Power ISO3745 / ISO 3743-1
		Watts	BTU/h	
EN12900 / R1234yf	50 Hz	842	2872	

<b>Displacement (cc)</b>	10.33
<b>Net Weight (Kg)</b>	9.7
<b>Oil Quantity (cc)</b>	280.0
<b>Oil Type</b>	Polyolester
<b>Expansion Device</b>	Capillary_Tube/Expansion_Valve
<b>Cooling</b>	Fan
<b>Main Winding (Ohm)</b>	8.29
<b>Start Winding (Ohm)</b>	19.16
<b>Current</b>	
RLA (A)	2.56
LRA (A)	13.5
<b>Electrical Equipment</b>	CSIR
<b>Overload</b>	MSP40AMW
Time Check	6.5s - 16s / 11.2 A
Open Temp	135° C
Close Temp	61° C
<b>Start Capacitor</b>	88 µF / 330 V
<b>Current Relay</b>	9660C***-149
Pick Up	7.70A
Drop Out	6.50A
<b>Refrigerating connection for OD</b>	
Suction Tube	7.9 (5/16")
Discharge Tube	6.35 (1/4")
Process Tube	6.35 (1/4")



\* EN12900 : T°Cond. 50.0°C / T°Evap. 5.0°C / T°Return gas temp.. 20.0°C  
T°Subcooling. 0.0K

Certificates :



Note : Tecumseh reserves the right to change information contained in this document without notification.





**Tecumseh**

<b>AE4440N-FZ1A</b>	<b>Tension FZ : 220 - 240V 1~ 50 Hz</b>
---------------------	---

Les performances sont données dans les <b>conditions EN12900</b> :	Gaz aspirés :	20.0 °C
Condition Dew	Sous refroidissement :	0.0 K
The performance data are in <b>EN12900 conditions</b> :	Return gas :	20.0 °C
Dew Condition	Subcooling :	0.0 K

**50 Hz R1234yf**



**N°3058**

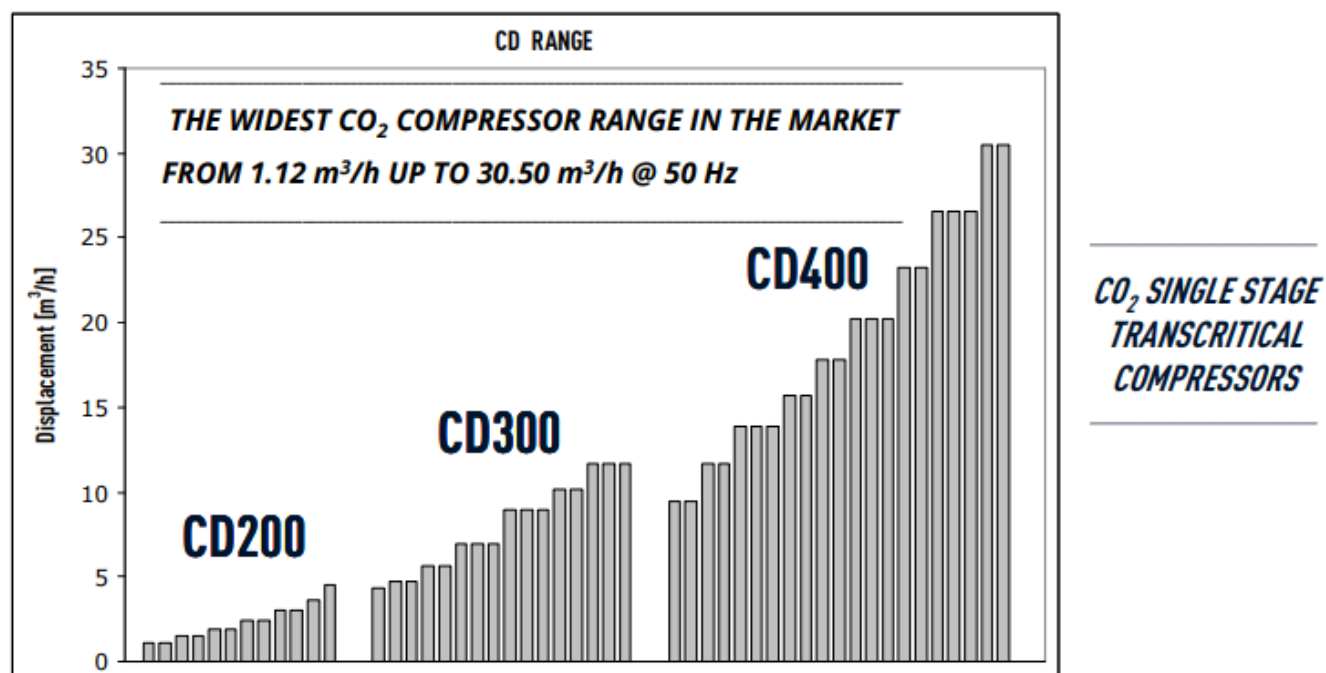
4   T condensation	5   T évaporation	(°C)	-25	-20	-15	-10	-5	0	5	10	15
<b>30</b>	1   P frigorifique	(Watt)	300	392	500	627	775	947	1144	1370	1626
	2   P absorbée	(W)	226	250	274	296	316	333	347	357	362
	3   I absorbée	(A)	1.85	1.91	1.97	2.03	2.08	2.13	2.18	2.22	2.27
<b>40</b>	1   P frigorifique	(Watt)	250	336	433	546	675	824	995	1190	1412
	2   P absorbée	(W)	232	260	289	317	344	369	392	412	429
	3   I absorbée	(A)	1.81	1.91	2.01	2.10	2.19	2.27	2.35	2.43	2.51
<b>50</b>	1   P frigorifique	(Watt)		277	364	461	572	698	842	1007	1194
	2   P absorbée	(W)		269	302	335	368	401	432	461	488
	3   I absorbée	(A)		1.90	2.03	2.15	2.28	2.40	2.52	2.63	2.74
<b>60</b>	1   P frigorifique	(Watt)			292	375	467	570	688	822	975
	2   P absorbée	(W)			315	353	392	430	469	507	543
	3   I absorbée	(A)			2.04	2.20	2.36	2.51	2.67	2.82	2.96

1 = cooling capacity 2 = power input 3 = current 4 = condensing temperature 5 = evaporating temperature

**Nota :** Tecumseh se réserve le droit de modifier les informations contenues dans ce document sans préavis.

**Note :** Tecumseh reserves the right to change information contained in this document without notification.

## APPENDIX E – R744 COMPRESSOR EFFICIENCY MAP DATA



OFFICINE MARIO DORIN SINCE 1918  
**DORIN**  
INNOVATION

CARATTERISTICHE TECNICHE / TECHNICAL DATA / CARACTERISTIQUES TECHNIQUES / TECHNISCHE MERKMALE

Serie Range Serie Serie	Modello Model Modèle Typ	Cilindri Cylinders Cylindres Zylinder	Volume Spost. Displacement Volume bal. Fördervolumen [m <sup>3</sup> /h] @ 50 Hz	HP	RPM @ 50 Hz	Aspirazione Suction Aspiration Saugventil		Scarico Discharge Refoulement Druckventil		Peso netto Net weight Poids net Nettogewicht [kg]	Carica olio Oil charge Charge huile Ölfüllung [kg]
						socket welding [mm]	butt welding [mm]	socket welding [mm]	butt welding [mm]		
CD200	CD 150M	2	1,12	1,5	1450	10	14	10	14	71	1,3
	CD 180H	2	1,12	1,8	1450	10	14	10	14	72	1,3
	CD 180M	2	1,46	1,8	1450	10	14	10	14	73	1,3
	CD 300H	2	1,46	3,0	1450	10	14	10	14	73	1,3
	CD 300M	2	1,88	3,0	1450	10	14	10	14	73	1,3
	CD 350H	2	1,88	3,5	1450	10	14	10	14	76	1,3
	CD 350M	2	2,39	3,5	1450	10	14	10	14	76	1,3
	CD 360H	2	2,39	3,8	1450	10	14	10	14	78	1,3
	CD 360M	2	3,00	3,6	1450	10	14	10	14	77	1,3
	CD 380H	2	3,00	3,8	1450	10	14	10	14	77	1,3

Serie Range Serie Serie	Modello Model Modèle Typ	Condizioni operative Operating conditions Conditions d'utilisation Betriebsbedingungen			Q [W]	Capacità frigorifera Refrigerating capacity Puissance frigorifique Kälteleistung					P [kW]	Potenza assorbita Power input Puissance absorbée Leistungsaufnahme				
		Tc	Tgcout	pc		Temperatura evaporazione / Evaporating temperature Température d'évaporation / Verdampfungstemperatur [°C]										
		[°C]	[°C]	[bar]	+10	+5	0	-5	-10	-15	-20	-25	-30	-35	-40	
CD200	CD150M	0	--	(34,9)	Q						3720	3050	2480	2000	1600	1300
					P						0,47	0,52	0,54	0,56	0,56	0,55
		5	--	(39,7)	Q					4110	3410	2800	2260	1810	1440	1170
					P					0,52	0,58	0,61	0,62	0,63	0,62	0,60
		10	--	(45,0)	Q			5270	4480	3760	3110	2540	2040	1620	1290	1040
					P			0,50	0,58	0,64	0,68	0,70	0,70	0,69	0,67	0,65
		15	--	(50,9)	Q			4790	4070	3400	2800	2270	1820	1440	1140	905
					P			0,66	0,72	0,76	0,78	0,78	0,77	0,75	0,73	0,69
		20	--	(57,3)	Q			4290	3630	3030	2480	2000	1590	1250	980	
					P			0,81	0,85	0,87	0,88	0,86	0,84	0,81	0,77	
	25	--	(64,3)	Q			3740	3160	2620	2140	1720	1360	1060	825		
				P			0,95	0,97	0,97	0,96	0,94	0,90	0,86	0,81		
	--	30	75	Q			3220	2710	2240	1820	1450	1140	880			
				P			1,13	1,12	1,10	1,07	1,02	0,97	0,92			
	--	35	90	Q			2880	2410	1980	1600	1260	980				
				P			1,33	1,29	1,24	1,18	1,11	1,05				
	--	40	100	Q			2510	2090	1720	1380	1090					
				P			1,45	1,39	1,32	1,25	1,17					
	--	45	110	Q			2200	1830	1500	1200	950					
				P			1,55	1,48	1,40	1,32	1,24					
	CD180H	0	--	(34,9)	Q						3710	3060	2510	2060		
				P							0,49	0,54	0,57	0,58		
5		--	(39,7)	Q						4110	3410	2800	2290	1870		
				P						0,54	0,60	0,64	0,66	0,66		
10		--	(45,0)	Q			5310	4500	3760	3110	2540	2060	1680			
				P			0,50	0,60	0,67	0,71	0,73	0,74	0,73			
15		--	(50,9)	Q			5640	4830	4080	3400	2800	2280	1840	1490		
				P			0,55	0,66	0,74	0,79	0,82	0,83	0,82	0,79		
20		--	(57,3)	Q	5850	5070	4330	3650	3030	2490	2010	1620	1300			
				P	0,61	0,73	0,82	0,88	0,91	0,92	0,91	0,89	0,85			
25	--	(64,3)	Q	5130	4440	3780	3180	2630	2150	1730	1380	1100				
			P	0,81	0,91	0,97	1,01	1,02	1,02	0,99	0,96	0,90				
--	30	75	Q	4450	3840	3260	2730	2250	1830	1460	1160	915				
			P	1,07	1,13	1,17	1,18	1,16	1,13	1,09	1,03	0,96				
--	35	90	Q	4020	3460	2930	2440	2000	1610	1280	1000					
			P	1,37	1,39	1,38	1,35	1,31	1,25	1,18	1,10					
--	40	100	Q	3530	3030	2560	2130	1740	1400	1100						
			P	1,53	1,52	1,49	1,45	1,38	1,30	1,22						
--	45	110	Q	3100	2670	2250	1870	1520	1220							
			P	1,67	1,64	1,59	1,52	1,44	1,35							
--	25	100	Q	5050	4320	3640	3020	2460	1970	1560						
			P	1,53	1,52	1,49	1,45	1,38	1,30	1,22						
--	25	120	Q	4900	4170	3500	2890	2350	1880							
			P	1,79	1,74	1,67	1,59	1,50	1,40							
--	25	140	Q	4770	4060	3400	2810									
			P	2,01	1,93	1,83	1,73									
	0	--	(34,9)	Q						5020	4140	3380	2730	2200	1780	

## APPENDIX F – CATALOG CONCERNING THE GEOMETRIC ASPECTS OF COPPER TUBES USED IN THE SIMULATION

O Departamento de Engenharia de Aplicações da ELUMA, estuda e recomenda soluções técnicas para projetos hidráulicos, efetua levantamentos e orçamentos de materiais, sem qualquer ônus para o solicitante.

Através de suas Unidades Volantes de Treinamento (UVT's) que estão tecnicamente equipadas, oferecem treinamento na própria obra para profissionais da área, afim de torná-los aptos a executarem as instalações hidráulicas com a mesma qualidade que são produzidos os tubos e conexões ELUMA.

Regularmente promove palestras e treinamentos técnicos para construtores, instaladores, projetistas hidráulicos, revendedores e também para estudantes de engenharia, arquitetura e escolas técnicas.

### Aplicações:

Os Tubos de Cobre sem costura e as Conexões de Cobre e Bronze ELUMA são utilizados para as seguintes aplicações: Instalações Hidráulicas (Água Quente e Água Fria), Instalações de Combate a Incêndio (Hidrante e Sprinkler), Instalações de Gás Combustível e Medicinal e Instalações Industriais.

### Vantagens e Propriedades do Cobre:

- Suporta altas temperaturas
- Sistema normatizado
- Segurança nas instalações
- Ecológico
- Material nobre
- Durabilidade

### Tubos de Cobre HIDROLAR®



Os tubos de cobre **HIDROLAR®** são rígidos, **sem costura**, fabricados pelo processo de extrusão e em seguida calibrados nos diâmetros comerciais por trefilação. São produzidos de acordo com a norma ABNT-NBR 13206\*. Comercializados em barras de 5,0 e 2,5 metros.

Sua composição química é de 99,9% de cobre (no mínimo). Os tubos de cobre apresentam as seguintes características: **boa resistência química**; **boa resistência à corrosão**; **fácil de manusear**; **pouca tendência à incrustação**; **boa resistência mecânica**; **longa vida útil** e é **reciclável**.

DIÂMETRO NOMINAL (pol.)	DIÂMETRO EXTERNO x ESP. PAREDE (mm)	CLASSE E		CLASSE A		CLASSE I			
		DIÂMETRO EXTERNO x ESP. PAREDE (mm)	PRESSÃO SERVIÇO Kg/m	DIÂMETRO EXTERNO x ESP. PAREDE (mm)	Kg/m	DIÂMETRO EXTERNO x ESP. PAREDE (mm)	PRESSÃO SERVIÇO Kg/m		
1/2"	15	15 x 0,50	0,203	41,0	0,318	69,0	15 x 1,0	0,392	88,0
3/4"	22	22 x 0,60	0,360	34,0	0,532	50,0	22 x 1,1	0,644	60,0
1"	28	28 x 0,60	0,460	26,0	0,683	40,0	28 x 1,2	0,901	55,0
1 1/4"	35	35 x 0,70	0,673	25,0	1,045	40,0	35 x 1,4	1,318	45,0
1 1/2"	42	42 x 0,80	0,923	24,0	1,261	35,0	42 x 1,4	1,593	42,0
2"	54	54 x 0,90	1,339	21,0	1,775	28,0	54 x 1,5	2,206	34,0
2 1/2"	66	66,7 x 1,00	1,839	20,0	2,200	24,0	66,7 x 1,5	2,737	28,0
3"	79	79,4 x 1,20	2,627	19,0	3,271	24,0	79,4 x 1,9	4,122	27,0
4"	104	104,8 x 1,20	3,480	14,0	4,337	18,0	104,8 x 2,0	5,755	20,0

\*Tubos de Cobre sem costura, conforme Normas de Instalações Hidráulicas e Gás da ABNT.

De acordo com a aplicação e identificação do tubo de cobre, são especificadas suas classes. Salvo indicação do projetista hidráulico, normalmente são utilizados para:

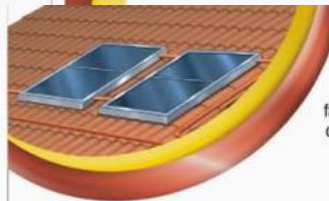
- Instalações de água fria e água quente, instalações de combate a incêndio por hidrante e sprinklers: **TUBOS CLASSE E - Identificados por tampões plásticos na cor Verde**. São acoplados com conexões por soldagem ou brasagem capilar.
- Todas as instalações indicadas para tubo classe **E**, instalações de gases combustíveis<sup>(\*)</sup> e medicinais: **TUBOS CLASSE A - Identificados por tampões plásticos na cor Amarela**. São acoplados com conexões por soldagem ou brasagem capilar.
- Todas as instalações indicadas para tubo classe **A** e instalações industriais de alta pressão e vapor: **TUBOS CLASSE I - Identificados por tampões plásticos na cor Azul**. São acoplados com conexões por soldagem ou brasagem capilar.

EDIÇÃO: JANEIRO/2009



**ELUMA**  
A marca do cobre

### Tubos de Cobre SOLAR



Tubos de cobre **SOLAR** são rígidos sem costura, fabricados pelo processo de extrusão e em seguida calibrados nos diâmetros comerciais por trefilação.

DIMENSÕES (mm)	PESO (kg/m)
9,52 x 0,40	0,102
12,70 x 0,40	0,138
15,00 x 0,40	0,164
22,00 x 0,50	0,301
28,00 x 0,50	0,385

Sua composição química é de 99,9% de cobre (no mínimo).

**Aplicação:** Fabricação de coletores solares para água quente.

### Tubos de Cobre ELUMAGÁS®

Tubos de cobre **ELUMAGÁS®** são produzidos sem costura, com processo de fabricação semelhante aos tubos **HIDROLAR®** e **SOLAR**, recebendo tratamento térmico posterior a trefilação, tornando-os flexíveis. São utilizados em instalações de gás para interligações com aparelhos (medidores de gás, botijões, etc). São fornecidos em rolos.

DIÂMETRO EXTERNO EM POLEGADA	DIMENSÕES (mm)	PESO (kg/m)	PRESSÃO SERVIÇO kgf/cm <sup>2</sup>
3/16"	4,76 x 0,79	0,088	190
1/4"	6,35 x 0,79	0,123	132
5/16"	7,94 x 0,79	0,158	100
3/8"	9,52 x 0,79	0,193	85
1/2"	12,70 x 0,79	0,263	60
5/8"	15,87 x 0,79	0,333	50
3/4"	19,05 x 0,79	0,403	40



Normas Técnicas de Instalação: NBR 7541  
NBR 13523, NBR 15526.

### COMPOSIÇÃO QUÍMICA

LIGA ELUMA	ESPEC. ASTM CDA	COMPOSIÇÃO%		LIGAS EQUIVALENTES
		Cu	P	
Nº	DENOMINAÇÃO			EN
122	Cobre Fosforoso DHP	C12200	99,90 min 0,015 0,040	CR024A

## APPENDIX G – METHOD USED TO SELECT OF COMMERCIAL DIAMETERS FOR EACH REFRIGERANT

As informed in topic 3.10, the diameters used in both the evaporator and condenser/gas cooler in each analyzed system were selected based on the values of COP and TEWI, considering different evaporation temperatures, condensation temperatures and commercial diameters.

For the **reference cooling capacity of 0.5 kW**, the results for the systems operating with **R134a, R290, R600a, and R1234yf** are shown in the tables below.

<b>R134a: <math>T_{\text{evap}} = -5^{\circ}\text{C}</math>, <math>T_{\text{cond}} = 50^{\circ}\text{C}</math>, <math>T_{\text{WI}} = 12^{\circ}\text{C}</math>, <math>T_{\text{WO}} = 5^{\circ}\text{C}</math>, <math>T_{\text{WCI}} = 25^{\circ}\text{C}</math>, <math>T_{\text{WCO}} = 40^{\circ}\text{C}</math></b>					
$D_{\text{REF}}$ (mm)	$D_{\text{oi}}$ (mm)	$D_{\text{W}}$ (mm)	COP (-)	TEWI (kgCO <sub>2</sub> )	Efficiency exergy (%)
6.36	7.94	26.8	1.795	2324	37.2
6.36	7.94	20.8	1.795	2128	37.2
6.36	7.94	14	1.794	1906	37.2
7.94	9.52	26.8	1.795	2829	37.2
7.94	9.52	20.8	1.795	2566	37.2
7.94	9.52	14	1.794	2270	37.2
11.12	12.7	26.8	1.795	3889	37.2
11.12	12.7	20.8	1.795	3482	37.2
11.12	12.7	14	1.794	3030	37.2
<b>R134a: <math>T_{\text{evap}} = -4^{\circ}\text{C}</math>, <math>T_{\text{cond}} = 50^{\circ}\text{C}</math>, <math>T_{\text{WI}} = 12^{\circ}\text{C}</math>, <math>T_{\text{WO}} = 5^{\circ}\text{C}</math>, <math>T_{\text{WCI}} = 25^{\circ}\text{C}</math>, <math>T_{\text{WCO}} = 40^{\circ}\text{C}</math></b>					
6.36	7.94	26.8	1.827	2363	37
6.36	7.94	20.8	1.827	2149	37
6.36	7.94	14	1.826	1906	37
7.94	9.52	26.8	1.827	2930	37
7.94	9.52	20.8	1.827	2642	37
7.94	9.52	14	1.826	2317	37
11.12	12.7	26.8	1.827	4088	37
11.12	12.7	20.8	1.827	3642	37
11.12	12.7	14	1.826	3145	37
<b>R134a: <math>T_{\text{evap}} = -3^{\circ}\text{C}</math>, <math>T_{\text{cond}} = 50^{\circ}\text{C}</math>, <math>T_{\text{WI}} = 12^{\circ}\text{C}</math>, <math>T_{\text{WO}} = 5^{\circ}\text{C}</math>, <math>T_{\text{WCI}} = 25^{\circ}\text{C}</math>, <math>T_{\text{WCO}} = 40^{\circ}\text{C}</math></b>					
6.36	7.94	26.8	1.859	2421	36.79
6.36	7.94	20.8	1.858	2184	36.79
6.36	7.94	14	1.858	1916	36.79
7.94	9.52	26.8	1.859	2740	36.79
7.94	9.52	20.8	1.858	2740	36.79
7.94	9.52	14	1.858	2380	36.79
11.12	12.7	26.8	1.859	4343	36.79

11.12	12.7	20.8	1.858	3848	36.79
11.12	12.7	14	1.858	3297	36.79
<b>R134a: <math>T_{\text{evap}} = -5^{\circ}\text{C}</math>, <math>T_{\text{cond}} = 45^{\circ}\text{C}</math>, <math>T_{\text{WI}} = 12^{\circ}\text{C}</math>, <math>T_{\text{WO}} = 5^{\circ}\text{C}</math>, <math>T_{\text{WCI}} = 25^{\circ}\text{C}</math>, <math>T_{\text{WCO}} = 40^{\circ}\text{C}</math></b>					
6.36	7.94	26.8	1.979	2376	36.98
6.36	7.94	20.8	1.979	2135	36.98
6.36	7.94	14	1.978	1862	36.98
7.94	9.52	26.8	1.979	2942	36.98
7.94	9.52	20.8	1.979	2621	36.98
7.94	9.52	14	1.978	2257	36.98
11.12	12.7	26.8	1.979	4115	36.98
11.12	12.7	20.8	1.979	3619	36.98
11.12	12.7	14	1.978	3066	36.98
<b>R134a: <math>T_{\text{evap}} = -4^{\circ}\text{C}</math>, <math>T_{\text{cond}} = 45^{\circ}\text{C}</math>, <math>T_{\text{WI}} = 12^{\circ}\text{C}</math>, <math>T_{\text{WO}} = 5^{\circ}\text{C}</math>, <math>T_{\text{WCI}} = 25^{\circ}\text{C}</math>, <math>T_{\text{WCO}} = 40^{\circ}\text{C}</math></b>					
6.36	7.94	26.8	2.014	2428	36.72
6.36	7.94	20.8	2.014	2165	36.72
6.36	7.94	14	2.013	1868	36.72
7.94	9.52	26.8	2.014	3062	36.72
7.94	9.52	20.8	2.014	2711	36.72
7.94	9.52	14	2.011	2314	36.72
11.12	12.7	26.8	2.014	4346	36.72
11.12	12.7	20.8	2.013	3803	36.72
11.12	12.7	14	1.996	3199	36.72
<b>R134a: <math>T_{\text{evap}} = -3^{\circ}\text{C}</math>, <math>T_{\text{cond}} = 45^{\circ}\text{C}</math>, <math>T_{\text{WI}} = 12^{\circ}\text{C}</math>, <math>T_{\text{WO}} = 5^{\circ}\text{C}</math>, <math>T_{\text{WCI}} = 25^{\circ}\text{C}</math>, <math>T_{\text{WCO}} = 40^{\circ}\text{C}</math></b>					
6.36	7.94	26.8	2.048	2499	36.45
6.36	7.94	20.8	2.048	2211	36.45
6.36	7.94	14	2.048	1884	36.45
7.94	9.52	26.8	2.048	3212	36.45
7.94	9.52	20.8	2.048	2825	36.45
7.94	9.52	14	2.048	2389	36.45
11.12	12.7	26.8	2.048	4636	36.45
11.12	12.7	20.8	2.048	4038	36.45
11.12	12.7	14	2.048	3373	36.45

<b>R290: <math>T_{\text{evap}} = -5^{\circ}\text{C}</math>, <math>T_{\text{cond}} = 50^{\circ}\text{C}</math>, <math>T_{\text{WI}} = 12^{\circ}\text{C}</math>, <math>T_{\text{WO}} = 5^{\circ}\text{C}</math>, <math>T_{\text{WCI}} = 25^{\circ}\text{C}</math>, <math>T_{\text{WCO}} = 40^{\circ}\text{C}</math></b>					
$D_{\text{REF}}$ (mm)	$D_{\text{oi}}$ (mm)	$D_{\text{W}}$ (mm)	COP (-)	TEWI (kgCO2)	Efficiency exergy (%)
6.36	7.94	26.8	2.496	913.4	51.84
6.36	7.94	20.8	2.495	912.1	51.84
6.36	7.94	14	2.494	911	51.84
7.94	9.52	26.8	2.496	916.2	51.84
7.94	9.52	20.8	2.495	914.6	51.84

7.94	9.52	14	2.493	913.4	51.84
11.12	12.7	26.8	2.495	922.1	51.84
11.12	12.7	20.8	2.495	919.6	51.84
11.12	12.7	14	2.497	922.4	51.84
<b>R290: <math>T_{\text{evap}} = -4^{\circ}\text{C}</math>, <math>T_{\text{cond}} = 50^{\circ}\text{C}</math>, <math>T_{\text{WI}} = 12^{\circ}\text{C}</math>, <math>T_{\text{WO}} = 5^{\circ}\text{C}</math>, <math>T_{\text{WCI}} = 25^{\circ}\text{C}</math>, <math>T_{\text{WCO}} = 40^{\circ}\text{C}</math></b>					
6.36	7.94	26.8	2.556	892.5	51.89
6.36	7.94	20.8	2.555	891.1	51.89
6.36	7.94	14	2.554	890	51.89
7.94	9.52	26.8	2.556	895.7	51.89
7.94	9.52	20.8	2.555	893.9	51.89
7.94	9.52	14	2.553	892.7	51.89
11.12	12.7	26.8	2.556	901.9	51.89
11.12	12.7	20.8	2.555	899.2	51.89
11.12	12.7	14	2.537	902.3	51.89
<b>R290: <math>T_{\text{evap}} = -3^{\circ}\text{C}</math>, <math>T_{\text{cond}} = 50^{\circ}\text{C}</math>, <math>T_{\text{WI}} = 12^{\circ}\text{C}</math>, <math>T_{\text{WO}} = 5^{\circ}\text{C}</math>, <math>T_{\text{WCI}} = 25^{\circ}\text{C}</math>, <math>T_{\text{WCO}} = 40^{\circ}\text{C}</math></b>					
6.36	7.94	26.8	2.617	872.3	51.92
6.36	7.94	20.8	2.617	870.8	51.92
6.36	7.94	14	2.615	869.5	51.92
7.94	9.52	26.8	2.617	874	51.92
7.94	9.52	20.8	2.617	874	51.92
7.94	9.52	14	2.613	872.7	51.92
11.12	12.7	26.8	2.617	882.5	51.92
11.12	12.7	20.8	2.616	879.5	51.92
11.12	12.7	14	2.595	883.1	51.92
<b>R290: <math>T_{\text{evap}} = -5^{\circ}\text{C}</math>, <math>T_{\text{cond}} = 45^{\circ}\text{C}</math>, <math>T_{\text{WI}} = 12^{\circ}\text{C}</math>, <math>T_{\text{WO}} = 5^{\circ}\text{C}</math>, <math>T_{\text{WCI}} = 25^{\circ}\text{C}</math>, <math>T_{\text{WCO}} = 40^{\circ}\text{C}</math></b>					
$D_{\text{REF}}$ (mm)	$D_{\text{oi}}$ (mm)	$D_{\text{W}}$ (mm)	COP (-)	TEWI (kgCO2)	Efficiency exergy (%)
6.36	7.94	26.8	2.819	810.5	52.77
6.36	7.94	20.8	2.819	809	52.77
6.36	7.94	14	2.817	807.6	52.77
7.94	9.52	26.8	2.819	813.8	52.77
7.94	9.52	20.8	2.819	811.7	52.77
7.94	9.52	14	2.815	810.3	52.77
11.12	12.7	26.8	2.819	820.2	52.77
11.12	12.7	20.8	2.818	817.1	52.77
11.12	12.7	14	2.796	819.9	52.77
<b>R290: <math>T_{\text{evap}} = -4^{\circ}\text{C}</math>, <math>T_{\text{cond}} = 45^{\circ}\text{C}</math>, <math>T_{\text{WI}} = 12^{\circ}\text{C}</math>, <math>T_{\text{WO}} = 5^{\circ}\text{C}</math>, <math>T_{\text{WCI}} = 25^{\circ}\text{C}</math>, <math>T_{\text{WCO}} = 40^{\circ}\text{C}</math></b>					
6.36	7.94	26.8	2.888	792	52.75
6.36	7.94	20.8	2.887	790.3	52.75
6.36	7.94	14	2.885	788.8	52.75
7.94	9.52	26.8	2.888	795.6	52.75

7.94	9.52	20.8	2.887	793.4	52.75
7.94	9.52	14	2.883	791.8	52.75
11.12	12.7	26.8	2.888	802.4	52.75
11.12	12.7	20.8	2.887	799.1	52.75
11.12	12.7	14	2.861	802.2	52.75
<b>R290: <math>T_{\text{evap}} = -3^{\circ}\text{C}</math>, <math>T_{\text{cond}} = 45^{\circ}\text{C}</math>, <math>T_{\text{WI}} = 12^{\circ}\text{C}</math>, <math>T_{\text{WO}} = 5^{\circ}\text{C}</math>, <math>T_{\text{WCI}} = 25^{\circ}\text{C}</math>, <math>T_{\text{WCO}} = 40^{\circ}\text{C}</math></b>					
6.36	7.94	26.8	2.958	773.9	52.71
6.36	7.94	20.8	2.958	772	52.71
6.36	7.94	14	2.956	770.4	52.71
7.94	9.52	26.8	2.958	777.7	52.71
7.94	9.52	20.8	2.958	775.1	52.71
7.94	9.52	14	2.954	773.2	52.71
11.12	12.7	26.8	2.958	785.2	52.71
11.12	12.7	20.8	2.958	781.5	52.71
11.12	12.7	14	2.927	785.2	52.71

<b>R600a: <math>T_{\text{evap}} = -5^{\circ}\text{C}</math>, <math>T_{\text{cond}} = 50^{\circ}\text{C}</math>, <math>T_{\text{WI}} = 12^{\circ}\text{C}</math>, <math>T_{\text{WO}} = 5^{\circ}\text{C}</math>, <math>T_{\text{WCI}} = 25^{\circ}\text{C}</math>, <math>T_{\text{WCO}} = 40^{\circ}\text{C}</math></b>					
DREF (mm)	Doi (mm)	DW (mm)	COP (-)	TEWi (kgco2)	Efficiency exergy (%)
6.36	7.94	26.8	1.815	1254	37.52
6.36	7.94	20.8	1.815	1252	37.52
6.36	7.94	14	1.814	1251	37.52
7.94	9.52	26.8	1.815	1257	37.52
7.94	9.52	20.8	1.815	1255	37.52
7.94	9.52	14	1.813	1254	37.52
11.12	12.7	26.8	1.815	1264	37.52
11.12	12.7	20.8	1.814	1261	37.52
11.12	12.7	14	1.804	1265	37.52
<b>R600a: <math>T_{\text{evap}} = -4^{\circ}\text{C}</math>, <math>T_{\text{cond}} = 50^{\circ}\text{C}</math>, <math>T_{\text{WI}} = 12^{\circ}\text{C}</math>, <math>T_{\text{WO}} = 5^{\circ}\text{C}</math>, <math>T_{\text{WCI}} = 25^{\circ}\text{C}</math>, <math>T_{\text{WCO}} = 40^{\circ}\text{C}</math></b>					
6.36	7.94	26.8	1.867	1219	37.73
6.36	7.94	20.8	1.867	1218	37.73
6.36	7.94	14	1.866	1217	37.73
7.94	9.52	26.8	1.867	1222	37.73
7.94	9.52	20.8	1.867	1221	37.73
7.94	9.52	14	1.865	1219	37.73
11.12	12.7	26.8	1.867	1230	37.73
11.12	12.7	20.8	1.867	1227	37.73
11.12	12.7	14	1.855	1231	37.73
<b>R600a: <math>T_{\text{evap}} = -3^{\circ}\text{C}</math>, <math>T_{\text{cond}} = 50^{\circ}\text{C}</math>, <math>T_{\text{WI}} = 12^{\circ}\text{C}</math>, <math>T_{\text{WO}} = 5^{\circ}\text{C}</math>, <math>T_{\text{WCI}} = 25^{\circ}\text{C}</math>, <math>T_{\text{WCO}} = 40^{\circ}\text{C}</math></b>					
6.36	7.94	26.8	1.92	1186	37.93
6.36	7.94	20.8	1.92	1185	37.93



6.36	7.94	14	1.92	1184	37.93
7.94	9.52	26.8	1.92	1187	37.93
7.94	9.52	20.8	1.92	1187	37.93
7.94	9.52	14	1.92	1186	37.93
11.12	12.7	26.8	1.92	1198	37.93
11.12	12.7	20.8	1.92	1194	37.93
11.12	12.7	14	1.92	1200	37.93
<b>R600a: <math>T_{\text{evap}} = -5^{\circ}\text{C}</math>, <math>T_{\text{cond}} = 45^{\circ}\text{C}</math>, <math>T_{\text{WI}} = 12^{\circ}\text{C}</math>, <math>T_{\text{WO}} = 5^{\circ}\text{C}</math>, <math>T_{\text{WCI}} = 25^{\circ}\text{C}</math>, <math>T_{\text{WCO}} = 40^{\circ}\text{C}</math></b>					
DREF (mm)	Doi (mm)	DW (mm)	COP (-)	TEWI (kgCO2)	Efficiency exergy (%)
6.36	7.94	26.8	2.069	1103	38.6
6.36	7.94	20.8	2.069	1101	38.6
6.36	7.94	14	2.069	1099	38.6
7.94	9.52	26.8	2.069	1106	38.6
7.94	9.52	20.8	2.069	1104	38.6
7.94	9.52	14	2.068	1102	38.6
11.12	12.7	26.8	2.069	1114	38.6
11.12	12.7	20.8	2.068	1110	38.6
11.12	12.7	14	2.054	1114	38.6
<b>R600a: <math>T_{\text{evap}} = -4^{\circ}\text{C}</math>, <math>T_{\text{cond}} = 45^{\circ}\text{C}</math>, <math>T_{\text{WI}} = 12^{\circ}\text{C}</math>, <math>T_{\text{WO}} = 5^{\circ}\text{C}</math>, <math>T_{\text{WCI}} = 25^{\circ}\text{C}</math>, <math>T_{\text{WCO}} = 40^{\circ}\text{C}</math></b>					
6.36	7.94	26.8	2.127	1073	38.72
6.36	7.94	20.8	2.127	1071	38.72
6.36	7.94	14	2.125	1070	38.72
7.94	9.52	26.8	2.127	1077	38.72
7.94	9.52	20.8	2.127	1074	38.72
7.94	9.52	14	2.124	1073	38.72
11.12	12.7	26.8	2.127	1085	38.72
11.12	12.7	20.8	2.126	1081	38.72
11.12	12.7	14	2.109	1086	38.72
<b>R600a: <math>T_{\text{evap}} = -3^{\circ}\text{C}</math>, <math>T_{\text{cond}} = 45^{\circ}\text{C}</math>, <math>T_{\text{WI}} = 12^{\circ}\text{C}</math>, <math>T_{\text{WO}} = 5^{\circ}\text{C}</math>, <math>T_{\text{WCI}} = 25^{\circ}\text{C}</math>, <math>T_{\text{WCO}} = 40^{\circ}\text{C}</math></b>					
6.36	7.94	26.8	2.185	1045	38.81
6.36	7.94	20.8	2.185	1043	38.81
6.36	7.94	14	2.183	1042	38.81
7.94	9.52	26.8	2.185	1049	38.81
7.94	9.52	20.8	2.185	1047	38.81
7.94	9.52	14	2.182	1045	38.81
11.12	12.7	26.8	2.185	1059	38.81
11.12	12.7	20.8	2.185	1054	38.81
11.12	12.7	14	2.163	1060	38.81

<b>R1234yf: <math>T_{\text{evap}} = -5^{\circ}\text{C}</math>, <math>T_{\text{cond}} = 50^{\circ}\text{C}</math>, <math>T_{\text{WI}} = 12^{\circ}\text{C}</math>, <math>T_{\text{WO}} = 5^{\circ}\text{C}</math>, <math>T_{\text{WCI}} = 25^{\circ}\text{C}</math>, <math>T_{\text{WCO}} = 40^{\circ}\text{C}</math></b>					
$D_{\text{REF}}$ (mm)	$D_{\text{oi}}$ (mm)	$D_{\text{W}}$ (mm)	COP (-)	TEWI (kgCO <sub>2</sub> )	Efficiency exergy (%)
6.36	7.94	26.8	1.508	1504	31.38
6.36	7.94	20.8	1.508	1503	31.38
6.36	7.94	14	1.507	1503	31.38
7.94	9.52	26.8	1.508	1505	31.38
7.94	9.52	20.8	1.508	1504	31.38
7.94	9.52	14	1.507	1504	31.38
11.12	12.7	26.8	1.508	1508	31.38
11.12	12.7	20.8	1.507	1507	31.38
11.12	12.7	14	1.5	1513	31.38
<b>R1234yf: <math>T_{\text{evap}} = -4^{\circ}\text{C}</math>, <math>T_{\text{cond}} = 50^{\circ}\text{C}</math>, <math>T_{\text{WI}} = 12^{\circ}\text{C}</math>, <math>T_{\text{WO}} = 5^{\circ}\text{C}</math>, <math>T_{\text{WCI}} = 25^{\circ}\text{C}</math>, <math>T_{\text{WCO}} = 40^{\circ}\text{C}</math></b>					
6.36	7.94	26.8	1.553	1460	31.59
6.36	7.94	20.8	1.553	1459	31.59
6.36	7.94	14	1.552	1459	31.59
7.94	9.52	26.8	1.553	1461	31.59
7.94	9.52	20.8	1.553	1460	31.59
7.94	9.52	14	1.552	1460	31.59
11.12	12.7	26.8	1.553	1465	31.59
11.12	12.7	20.8	1.553	1463	31.59
11.12	12.7	14	1.544	1470	31.59
<b>R1234yf: <math>T_{\text{evap}} = -3^{\circ}\text{C}</math>, <math>T_{\text{cond}} = 50^{\circ}\text{C}</math>, <math>T_{\text{WI}} = 12^{\circ}\text{C}</math>, <math>T_{\text{WO}} = 5^{\circ}\text{C}</math>, <math>T_{\text{WCI}} = 25^{\circ}\text{C}</math>, <math>T_{\text{WCO}} = 40^{\circ}\text{C}</math></b>					
6.36	7.94	26.8	1.6	1418	31.79
6.36	7.94	20.8	1.6	1417	31.79
6.36	7.94	14	1.6	1417	31.79
7.94	9.52	26.8	1.6	1418	31.79
7.94	9.52	20.8	1.6	1418	31.79
7.94	9.52	14	1.6	1418	31.79
11.12	12.7	26.8	1.6	1423	31.79
11.12	12.7	20.8	1.6	1421	31.79
11.12	12.7	14	1.6	1429	31.79
<b>R1234yf: <math>T_{\text{evap}} = -5^{\circ}\text{C}</math>, <math>T_{\text{cond}} = 45^{\circ}\text{C}</math>, <math>T_{\text{WI}} = 12^{\circ}\text{C}</math>, <math>T_{\text{WO}} = 5^{\circ}\text{C}</math>, <math>T_{\text{WCI}} = 25^{\circ}\text{C}</math>, <math>T_{\text{WCO}} = 40^{\circ}\text{C}</math></b>					
$D_{\text{REF}}$ (mm)	$D_{\text{oi}}$ (mm)	$D_{\text{W}}$ (mm)	COP (-)	TEWI (kgCO <sub>2</sub> )	Efficiency exergy (%)
6.36	7.94	26.8	1.744	1301	32.66
6.36	7.94	20.8	1.744	1300	32.66
6.36	7.94	14	1.743	1300	32.66
7.94	9.52	26.8	1.744	1303	32.66
7.94	9.52	20.8	1.744	1302	32.66
7.94	9.52	14	1.743	1301	32.66
11.12	12.7	26.8	1.744	1307	32.66

11.12	12.7	20.8	1.744	1305	32.66
11.12	12.7	14	1.732	1311	32.66
<b>R1234yf: <math>T_{\text{evap}} = -4^{\circ}\text{C}</math>, <math>T_{\text{cond}} = 45^{\circ}\text{C}</math>, <math>T_{\text{WI}} = 12^{\circ}\text{C}</math>, <math>T_{\text{WO}} = 5^{\circ}\text{C}</math>, <math>T_{\text{WCI}} = 25^{\circ}\text{C}</math>, <math>T_{\text{WCO}} = 40^{\circ}\text{C}</math></b>					
6.36	7.94	26.8	1.795	1265	32.8
6.36	7.94	20.8	1.795	1264	32.8
6.36	7.94	14	1.794	1263	32.8
7.94	9.52	26.8	1.795	1266	32.8
7.94	9.52	20.8	1.795	1265	32.8
7.94	9.52	14	1.794	1264	32.8
11.12	12.7	26.8	1.795	1270	32.8
11.12	12.7	20.8	1.795	1268	32.8
11.12	12.7	14	1.781	1275	32.8
<b>R1234yf: <math>T_{\text{evap}} = -3^{\circ}\text{C}</math>, <math>T_{\text{cond}} = 45^{\circ}\text{C}</math>, <math>T_{\text{WI}} = 12^{\circ}\text{C}</math>, <math>T_{\text{WO}} = 5^{\circ}\text{C}</math>, <math>T_{\text{WCI}} = 25^{\circ}\text{C}</math>, <math>T_{\text{WCO}} = 40^{\circ}\text{C}</math></b>					
6.36	7.94	26.8	1.847	1230	32.91
6.36	7.94	20.8	1.847	1229	32.91
6.36	7.94	14	1.846	1228	32.91
7.94	9.52	26.8	1.847	1231	32.91
7.94	9.52	20.8	1.847	1230	32.91
7.94	9.52	14	1.845	1229	32.91
11.12	12.7	26.8	1.847	1235	32.91
11.12	12.7	20.8	1.847	1233	32.91
11.12	12.7	14	1.831	1241	32.91

For the **reference cooling capacity of 1.2 kW**, the results for the systems operating with **R134a, R290, R744, and R1234yf** are shown in the tables below.

<b>R134a: <math>T_{\text{evap}} = -5^{\circ}\text{C}</math>, <math>T_{\text{cond/gc}} = 50^{\circ}\text{C}</math>, <math>T_{\text{WI}} = 12^{\circ}\text{C}</math>, <math>T_{\text{WO}} = 5^{\circ}\text{C}</math>, <math>T_{\text{WCI}} = 25^{\circ}\text{C}</math>, <math>T_{\text{WCO}} = 40^{\circ}\text{C}</math></b>						
$D_{\text{REF}}$ (mm)	$D_{\text{oi}}$ (mm)	$D_{\text{w}}$ (mm)	COP (-)	TEWI (kgCO <sub>2</sub> )	Efficiency exergy (%)	Total plant cost rate (R\$/year)
6.36	7.94	26.8	1.983	3883	41.1	2043
6.36	7.94	20.8	1.983	3494	41.1	2018
6.36	7.94	14	1.981	3054	41.1	2008
7.94	9.52	26.8	1.983	4451	41.1	2038
7.94	9.52	20.8	1.983	3925	41.1	2014
7.94	9.52	14	1.98	3332	41.1	2012
11.12	12.7	26.8	1.983	5597	41.1	2035
11.12	12.7	20.8	1.983	4756	41.1	2016
11.12	12.7	14	1.955	3834	41.1	2067
<b>R134a: <math>T_{\text{evap}} = -4^{\circ}\text{C}</math>, <math>T_{\text{cond/gc}} = 50^{\circ}\text{C}</math>, <math>T_{\text{WI}} = 12^{\circ}\text{C}</math>, <math>T_{\text{WO}} = 5^{\circ}\text{C}</math>, <math>T_{\text{WCI}} = 25^{\circ}\text{C}</math>, <math>T_{\text{WCO}} = 40^{\circ}\text{C}</math></b>						
6.36	7.94	26.8	2.026	3959	41.1	2023

6.36	7.94	20.8	2.026	3535	41.1	1994
6.36	7.94	14	2.023	3057	41.1	1980
7.94	9.52	26.8	2.026	4568	41.1	2017
7.94	9.52	20.8	2.026	3993	41.1	1989
7.94	9.52	14	2.022	3346	41.1	1984
11.12	12.7	26.8	2.026	5779	41.1	2011
11.12	12.7	20.8	2.026	4857	41.1	1989
11.12	12.7	14	1.994	3846	41.1	2037
<b>R134a: <math>T_{\text{evap}} = -3^{\circ}\text{C}</math>, <math>T_{\text{cond/gc}} = 50^{\circ}\text{C}</math>, <math>T_{\text{WI}} = 12^{\circ}\text{C}</math>, <math>T_{\text{WO}} = 5^{\circ}\text{C}</math>, <math>T_{\text{WCI}} = 25^{\circ}\text{C}</math>, <math>T_{\text{WCO}} = 40^{\circ}\text{C}</math></b>						
6.36	7.94	26.8	2.07	4062	41	2008
6.36	7.94	20.8	2.07	3596	41	1974
6.36	7.94	14	2.07	3070	41	1955
7.94	9.52	26.8	2.07	4720	41	2001
7.94	9.52	20.8	2.07	4086	41	1968
7.94	9.52	14	2.07	3373	41	1958
11.12	12.7	26.8	2.07	6017	41	1993
11.12	12.7	20.8	2.07	4998	41	1965
11.12	12.7	14	2.033	3880	41	2010
<b>R134a: <math>T_{\text{evap}} = -5^{\circ}\text{C}</math>, <math>T_{\text{cond/gc}} = 45^{\circ}\text{C}</math>, <math>T_{\text{WI}} = 12^{\circ}\text{C}</math>, <math>T_{\text{WO}} = 5^{\circ}\text{C}</math>, <math>T_{\text{WCI}} = 25^{\circ}\text{C}</math>, <math>T_{\text{WCO}} = 40^{\circ}\text{C}</math></b>						
D <sub>REF</sub> (mm)	D <sub>oi</sub> (mm)	D <sub>w</sub> (mm)	COP (-)	TEWI (kgCO <sub>2</sub> )	Efficiency exergy (%)	Total plant cost rate (R\$/year)
6.36	7.94	26.8	2.216	3991	41.4	1883
6.36	7.94	20.8	2.215	3508	41.4	1852
6.36	7.94	14	2.212	2963	41.4	1836
7.94	9.52	26.8	2.216	4644	41.4	1877
7.94	9.52	20.8	2.215	3995	41.4	1847
7.94	9.52	14	2.21	3263	41.4	1840
11.12	12.7	26.8	2.215	5906	41.4	1869
11.12	12.7	20.8	2.215	4875	41.4	1845
11.12	12.7	14	2.177	3739	41.4	1891
<b>R134a: <math>T_{\text{evap}} = -4^{\circ}\text{C}</math>, <math>T_{\text{cond/gc}} = 45^{\circ}\text{C}</math>, <math>T_{\text{WI}} = 12^{\circ}\text{C}</math>, <math>T_{\text{WO}} = 5^{\circ}\text{C}</math>, <math>T_{\text{WCI}} = 25^{\circ}\text{C}</math>, <math>T_{\text{WCO}} = 40^{\circ}\text{C}</math></b>						
6.36	7.94	26.8	2.263	4096	41.26	1869
6.36	7.94	20.8	2.262	3571	41.26	1834
6.36	7.94	14	2.26	2980	41.26	1814
7.94	9.52	26.8	2.263	4796	41.26	1862
7.94	9.52	20.8	2.262	4089	41.26	1828
7.94	9.52	14	2.257	3293	41.26	1816
11.12	12.7	26.8	2.263	6132	41.26	1852
11.12	12.7	20.8	2.262	5006	41.26	1823
11.12	12.7	14	2.219	3767	41.26	1867

<b>R134a: <math>T_{\text{evap}} = -3^{\circ}\text{C}</math>, <math>T_{\text{cond/gc}} = 45^{\circ}\text{C}</math>, <math>T_{\text{WI}} = 12^{\circ}\text{C}</math>, <math>T_{\text{WO}} = 5^{\circ}\text{C}</math>, <math>T_{\text{WCI}} = 25^{\circ}\text{C}</math>, <math>T_{\text{WCO}} = 40^{\circ}\text{C}</math></b>						
6.36	7.94	26.8	2.311	4230	41.11	1861
6.36	7.94	20.8	2.311	3656	41.11	1820
6.36	7.94	14	2.306	3009	41.11	1794
7.94	9.52	26.8	2.311	4985	41.11	1852
7.94	9.52	20.8	2.31	4210	41.11	1813
7.94	9.52	14	2.304	3336	41.11	1796
11.12	12.7	26.8	2.311	6420	41.11	1840
11.12	12.7	20.8	2.31	5181	41.11	1805
11.12	12.7	14	2.261	3818	41.11	1845

<b>R290: <math>T_{\text{evap}} = -5^{\circ}\text{C}</math>, <math>T_{\text{cond/gc}} = 50^{\circ}\text{C}</math>, <math>T_{\text{WI}} = 12^{\circ}\text{C}</math>, <math>T_{\text{WO}} = 5^{\circ}\text{C}</math>, <math>T_{\text{WCI}} = 25^{\circ}\text{C}</math>, <math>T_{\text{WCO}} = 40^{\circ}\text{C}</math></b>						
$D_{\text{REF}}$ (mm)	$D_{\text{oi}}$ (mm)	$D_{\text{w}}$ (mm)	COP (-)	TEWI (kgCO <sub>2</sub> )	Efficiency exergy (%)	Total plant cost rate (R\$/year)
6.36	7.94	26.8	1.982	2221	41.17	2057
6.36	7.94	20.8	1.982	2219	41.17	2030
6.36	7.94	14	1.979	2218	41.17	2016
7.94	9.52	26.8	1.982	2225	41.17	2050
7.94	9.52	20.8	1.982	2222	41.17	2024
7.94	9.52	14	1.978	2221	41.17	2020
11.12	12.7	26.8	1.982	2233	41.17	2041
11.12	12.7	20.8	1.981	2227	41.17	2020
11.12	12.7	14	1.953	2252	41.17	2070
<b>R290: <math>T_{\text{evap}} = -4^{\circ}\text{C}</math>, <math>T_{\text{cond/gc}} = 50^{\circ}\text{C}</math>, <math>T_{\text{WI}} = 12^{\circ}\text{C}</math>, <math>T_{\text{WO}} = 5^{\circ}\text{C}</math>, <math>T_{\text{WCI}} = 25^{\circ}\text{C}</math>, <math>T_{\text{WCO}} = 40^{\circ}\text{C}</math></b>						
6.36	7.94	26.8	2.027	2170	41.18	2003
6.36	7.94	20.8	2.024	2169	41.18	1987
6.36	7.94	14	2.024	2169	41.18	1985
7.94	9.52	26.8	2.028	2177	41.18	2027
7.94	9.52	20.8	2.027	2173	41.18	1997
7.94	9.52	14	2.023	2172	41.18	1989
11.12	12.7	26.8	2.028	2185	41.18	2016
11.12	12.7	20.8	2.027	2179	41.18	1991
11.12	12.7	14	1.995	2206	41.18	2039
<b>R290: <math>T_{\text{evap}} = -3^{\circ}\text{C}</math>, <math>T_{\text{cond/gc}} = 50^{\circ}\text{C}</math>, <math>T_{\text{WI}} = 12^{\circ}\text{C}</math>, <math>T_{\text{WO}} = 5^{\circ}\text{C}</math>, <math>T_{\text{WCI}} = 25^{\circ}\text{C}</math>, <math>T_{\text{WCO}} = 40^{\circ}\text{C}</math></b>						
6.36	7.94	26.8	2.07	2126	41.16	2019
6.36	7.94	20.8	2.07	2122	41.16	1982
6.36	7.94	14	2.07	2122	41.16	1959
7.94	9.52	26.8	2.074	2130	41.16	2010
7.94	9.52	20.8	2.073	2126	41.16	1975
7.94	9.52	14	2.068	2126	41.16	1961

11.12	12.7	26.8	2.074	2139	41.16	1996
11.12	12.7	20.8	2.073	2132	41.16	1967
11.12	12.7	14	2.035	2162	41.16	2010
<b>R290: <math>T_{\text{evap}} = -5^{\circ}\text{C}</math>, <math>T_{\text{cond/gc}} = 45^{\circ}\text{C}</math>, <math>T_{\text{WI}} = 12^{\circ}\text{C}</math>, <math>T_{\text{WO}} = 5^{\circ}\text{C}</math>, <math>T_{\text{WCI}} = 25^{\circ}\text{C}</math>, <math>T_{\text{WCO}} = 40^{\circ}\text{C}</math></b>						
6.36	7.94	26.8	2.229	1979	41.73	1890
6.36	7.94	20.8	2.229	1976	41.73	1855
6.36	7.94	14	2.225	1975	41.73	1835
7.94	9.52	26.8	2.229	1985	41.73	1893
7.94	9.52	20.8	2.228	1979	41.73	1848
7.94	9.52	14	2.223	1978	41.73	1838
11.12	12.7	26.8	2.229	1992	41.73	1868
11.12	12.7	20.8	2.228	1985	41.73	1840
11.12	12.7	14	2.189	2012	41.73	1886
<b>R290: <math>T_{\text{evap}} = -4^{\circ}\text{C}</math>, <math>T_{\text{cond/gc}} = 45^{\circ}\text{C}</math>, <math>T_{\text{WI}} = 12^{\circ}\text{C}</math>, <math>T_{\text{WO}} = 5^{\circ}\text{C}</math>, <math>T_{\text{WCI}} = 25^{\circ}\text{C}</math>, <math>T_{\text{WCO}} = 40^{\circ}\text{C}</math></b>						
6.36	7.94	26.8	2.279	1937	41.64	1876
6.36	7.94	20.8	2.279	1934	41.64	1837
6.36	7.94	14	2.274	1932	41.64	1812
7.94	9.52	26.8	2.279	1942	41.64	1866
7.94	9.52	20.8	2.279	1937	41.64	1829
7.94	9.52	14	2.272	1936	41.64	1814
11.12	12.7	26.8	2.279	1951	41.64	1850
11.12	12.7	20.8	2.278	1943	41.64	1818
11.12	12.7	14	2.233	1972	41.64	1861
<b>R290: <math>T_{\text{evap}} = -3^{\circ}\text{C}</math>, <math>T_{\text{cond/gc}} = 45^{\circ}\text{C}</math>, <math>T_{\text{WI}} = 12^{\circ}\text{C}</math>, <math>T_{\text{WO}} = 5^{\circ}\text{C}</math>, <math>T_{\text{WCI}} = 25^{\circ}\text{C}</math>, <math>T_{\text{WCO}} = 40^{\circ}\text{C}</math></b>						
6.36	7.94	26.8	2.324	1892	41.53	1793
6.36	7.94	20.8	2.33	1892	41.53	1822
6.36	7.94	14	2.325	1891	41.53	1791
7.94	9.52	26.8	2.33	1901	41.53	1855
7.94	9.52	20.8	2.33	1896	41.53	1812
7.94	9.52	14	2.322	1896	41.53	1792
11.12	12.7	26.8	2.33	1911	41.53	1837
11.12	12.7	20.8	2.329	1903	41.53	1800
11.12	12.7	14	2.277	1936	41.53	1838

<b>R744: <math>T_{\text{evap}} = -5^{\circ}\text{C}</math>, <math>T_{\text{cond/gc}} = 50^{\circ}\text{C}</math>, <math>T_{\text{WI}} = 12^{\circ}\text{C}</math>, <math>T_{\text{WO}} = 5^{\circ}\text{C}</math>, <math>T_{\text{WCI}} = 25^{\circ}\text{C}</math>, <math>T_{\text{WCO}} = 40^{\circ}\text{C}</math></b>						
$D_{\text{REF}}$ (mm)	$D_{\text{oi}}$ (mm)	$D_{\text{w}}$ (mm)	COP (-)	TEWI (kgCO <sub>2</sub> )	Efficiency exergy (%)	Total plant cost rate (R\$/year)
6.36	7.94	26.8	1.891	2647	36.21	2458
6.36	7.94	20.8	1.888	2650	36.21	2379
6.36	7.94	14	1.888	2650	36.21	2378

7.94	9.52	26.8	1.891	2647	36.21	2458
7.94	9.52	20.8	1.890	2648	36.21	2425
7.94	9.52	14	1.886	2654	36.21	2417
11.12	12.7	26.8	1.891	2648	36.21	2468
11.12	12.7	20.8	1.89	2649	36.21	2442
11.12	12.7	14	1.857	2695	36.21	2498
<b>R744: <math>T_{\text{evap}} = -4^{\circ}\text{C}</math>, <math>T_{\text{cond/gc}} = 50^{\circ}\text{C}</math>, <math>T_{\text{WI}} = 12^{\circ}\text{C}</math>, <math>T_{\text{WO}} = 5^{\circ}\text{C}</math>, <math>T_{\text{WCI}} = 25^{\circ}\text{C}</math>, <math>T_{\text{WCO}} = 40^{\circ}\text{C}</math></b>						
6.36	7.94	26.8	1.934	2588	36.17	2426
6.36	7.94	20.8	1.934	2588	36.17	2388
6.36	7.94	14	1.931	2591	36.17	2339
7.94	9.52	26.8	1.934	2588	36.17	2425
7.94	9.52	20.8	1.934	2588	36.17	2389
7.94	9.52	14	1.929	2595	36.17	2377
11.12	12.7	26.8	1.934	2589	36.17	2435
11.12	12.7	20.8	1.933	2590	36.17	2405
11.12	12.7	14	1.896	2641	36.17	2460
<b>R744: <math>T_{\text{evap}} = -3^{\circ}\text{C}</math>, <math>T_{\text{cond/gc}} = 50^{\circ}\text{C}</math>, <math>T_{\text{WI}} = 12^{\circ}\text{C}</math>, <math>T_{\text{WO}} = 5^{\circ}\text{C}</math>, <math>T_{\text{WCI}} = 25^{\circ}\text{C}</math>, <math>T_{\text{WCO}} = 40^{\circ}\text{C}</math></b>						
6.36	7.94	26.8	1.978	2530	36.11	2400
6.36	7.94	20.8	1.978	2531	36.11	2357
6.36	7.94	14	1.974	2535	36.11	2304
7.94	9.52	26.8	1.978	2531	36.11	2399
7.94	9.52	20.8	1.978	2531	36.11	2358
7.94	9.52	14	1.972	2538	36.11	2321
11.12	12.7	26.8	1.978	2532	36.11	2407
11.12	12.7	20.8	1.977	2532	36.11	2373
11.12	12.7	14	1.934	2589	36.11	2425
<b>R744: <math>T_{\text{evap}} = -5^{\circ}\text{C}</math>, <math>T_{\text{cond/gc}} = 45^{\circ}\text{C}</math>, <math>T_{\text{WI}} = 12^{\circ}\text{C}</math>, <math>T_{\text{WO}} = 5^{\circ}\text{C}</math>, <math>T_{\text{WCI}} = 25^{\circ}\text{C}</math>, <math>T_{\text{WCO}} = 40^{\circ}\text{C}</math></b>						
6.36	7.94	26.8	2.102	2381	39.9	2273
6.36	7.94	20.8	2.102	2381	39.9	2232
6.36	7.94	14	2.099	2384	39.9	2173
7.94	9.52	26.8	2.102	2381	39.9	2273
7.94	9.52	20.8	2.102	2382	39.9	2233
7.94	9.52	14	2.096	2388	39.9	2218
11.12	12.7	26.8	2.102	2382	39.9	2282
11.12	12.7	20.8	2.101	2383	39.9	2250
11.12	12.7	14	2.058	2433	39.9	2302
<b>R744: <math>T_{\text{evap}} = -4^{\circ}\text{C}</math>, <math>T_{\text{cond/gc}} = 45^{\circ}\text{C}</math>, <math>T_{\text{WI}} = 12^{\circ}\text{C}</math>, <math>T_{\text{WO}} = 5^{\circ}\text{C}</math>, <math>T_{\text{WCI}} = 25^{\circ}\text{C}</math>, <math>T_{\text{WCO}} = 40^{\circ}\text{C}</math></b>						
6.36	7.94	26.8	2.152	2326	39.88	2243
6.36	7.94	20.8	2.152	2326	39.88	2199
6.36	7.94	14	2.148	2330	39.88	2138

7.94	9.52	26.8	2.152	2326	39.88	2242
7.94	9.52	20.8	2.151	2327	39.88	2200
7.94	9.52	14	2.145	2333	39.88	2156
11.12	12.7	26.8	2.152	2327	39.88	2250
11.12	12.7	20.8	2.151	2328	39.88	2215
11.12	12.7	14	2.101	2382	39.88	2266
<b>R744: <math>T_{\text{evap}} = -3^{\circ}\text{C}</math>, <math>T_{\text{cond/gc}} = 45^{\circ}\text{C}</math>, <math>T_{\text{WI}} = 12^{\circ}\text{C}</math>, <math>T_{\text{WO}} = 5^{\circ}\text{C}</math>, <math>T_{\text{WCI}} = 25^{\circ}\text{C}</math>, <math>T_{\text{WCO}} = 40^{\circ}\text{C}</math></b>						
6.36	7.94	26.8	2.203	2272	39.84	2219
6.36	7.94	20.8	2.202	2273	39.84	2171
6.36	7.94	14	2.198	2277	39.84	2105
7.94	9.52	26.8	2.203	2273	39.84	2217
7.94	9.52	20.8	2.202	2273	39.84	2171
7.94	9.52	14	2.195	2280	39.84	2123
11.12	12.7	26.8	2.203	2274	39.84	2225
11.12	12.7	20.8	2.201	2275	39.84	2185
11.12	12.7	14	2.144	2335	39.84	2233

<b>R1234yf: <math>T_{\text{evap}} = -5^{\circ}\text{C}</math>, <math>T_{\text{cond/gc}} = 50^{\circ}\text{C}</math>, <math>T_{\text{WI}} = 12^{\circ}\text{C}</math>, <math>T_{\text{WO}} = 5^{\circ}\text{C}</math>, <math>T_{\text{WCI}} = 25^{\circ}\text{C}</math>, <math>T_{\text{WCO}} = 40^{\circ}\text{C}</math></b>						
$D_{\text{REF}}$ (mm)	$D_{\text{oi}}$ (mm)	$D_{\text{w}}$ (mm)	COP (-)	TEWI (kgCO <sub>2</sub> )	Efficiency exergy (%)	Total plant cost rate (R\$/year)
6.36	7.94	26.8	1.622	2707	33.73	2490
6.36	7.94	20.8	1.621	2706	33.73	2454
6.36	7.94	14	1.619	2707	33.73	2430
7.94	9.52	26.8	1.622	2709	33.73	2480
7.94	9.52	20.8	1.621	2707	33.73	2445
7.94	9.52	14	1.618	2710	33.73	2431
11.12	12.7	26.8	1.622	2712	33.73	2460
11.12	12.7	20.8	1.621	2710	33.73	2431
11.12	12.7	14	1.614	2739	33.73	2474
<b>R1234yf: <math>T_{\text{evap}} = -4^{\circ}\text{C}</math>, <math>T_{\text{cond/gc}} = 50^{\circ}\text{C}</math>, <math>T_{\text{WI}} = 12^{\circ}\text{C}</math>, <math>T_{\text{WO}} = 5^{\circ}\text{C}</math>, <math>T_{\text{WCI}} = 25^{\circ}\text{C}</math>, <math>T_{\text{WCO}} = 40^{\circ}\text{C}</math></b>						
6.36	7.94	26.8	1.669	2629	33.95	2450
6.36	7.94	20.8	1.668	2628	33.95	2409
6.36	7.94	14	1.667	2629	33.95	2354
7.94	9.52	26.8	1.669	2631	33.95	2439
7.94	9.52	20.8	1.668	2630	33.95	2399
7.94	9.52	14	1.665	2633	33.95	2380
11.12	12.7	26.8	1.669	2635	33.95	2416
11.12	12.7	20.8	1.668	2632	33.95	2382
11.12	12.7	14	1.645	2665	33.95	2422
<b>R1234yf: <math>T_{\text{evap}} = -3^{\circ}\text{C}</math>, <math>T_{\text{cond/gc}} = 50^{\circ}\text{C}</math>, <math>T_{\text{WI}} = 12^{\circ}\text{C}</math>, <math>T_{\text{WO}} = 5^{\circ}\text{C}</math>, <math>T_{\text{WCI}} = 25^{\circ}\text{C}</math>, <math>T_{\text{WCO}} = 40^{\circ}\text{C}</math></b>						



6.36	7.94	26.8	1.716	2553	34.17	2416
6.36	7.94	20.8	1.716	2552	34.17	2369
6.36	7.94	14	1.716	2553	34.17	2303
7.94	9.52	26.8	1.716	2556	34.17	2404
7.94	9.52	20.8	1.716	2554	34.17	2357
7.94	9.52	14	1.715	2558	34.17	2332
11.12	12.7	26.8	1.716	2559	34.17	2378
11.12	12.7	20.8	1.715	2557	34.17	2337
11.12	12.7	14	1.688	2594	34.17	2373
<b>R1234yf: <math>T_{\text{evap}} = -5^{\circ}\text{C}</math>, <math>T_{\text{cond/gc}} = 45^{\circ}\text{C}</math>, <math>T_{\text{WI}} = 12^{\circ}\text{C}</math>, <math>T_{\text{WO}} = 5^{\circ}\text{C}</math>, <math>T_{\text{WCI}} = 25^{\circ}\text{C}</math>, <math>T_{\text{WCO}} = 40^{\circ}\text{C}</math></b>						
6.36	7.94	26.8	1.876	2341	35.15	2251
6.36	7.94	20.8	1.875	2339	35.15	2202
6.36	7.94	14	1.874	2338	35.15	2124 (2080)
7.94	9.52	26.8	1.876	2343	35.15	2238
7.94	9.52	20.8	1.875	2341	35.15	2190
7.94	9.52	14	1.872	2344	35.15	2164
11.12	12.7	26.8	1.876	2347	35.15	2210
11.12	12.7	20.8	1.875	2344	35.15	2167
11.12	12.7	14	1.844	2377	35.15	2200
<b>R1234yf: <math>T_{\text{evap}} = -4^{\circ}\text{C}</math>, <math>T_{\text{cond/gc}} = 45^{\circ}\text{C}</math>, <math>T_{\text{WI}} = 12^{\circ}\text{C}</math>, <math>T_{\text{WO}} = 5^{\circ}\text{C}</math>, <math>T_{\text{WCI}} = 25^{\circ}\text{C}</math>, <math>T_{\text{WCO}} = 40^{\circ}\text{C}</math></b>						
6.36	7.94	26.8	1.936	2271	35.36	2221
6.36	7.94	20.8	1.935	2270	35.36	2166
6.36	7.94	14	1.934	2266	35.36	2027
7.94	9.52	26.8	1.936	2274	35.36	2206
7.94	9.52	20.8	1.935	2272	35.36	2153
7.94	9.52	14	1.929	2272	35.36	2086
11.12	12.7	26.8	1.936	2278	35.36	2176
11.12	12.7	20.8	1.935	2275	35.36	2127
11.12	12.7	14	1.899	2312	35.36	2156
<b>R1234yf: <math>T_{\text{evap}} = -3^{\circ}\text{C}</math>, <math>T_{\text{cond/gc}} = 45^{\circ}\text{C}</math>, <math>T_{\text{WI}} = 12^{\circ}\text{C}</math>, <math>T_{\text{WO}} = 5^{\circ}\text{C}</math>, <math>T_{\text{WCI}} = 25^{\circ}\text{C}</math>, <math>T_{\text{WCO}} = 40^{\circ}\text{C}</math></b>						
6.36	7.94	26.8	1.995	2204	35.56	2198
6.36	7.94	20.8	1.994	2202	35.56	2133
6.36	7.94	14	1.993	2198	35.56	1978
7.94	9.52	26.8	1.995	2207	35.56	2201
7.94	9.52	20.8	1.994	2204	35.56	2118
7.94	9.52	14	1.992	2200	35.56	1994
11.12	12.7	26.8	1.995	2212	35.56	2166
11.12	12.7	20.8	1.994	2207	35.56	2090
11.12	12.7	14	1.951	2250	35.56	2114